

THEME I a

MECHANICAL PROPERTIES OF STEEL UNDER LOAD CYCLES IDEALIZING  
SEISMIC ACTIONS

PROPRIETES MECANQUES DE L'ACIER SOUS CYCLES DE CHARGE REPRESENTATIFS DES ACTIONS SISMQUES

Reporter  
Rapporteur

Ben KATO  
University of Tokyo  
Tokyo, Japan



Ben KATO - Theme Ia

Errata Corrige

Page 13, line 7, should read:

,and the relationship between  $E_B$  and  $\epsilon_S$

Page 20, line 3, should read:

significance of their study may

Page 24, line 11, should read:

and introducing the relation of  $\phi = \epsilon / 0.75d$ , the



# MECHANICAL PROPERTIES OF STEEL UNDER LOAD CYCLES IDEALIZING SEISMIC ACTIONS

## PROPRIETES MECANQUES DE L'ACIER SOUS CYCLES REPRESENTATIFS DES ACTIONS SISMQUES

Ben KATO

University of Tokyo  
Tokyo, Japan

### SUMMARY

Stress-strain relations for reinforcing steel under repeated and reversed cyclic loading simulating seismic conditions are reviewed. An emphasis is made that these constitutive relations should provide the prediction on the limit of deformability of reinforcing steel which will be reached under any given loading cycles.

The prerequisite for a reinforced concrete member as a part of the seismic structures is that it should develop enough ductility or rotation capacity. Basic inelastic behaviors of reinforced concrete members are discussed in association with the influence of the steel performance to the ductility of the reinforced concrete members. Some comments on the behavior of prestressing steel are included incidentally.

### RESUME

On décrit d'abord les lois constitutives de l'acier sous l'action des charges répétées et alternées de type sismique. On souligne à ce propos l'importance d'une représentation fidèle des déformations atteintes après des histoires de charges quelconques.

La propriété fondamentale des éléments formant une structure asismique est celle de posséder une bonne capacité de rotation plastique. Le comportement inélastique des divers éléments en béton armé est discuté par rapport à la contribution de l'acier à la ductilité résultante. Des observations marginales concernant le béton précontraint sont aussi présentées.

### 1. INTRODUCTION

To study the behavior of reinforced concrete members under repeated and reversed loadings such as earthquakes it is very important to have basic information on the behavior of steel bars under such loadings. This information must be organized to give the basis for the two major achievements. Firstly, it should be so formulated that it will lead to the derivation of the moment-curvature diagrams of reinforced concrete members. In performing the formulation, it should be kept in mind whether it will be used in research or in design. In research, it should be accurate enough to be compared with experimental results and be clear enough to explain the physical mechanism involved. In design, with considerable variations likely in the actual strengths of both concrete and steel, a solution should provide only basic insight into the overall behavior of a structure,

and should be as simple as possible. Secondly, it should include the information on the amount of plastic strain in steel bars accumulated by a given load cycling so that it enables to predict the ultimate state of concrete members determined by the ultimate deformation capacity of steel.

This paper first traces the available mathematical models for inelastic cyclic behavior of reinforcing steel, including some comments on the accumulated plastic strain in the reinforcing steel due to any given stress cycles. Discussions on the deformability or the rotation capacity of reinforced concrete members then follow. Although they do not go far enough to evaluate under the cyclic loading conditions, clear understanding of the influence of the steel performance to the deformability of the reinforced concrete members under monotonic loading is prerequisite to proceed to the study of cyclic behavior. Some comments on the behavior of prestressing steel are included incidentally.

## 2. MONOTONIC UNIAXIAL STRESS-STRAIN RELATIONSHIP

In any type of analysis of the hysteretic behavior of reinforcing steels, it must be based on the accurate knowledge on the stress-strain relationship for the monotonic loading up to the maximum stress point through the strain-hardening range. Various grades of reinforcing steels are categorized in Table 1, and the stress-strain curves for typical ones representative for each grade are shown in Fig.1. 0-1, 0-2 are traditional

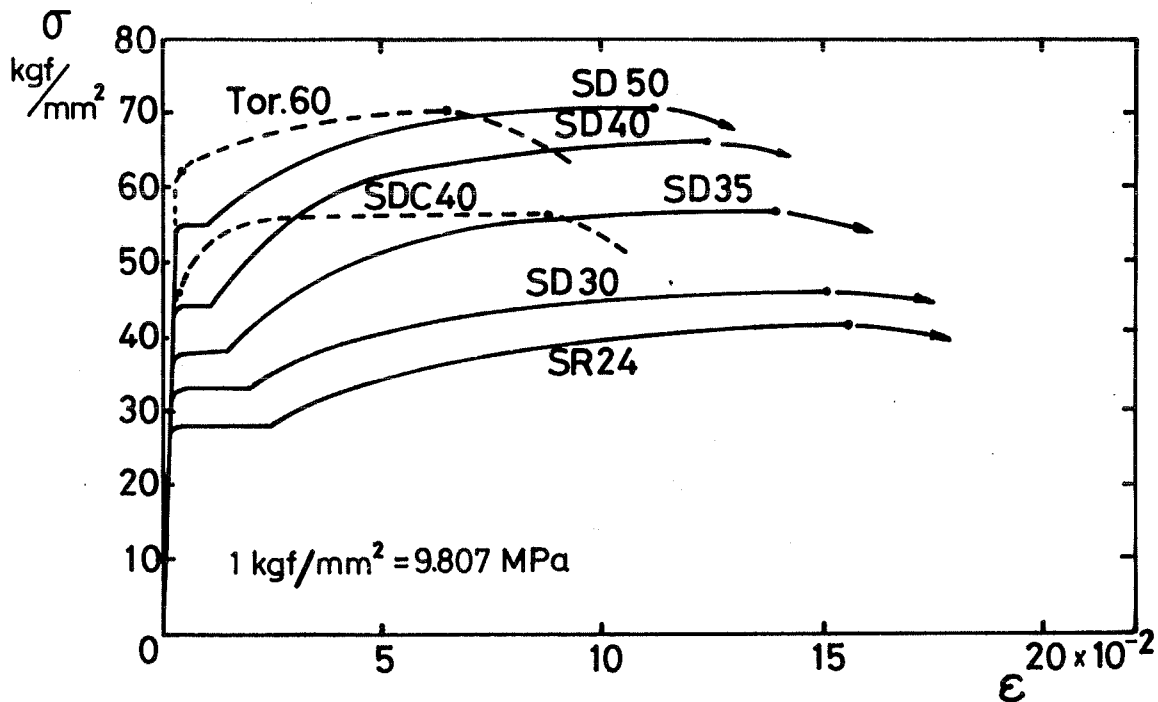


FIG.1. Stress-Strain Relationship of Steel Bars

mild steel, which are structural carbon steel if grouped according to metallurgical characteristics. I through V' are high strength steel, which are high-strength low-alloy steels in metallurgical sense. Among these, II', III', IV' and V' are cold-strained by twisting and/or stretching to increase the yield strength. In Table 1, the term Yield Ratio is the ratio of the yield strength to the tensile strength, and an alternative expression of this characteristic is the tensile-yield ratio which is the inverse of the yield ratio. The values of yield ratio listed in Table 1 are only the nominal, the figures which will be obtained on the basis of the actually market-supplied steels will be considerably higher. This ratio is

Table 1. Mechanical Properties of Reinforcing Bars

		Minimum Specified Values			Yield Ratio	Designation
		Yield Strength MPa (kgf/mm <sup>2</sup> )	Tens. Strength MPa (kgf/mm <sup>2</sup> )	Percentage Elongation %		
Mild Steel	0-1	216 (22)	412 (42)	30	0.524	Beton Stahl I(G), SR24(J)
	0-2	275 (28)	412 (47)	30	0.596	Grade 40(U), SR30(J)
High-Strength Steel	I	343 (35)	559 (57)	27	0.614	Beton Stahl II(G), Grade 50(U), SD35(J)
	II	392 (40)	647 (66)	23	0.606	Beton Stahl III(G), Grade 60(U), SD40(J)
	II'	392 (40)	539 (55)	16	0.727	Torsteel 40(A), Rippentorsteel(G) Tentorsteel(E), Kamsteel(Sn), SDC40(J)
	III	490 (50)	691 (70.5)	22	0.709	Beton Stahl IV(G), Grade 75(U), SD50(J)
	III'	490 (50)				Tentorsteel(E), Torsteel 50(A), SDC50(J)
	IV'	588 (60)	682 (69.5)	13	0.863	Torsteel 60(A), Kamsteel 60(Sn)
	V'	686 ~ 883 (70 ~ 90)				Torsteel 80(A), Kamsteel 90(Sn)

G = Germany, J = Japan, U = U.S.A., A = Austria, E = United Kingdom, Sn = Sweden

an important parameter to assess the deformation capacity or the rotation capacity of reinforced concrete members as will be discussed later. Generally speaking, the higher the yield strength, the higher the yield ratio and the smaller the percentage elongation. These tendencies are visualized in Table 1, and are especially remarkable for the pre-twisted and/or pre-stretched bars (Torsteel, Tentorsteel).

### 3. HYSTERETIC UNIAXIAL STRESS-STRAIN RELATIONSHIP

The available formulations for stress-strain relations for cyclic behavior can be classified into two groups. One of these groups is that consider the history dependence in the material behavior though there are considerable differences in their approaches. This group will be referred to as history dependent formulations. The other group is based on generalizations of Ramberg-Osgood equations (R-O equations). In this approach, history dependence is also taken into account, but not in a direct manner. Details of these approaches follow.

#### 3.1. History Dependent Formulations

Inelastic behavior of steel in cyclic loading is a strongly history dependent process. In this section three procedures for obtaining cyclic stress-strain relations based on a clearly recognized dependence on the past history of loadings are discussed. The first procedure has been developed by the writer and his associates [1],[2],[3], the second by Popov et.al. [4],[5], and the third by Sozen et.al. [6].

On the basis of a series of tests which includes a) progressively increasing stress amplitude, b) stationally cyclic process, c) steadily decreasing stress amplitude and d) random process, the writer and his associates [1],[2],[3], demonstrated that any stress-strain relation under repeated and reversed loading can be decomposed into three parts: skeleton part, unloading part and softened part. In a cluster of cyclic hysteretic loops such as shown in Fig.2, the bold lines are defined as the skeleton parts which are the portions of the curves at stresses of the same sign larger than the ones during the previous cycle, fine straight lines are the unloaded parts and the dashed lines are softened parts in which the Bauschinger effect is dominant. The characteristics of these three parts are described in the following;

##### 1) Skeleton Parts

Inter-connecting the skeleton lines end to start, either above or below the horizontal axis gives curves as shown in Fig.3. Curves found from monotonic experiments for the same size and grade of specimens are shown by dashed lines in the same figure, and it can be seen that these two pairs of curves agree satisfactorily each other except for the first yielding region in the compression side. Thus it can be concluded that any skeleton line is always a part of the monotonic stress-strain curve and that when the accumulated skeleton strains in either sign attain the maximum strain  $\epsilon_u$  found from the monotonic stress-strain relationship, the specimen will attain its ultimate load carrying capacity.

##### 2) Unloaded Parts

It was found any unloaded line can be approximated by the straight line.

##### 3) Softened Parts

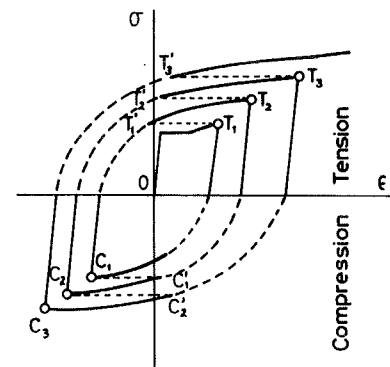


FIG.2. A Cluster of Hysteretic Loops



The behavior of a softened part depends strongly on the history of the opposite sign of stressing, and this behavior was investigated according to the following two categories; (a) being unloaded from a skeleton part and is reloaded into the reverse side of skeleton part, (b) being unloaded from a softened part, and reloaded into the skeleton part of the opposite side. As shown in Fig.4, cases (a') and (b') can be considered as being included in case (a) and case (b) respectively.

Category(a): Experimental data for the softened parts such as OA in Fig.5 are plotted in

Fig.6 for a particular grade of steel SM58 for various stages of cycles in nondimensional form where  $\sigma_s$  is the maximum skeleton part stress experienced in the preceding loading history in the same sign and  $\epsilon_B$  is the corresponding strain, and numerals shown in the box are the number of cycles hitherto experienced corresponding to each mark. These plots can be fitted by a hyperbolic equation as

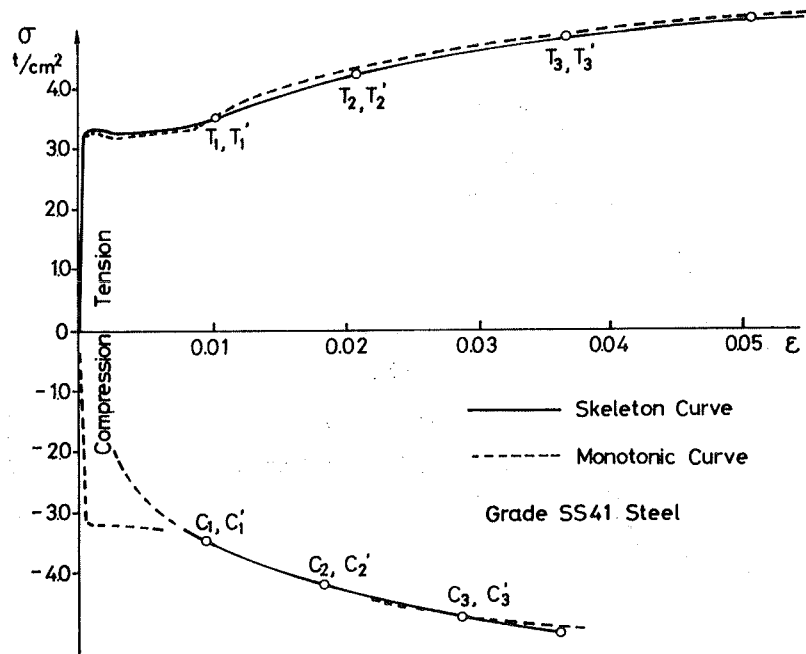


FIG.3. Comparison of Predicted and Experimental Curves

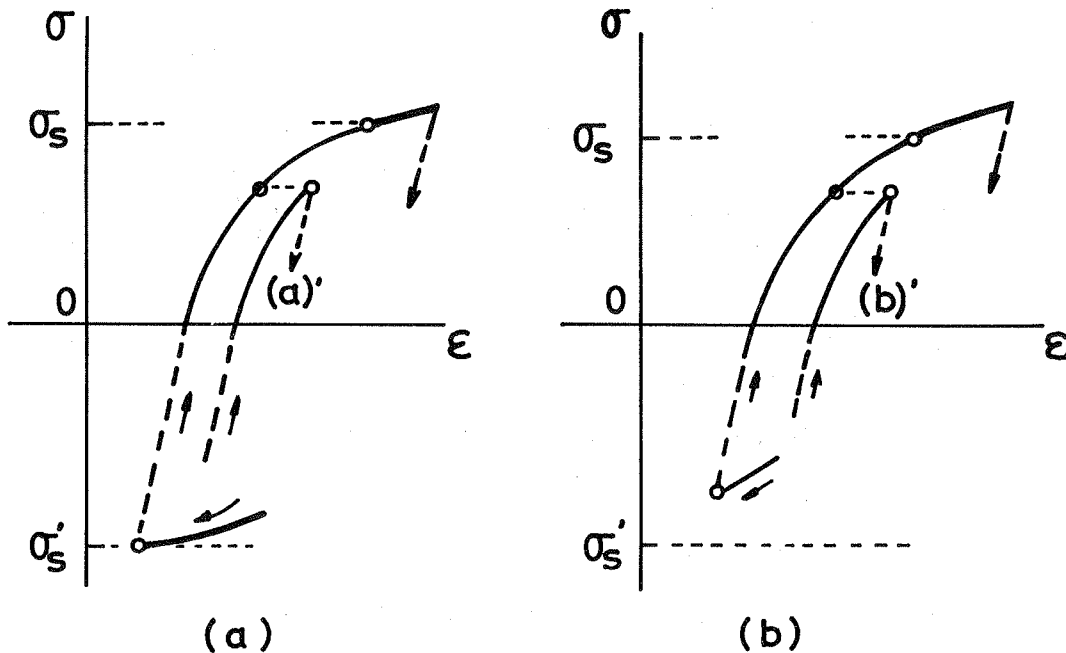


FIG.4. Classification of Softened Parts

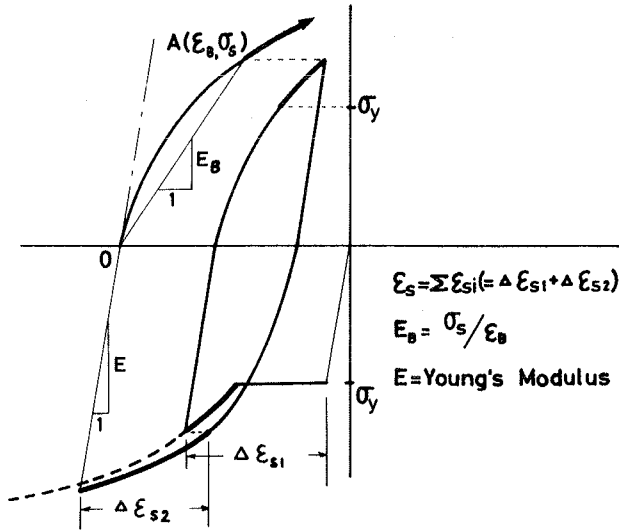


FIG.5. Softened Parts

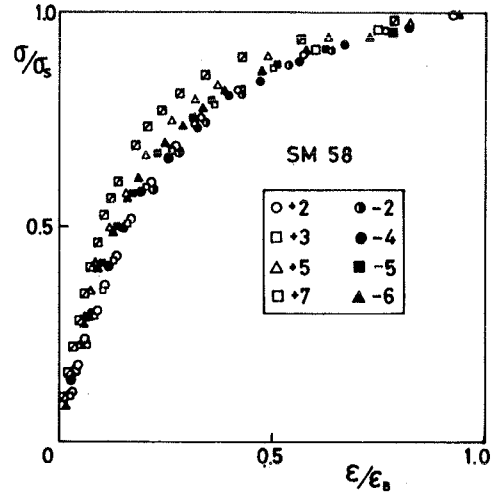


FIG.6. Measured Softened Parts

$$\begin{aligned}
 & \left( \frac{\sigma}{\sigma_s} - a \right) \left( \frac{E_B}{\sigma_s} \epsilon + a - 1 \right) - a(1 - a) = 0 \\
 \text{or} \quad & \left( \frac{\sigma}{\sigma_s} - a \right) \left( \frac{\epsilon}{\epsilon_B} + a - 1 \right) - a(1 - a) = 0
 \end{aligned} \quad (1)$$

The slope at the local origin 0 in Fig.6 is

$$\left[ \frac{d(\sigma/\sigma_s)}{d(\epsilon/\epsilon_B)} \right]_0 = \left( \frac{d\sigma}{d\epsilon} \right)_0 \frac{\epsilon_B}{\sigma_s} \quad (2)$$

$\left( \frac{d\sigma}{d\epsilon} \right)_0$  is the slope at the local origin 0 of the real softened diagram and is equal to the Young's modulus  $E$  since it shares the common tangent with the elastic unloading line, and  $\sigma_s/\epsilon_B$  is the secant modulus of the softened part and is denoted by  $E_B$  (see Fig.5), then eq.(2) can be written as

$$\left[ \frac{d(\sigma/\sigma_s)}{d(\epsilon/\epsilon_B)} \right]_0 = \frac{E}{E_B} \quad (3)$$

On the other hand, this term is led from eq.(1) as

$$\left[ \frac{d(\sigma/\sigma_s)}{d(\epsilon/\epsilon_B)} \right]_0 = \frac{a}{a - 1} \quad (4)$$

From eqs.(3) and (4), the parameter  $a$  is determined as

$$a = \frac{E}{E - E_B} \quad (5)$$

The characteristics of the softened parts are strongly influenced by the strain hysteresis in the opposite sign as mentioned earlier, and the effect of this strain hysteresis can be represented by the sum of all skeleton strains  $\Delta\epsilon_{si}$  hitherto experienced in the opposite side as shown in Fig.5 for an example. This accumulated skeleton strain is denoted by  $\epsilon_s (\epsilon_s = \sum \Delta\epsilon_{si})$ . The extension of the softened part is represented by the secant modulus  $E_B$ , on the other hand, and the relationship between  $E_B$  and  $\sigma_s$  were investigated on the experimental data. One of the results of this investigation is shown in Fig.7. From a series of test results for the various grades of steel, an empirical  $E_B$  vs.  $\epsilon_s$  relation on the basis of the lower bound was obtained as

$$E_B = -\frac{E}{6} \log_{10} 10\epsilon_s . \quad (6)$$

Eq.(6) is shown by the dashed line in Fig.7.

Thus the softened part in this category can be expressed by eqs.(1),(5) and (6).

Category(b): Depending on the preceding strain history, investigation was carried out according to the following sub-categories on the experimental data obtained from test series b) through

d): i) Unloaded from a boundary point between softened and skeleton part, stressed into the reverse side and unloaded again

at a intermediate point of this softened part followed by stressing into the previous domain as is illustrated by BMB'  $\rightarrow$  B'M'B in Fig.8(a), ii) Unloaded from a skeleton part, stressed into the opposite domain and unloaded again at a intermediate point of this softened part followed by stressing into the previous domain as is illustrated by ALA"  $\rightarrow$  A"L"A in Fig.8(b) and iii) Cyclic excursion inside the softened part region as is illustrated by A"L"B"  $\rightarrow$  B"M"A".

For all of these sub-categories, it has been demonstrated that any hysteresis curve for half-cycle (unloaded part plus softened part) could be obtained by the following procedure; Find the half-cycle curve which belongs to the category (a) experienced most recently to the curve in question in either sign which can be predicted by eq.(1). Then if one traces along this curve from the starting point of unloading to the specified stress point, this will give the half-cycle in question. This procedure is illustrated in Fig.8(c) and (d) for the cases of Fig.8(a) and (b) respectively, demonstrating that curve BMB' and curve B'M'B are the same shape and both are the part of the category (a) curve A'L'B.

These informations obtained above are sufficient enough to depict any random response of a steel bar if the loading pattern is specified. An example is shown in Fig.9, in which the prediction is compared with experimental result showing a good correlation.

A totally computer oriented approach was developed by Peterson and Popov [5]. This approach was developed on the basis of the following assumptions; a) The cyclic stress-strain curves tend to approach

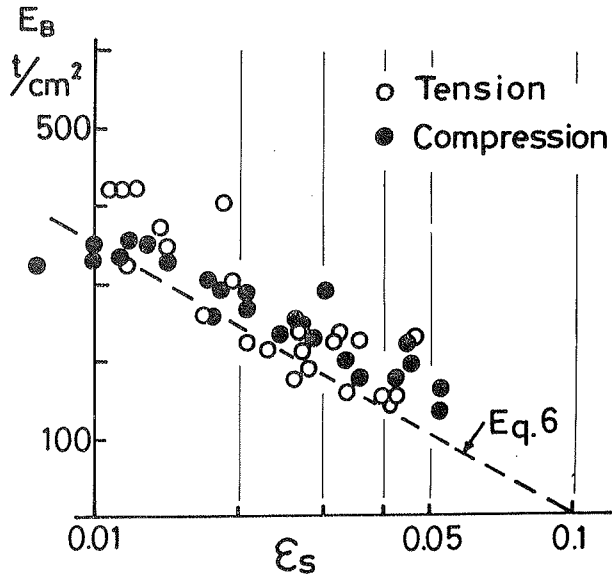


FIG.7.  $E_B \sim \epsilon_s$  Relation

asymptotically a pair of limiting or boundary lines [4] as shown in Fig.10(a), b) In any unloading process, linear portion is  $2K$ , twice the yield strength  $K$ , c) The experimental stress-strain curve is approximated by Hermitian polynomials to facilitate computer application.

In Fig.10, the elastic part of the strain is removed for the convenience of description. In the monotonic virgin curve as shown in Fig.10(b),  $AA'(2K)$  is the elastic range. Points 1, 2, 1" and 2" for the purpose of illustration only are so chosen as to result in equal stress increments  $\Delta\sigma$  for the different strain increments  $\epsilon_{p1}$ ,  $\epsilon_{p2}$ , and these increments remain the same in subsequent work. Suppose now that at some point B such as shown in Fig.10(c), the stress is unloaded. The segment BC whose length is  $2K$  represents elastic range. If loading were to continue beyond point C, it is assumed that for the various plastic strain increments such as  $\epsilon_{p1}$ , the vertical segment  $11'$  remains the same as in the virgin curve ( $11'$  in Fig.10(b)). Then, following to the same way as that of the virgin curve, the deformed point  $1''$  is obtained as illustrated in Fig.10(c). Point  $2''$  is established similarly. Since this construction makes use of the points B, 1, 2, etc. on the previous path of deformation, this becomes a history dependent description of the material behavior. If the load was again removed at point D such as shown in Fig. 10(d), the curve C2 (C2" in Fig.10(c)) determines the new locations of points E, 1" and 2". In this manner the history dependence of the cyclic process is brought in at each load reversal.

Since there is a good deal of difference in shapes between the initial monotonic stress-strain diagram and the curve generated during advanced stages of cycling, some modification of the curves for the advanced stages of cycles reflecting the experimental results must be introduced into the computer program.

A simple linear model was presented by Aktan, Karlsson and Sozen [6]. In this model, the strain-hardening slope or boundary curve and the expansion of the loop at any stage of cyclic loading are given as the functions of the plastic strain increment undergone in the preceding half-cycle of excursion.

The process of constructing the hysteresis curves is illustrated in

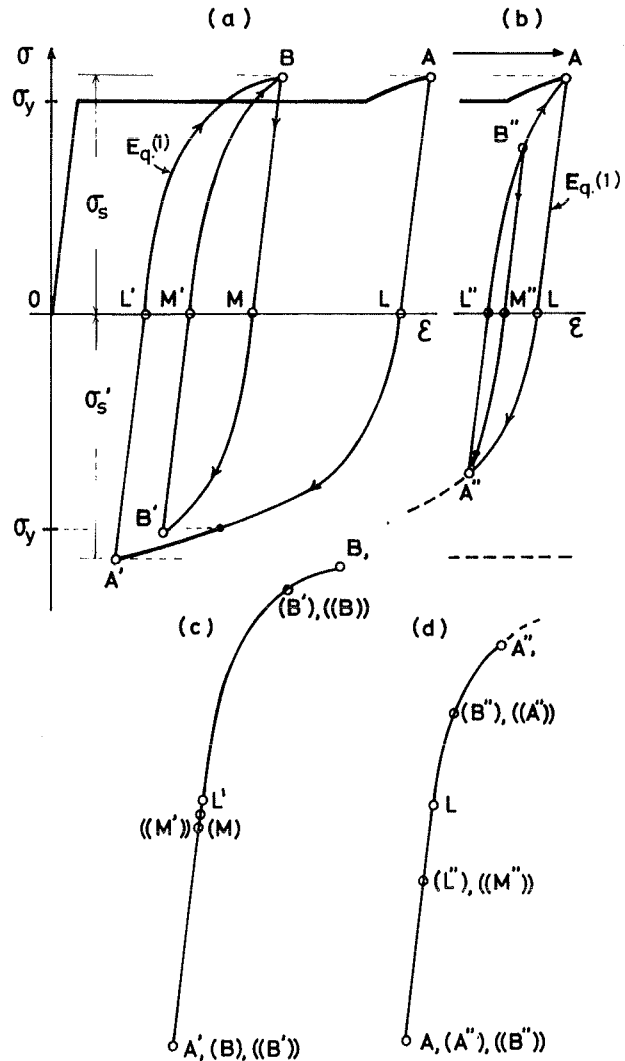


FIG.8. Characteristics of Softened Parts

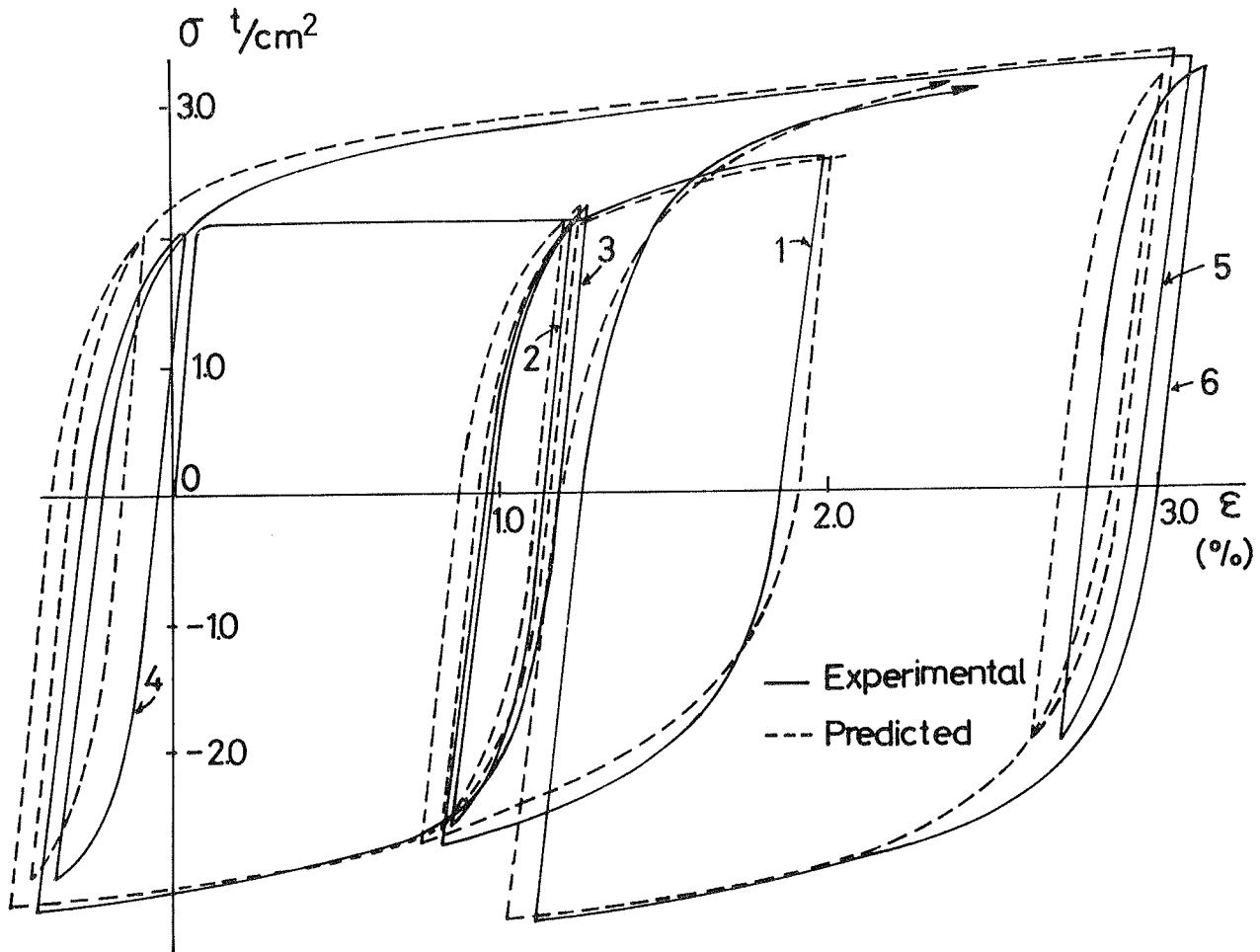


FIG.9. Comparison of Predicted and Experimental Loops

Fig.11. The initial stress-strain relation is bi-linear with a strain-hardening slope of 1,125,000 psi (791 kgf/mm<sup>2</sup>, 7,756 MPa) up to a stress of  $\pm 110,000$  psi (77 kgf/mm<sup>2</sup>, 758 MPa) in tension or compression.

At any reversal, if any plastic strain is obtained for the half-cycle before the reversal occurs, the boundary line after the reversal shifts from the previous one (in the same side) further into reverse direction by the stress increment  $\sigma_p$  corresponding to the plastic strain increment obtained before the reversal. At the first cycle, the virgin curve is considered to be the previous boundary line as shown by dashed line in the figure. The slope of this new boundary line is less than the previous boundary line and is given by  $K_o \frac{\pm 110,000 - \sigma_i}{\pm 110,000 - \sigma_n}$ , where  $K_o$  is the slope of the previous boundary line (in the same side),  $\sigma_n$ (psi) is the stress measured from the strain axis to the intersection of the unloading line and the previous boundary line, and  $\sigma_i = \sigma_n + \sigma_p$ . For further reversal, the plastic strain increment is defined as shown in the figure. If a plastic strain increment in this sense is not obtained before the reversal, the previous boundary line does not change. No information on the grade of steel used for this research was given.

### 3.2. Generalized Ramberg - Osgood Formulations

Originally Ramberg - Osgood equation (R-O equation) was proposed to

give a general stress-strain relationship of metallic materials for monotonic loading [7]. What actually happened was that the Ramberg - Osgood equation was used together with the Massing hypothesis [8] published earlier. The original Massing hypothesis asserts that initial monotonic curve such as given by the R-O equation, when magnified by a factor of two, will define the hysteretic loop shape of any branch when the origin of this new curve is placed at the point of stress reversal as illustrated in Fig. 12. Since this loop shape is most directly adaptable to the stationary cyclic process, this approach was successfully applied by a number of investigators to study the fatigue behavior of metals [9]. However, to apply to the non-stationary or random process such as earthquake response of structural members, a number of modifications are necessary. Among the researches intending to accomodate to the non-stationary process, those of  $M_a$ ,

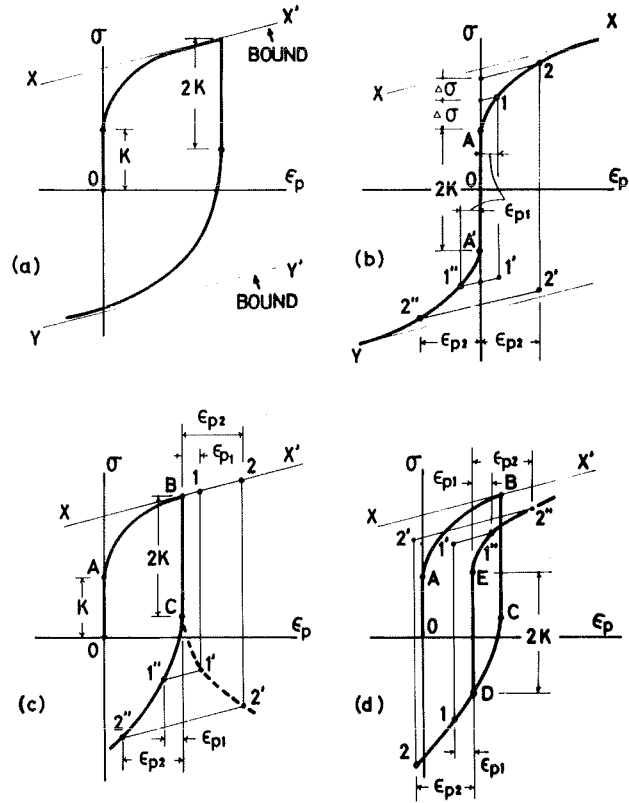
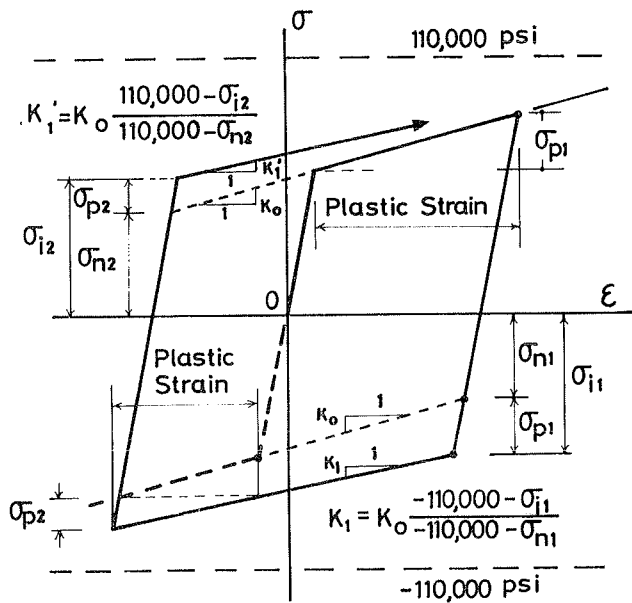


FIG.10. Construction of Hysteretic Curve (4), (5)



$$110,000 \text{ psi} = 77.3 \text{ kgf/mm}^2 = 758 \text{ MPa}$$

FIG.11. Construction of Hysteretic Curve (6)

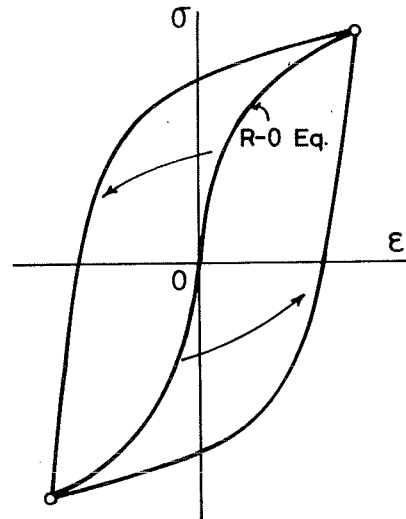


FIG.12. R-O Curve and Masing Hypothesis

Bertero and Popov [10],[11], Aktan, Karlson and Sozen [6], Yokoo and Nakamura [12] and Kent and Park [13] may be mentioned. In any approach, a monotonic stress-strain curve well into the strain-hardening range must be available.

M<sub>a</sub>, Bertero, Popov's Method [10], [11]

Two possible cases of first stress reversals are shown in Fig.13(a); one of them occurs in the plastic plateau range (Point A), the other in the strain-hardening range (Point A'). For the latter case, upon unloading, the stress is first reduced elastically from A' to A''. The  $\sigma$ - $\epsilon$  relationship between A and B or A'' and B' is given by a R-O equation:

$$\bar{\epsilon} = \beta(\bar{\sigma} + \alpha|\bar{\sigma}|^n) \quad (7)$$

where,  $\bar{\epsilon} = (\epsilon - \epsilon_A)/2\epsilon_y$ ,  $\bar{\sigma} = (\sigma - \sigma_A)/2\sigma_y$

in which  $\sigma$  and  $\epsilon$  define a point on AB (or A''B'), and  $\sigma_A$  and  $\epsilon_A$  define point A (or A').

Three parameters  $\alpha$ ,  $\beta$  and  $n$  are varied depending on the magnitude of the residual plastic strain  $\epsilon_{p.m}$ , which would develop upon the release of the previous loading as indicated in Fig.13(a). For the material used in this investigation,  $\alpha$  and  $\beta$  can be determined empirically by

$$\alpha = 2.3\epsilon_{p.m}/\epsilon_{sh} < 2.3$$

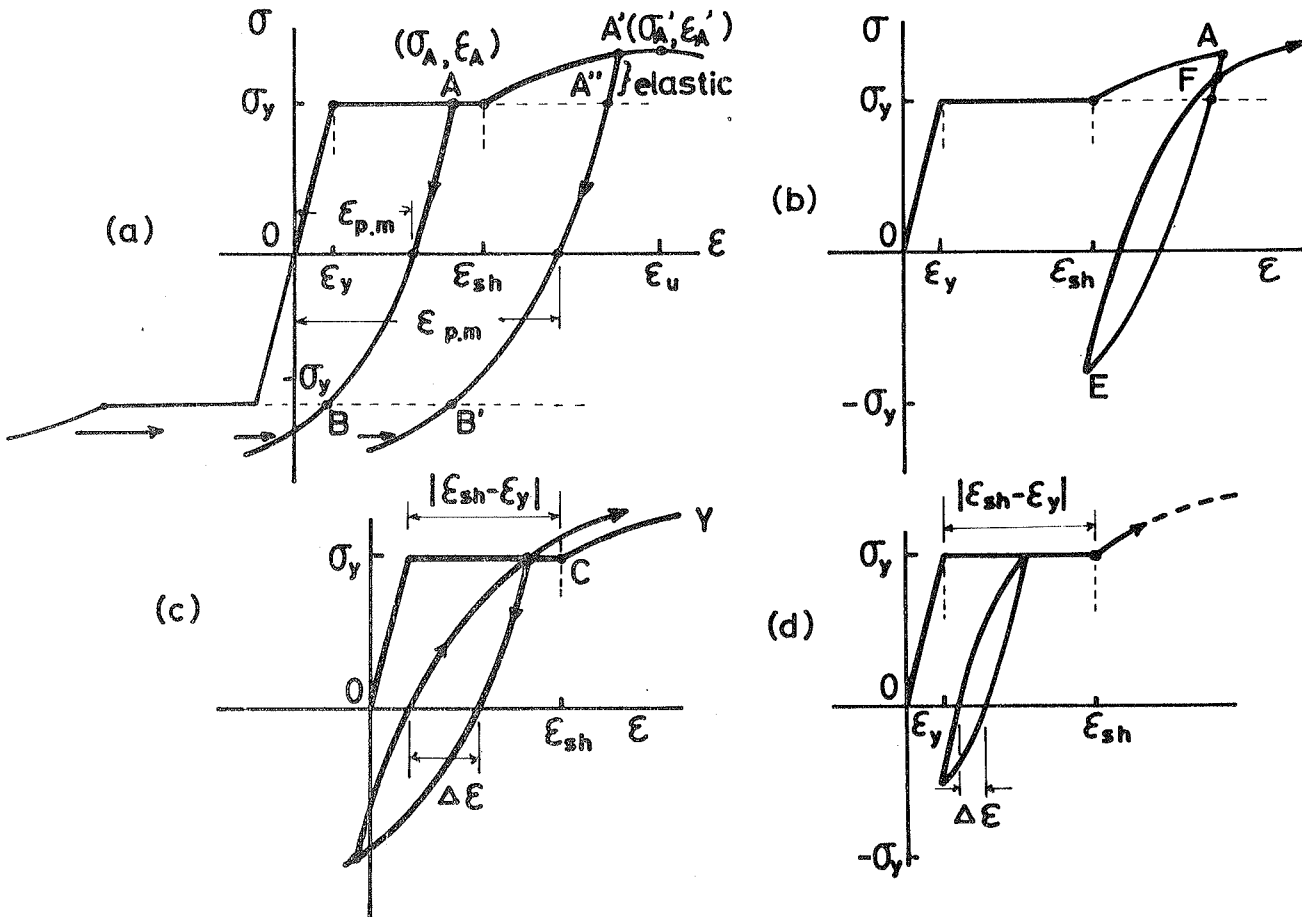


FIG.13. R-O Model by Popov [10]

$$\beta = (1 + 0.7\bar{\epsilon}_p - 0.3\bar{\epsilon}_p^{7/3}) < 1.4$$

where  $\bar{\epsilon}_p = \epsilon_{p,m}/(35 \times 10^{-3})$ .

For the two possible cases described above,  $n$  is 6 and 7 respectively. Beyond points such as B or B', the  $\sigma$ - $\epsilon$  relationship is assumed to be given by the translated monotonic strain-hardening curve.

If loading reverses a second time, similar to that shown at point E in Fig.13(b), the  $\sigma$ - $\epsilon$  relationship of the ascending curve EF is determined from the shape of the previous descending curve AE. For example, the curve EF is established by rotating the curve AE through  $180^\circ$  and translating it so that point A coincides with E. This procedure is applicable provided  $\epsilon_{p,m}$  for point F is equal to or less than that for point A. For loading beyond point F, the  $\sigma$ - $\epsilon$  relationship is assumed to follow the original monotonic  $\sigma$ - $\epsilon$  curve.

For an accurate modeling of the initiation of cyclic strain-hardening in the plastic plateau range, two cases are differentiated. The quantity  $0.5|\epsilon_{sh} - \epsilon_y|$  is used to separate the problem into the two cases. If the loop width  $\Delta\epsilon$  is wider than this quantity, the strain-hardening curve CY will be translated into the appropriate position as shown in Fig.13(c), if the loop width is smaller, strain-hardening will be initiated at the same strain value as that under monotonic loading as shown Fig.13(d). A computer program, BAUSCH, incorporating the above rules, has been written.

Aktan, Karlson, Sozen's Method [6]

A R-O function having the following form was used to describe the  $\sigma$ - $\epsilon$  relationship for each half-cycle between two stress reversals such as curves AB or BC in Fig.14.

$$\frac{\epsilon - \epsilon_i}{\epsilon_0} = \frac{\sigma - \sigma_i}{\sigma_0} + \left(\frac{\sigma - \sigma_i}{\sigma_0}\right)^\alpha \quad (8)$$

where  $\sigma_i$  and  $\epsilon_i$  are the initial values of the stress and strain at the beginning of the half cycle ( $\sigma_1, \epsilon_1$  for AB and  $\sigma_2, \epsilon_2$  for BC). The terms  $\sigma_0, \epsilon_0$  and  $\alpha$  are the three parameters of the R-O equation.

An iterative process of least squares curve fitting technique was applied to determine the three parameters for each half-cycle of the test data. The results of this analysis indicated that the ratio  $\sigma_0/\epsilon_0$  can be taken as the modulus of elasticity of steel E (29,000,000 psi, 20,400 kgf/mm<sup>2</sup>, 199,800 MPa). The number of parameters were thus reduced to two.

The Ramberg-Osgood model, obtained for the material used in this investigation, was generalized in terms of the yield stress of the coupons. The rules to determine the model are summarized in the following;

- 1)  $\sigma = E\epsilon$  for  $\epsilon < \epsilon_y$  (elastic region)

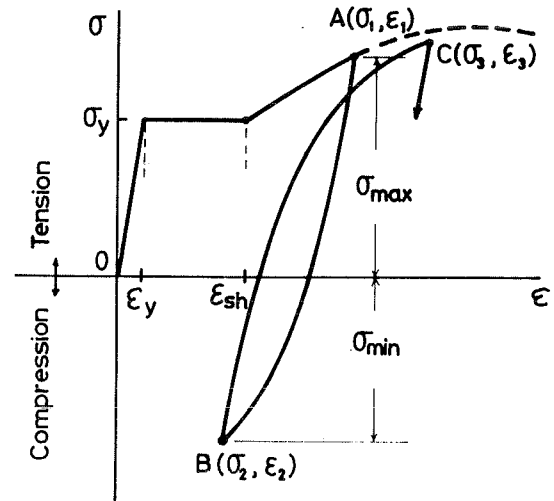


FIG.14. R-O Model by Sozen [6]



2)  $\sigma = \sigma_y$  for  $\epsilon_y < \epsilon < 4.2447\epsilon_y = \epsilon_{sh}$  (plastic plateau)

3)  $\frac{\sigma}{\epsilon_0} = \frac{\sigma}{\sigma_0} + \left(\frac{\sigma}{\sigma_0}\right)^\alpha$  for  $4.2447\epsilon_y < \epsilon$  (strain-hardening region)

before the first reversal, where  $\sigma_0 = 0.7\sigma_y$ ,  $\epsilon_0 = \sigma_0/E$ ,  $\alpha = 4.3$

4)  $\frac{\epsilon - \epsilon_1}{\epsilon_0} = \frac{\sigma - \sigma_1}{\sigma_0} + \left(\frac{\sigma - \sigma_1}{\sigma_0}\right)^\alpha$  for subsequent half cycles, where

$$\sigma_0/\epsilon_0 = E,$$

$\sigma_0 = 47,628 + 0.51723 (\sigma_{max} - \sigma_{min})$  for half-cycles starting from compression.

$\sigma_0 = 46,410 + 0.47989 (\sigma_{max} - \sigma_{min})$  for half-cycles starting from tension.

$\alpha$  can be determined from the following relations;

$\sigma = 110,000$  psi for  $\epsilon = \epsilon_1 + 0.09$  for ascending curve

$\sigma = -110,000$  psi for  $\epsilon = \epsilon_1 - 0.09$  for descending curve.

where

$\sigma_y$  = yield stress of the bar (psi)

$\epsilon_y$  = yield strain of the bar

$\sigma_{max}$  = maximum tensile stress reached prior to the half-cycle under consideration (psi)

$\sigma_{min}$  = maximum compressive stress reached prior to the half-cycle under consideration (psi)

For example, the curve AB in Fig.14 is expressed as

$$\frac{\epsilon - \epsilon_1}{\epsilon_0} = \frac{\sigma - \sigma_1}{\sigma_0} + \left(\frac{\sigma - \sigma_1}{\sigma_0}\right)^\alpha$$

where,

$$\sigma_0 = 46,410 + 0.47989\sigma_1$$

$$\epsilon_0 = \sigma_0/E$$

$\alpha$  can be determined from the condition that

$\sigma = -110,000$  psi. for  $\epsilon = \epsilon_1 - 0.09$

and the curve BC is expressed as

$$\frac{\epsilon - \epsilon_2}{\epsilon_0} = \frac{\sigma - \sigma_2}{\sigma_0} + \left(\frac{\sigma - \sigma_2}{\sigma_0}\right)^\alpha$$

where,

$$\sigma_0 = 47,628 + 0.51723 (\sigma_1 - \sigma_2)$$

$$\epsilon_0 = \sigma_0/E$$

$\alpha$  can be determined from the condition that

$\sigma = 110,000$  psi. for  $\epsilon = \epsilon_2 + 0.09$

A comparison of this Ramberg-Osgood model with a test result is shown in Fig.15.

#### Yokoo and Nakamura's Method [12]

In the foregoing analysis, it was seen that the parameters of R-O equation were given as the function of the residual plastic strain  $\epsilon_{p.m}$  in Popov's method, while they were given as the function of the maximum stress

amplitude reached prior to the half-cycle under consideration in Sozen's method. Yokoo and Nakamura's approach is similar to that of Sozen, but the significance of their study may be said to consist in the following points;

- 1) Linear regression and correlation analyses have been carried out with respect to the maximum stress amplitudes reached prior to the half-cycle under consideration, and obtained the different parameter from that of Sozen's.
- 2) The power  $\alpha$  in the R-O equation has also been regarded as dependent upon the previous maximum stress amplitudes.
- 3) A set of hysteretic  $\sigma$ - $\epsilon$  relations was proposed in the form of two R-O equations, one applicable to a small plastic strain range and the other to a moderate plastic strain range.

#### 4. DUCTILITY AND ENERGY ABSORPTION

The most essential requirement for reinforced concrete structures subject to earthquakes is to secure the sufficient ductility. In this chapter, the important factors which influence the ductility of reinforced

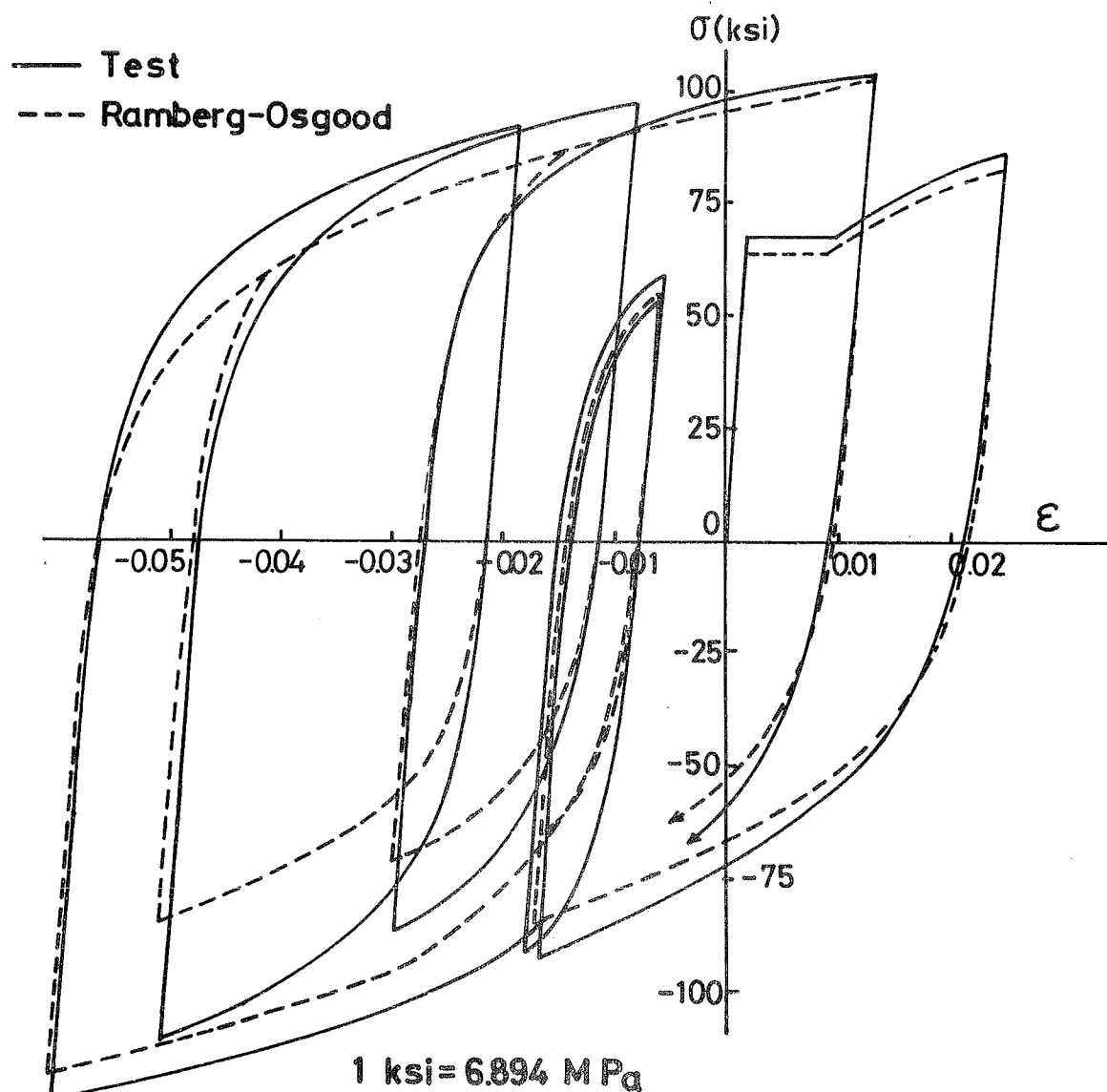


FIG.15. Comparison of Predicted and Experimental Loops [6]

concrete members such as reinforcing index, spread of plastic region, strain rate and buckling of steel bars will be discussed in association with the mechanical properties of the reinforcing steels.

#### 4.1. Influence of The Strength of Steel Bars on the Failure Modes

For reinforced concrete members (nonprestressed) subject to bending, to allow considerable inelastic rotation within a region of plastic hinging, reinforcing bars should develop sufficient plastic elongation before the local crushing of the concrete on the opposite side of the member takes place. Because of its brittleness and low tensile strength, nonprestressed concrete cracks early in the strain history and is not very effective in absorbing energy before concrete crushing. Therefore, the reinforcing steel in nonprestressed concrete receives a major portion of the energy absorption.

It has been noted [14] that optimizing the steel energy-absorption capacity involves using a low enough reinforcing index

$$\frac{(\rho - \rho')f_y}{f_c'}$$

so that the steel will yield considerably before concrete crushing on the other side of the member, but using a high enough reinforcing index so that the steel will not rupture before the concrete crushes;  $\rho$  and  $\rho'$  are the tension and compression steel percentages respectively,  $f_y$  is the steel yield strength and  $f_c'$  is the concrete compressive strength (see Fig.16).

According to the parametric study on the regular reinforced concrete beams [15] which have the properties that a) concrete with  $f_c' = 4,000$  psi (27.6 MPa) and crushing strain of 0.3 percent, b)  $\rho' > 0.5\rho$ , c) reinforcing bars are of Grade 60 ( $f_y = 60$  ksi = 414 MPa) and the balanced-design steel percentage  $\rho_b$  is computed to be 0.0285, more than 4% of steel strains can be developed before

the concrete on the other side of the member begins to crush. On the other hand, the results of reverse-loading tests on full-scale cross-shaped specimens in which 40 Grade ( $f_y = 40$  ksi = 276 MPa) and 60 Grade reinforcing steels were used [16], [17], had shown that even with a deflection ductility ratio of 5.0 induced in each specimen, the steel strains measured by attached strain gages did not exceed about 4% in any of the tests.

In this context, an upper limit on the as-furnished yield strength of the reinforcing bars is desirable. If an actual yield strength of the reinforcing bars are much higher than the specified value, the following unexpected modes of failure may take place all of which will impair the ductility of the members; a) premature crushing of concrete on the other side of the section, b) change of the failure mode from flexural to shear: the increase of yield strength of the reinforcing bars brings the increase of bending moment in the member and thus brings the greater shear and, as a result, a premature-stirrup or diagonal tension failure may occur before the moment capacity of the member is reached, c) in the actual steel products, the increase of the yield strength is usually much higher than that of tensile strength, which means that the yield ratio of steel is apt to become higher than the nominal value. The higher yield ratio will

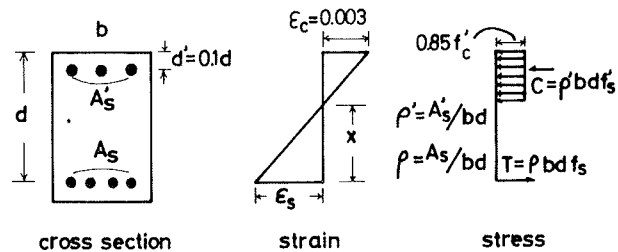


FIG.16. Calculation of Tensile-Steel  $\sigma - \epsilon$  condition

reduce the rotation capacity of the member of which some comments will be made later.

Reflecting these considerations, upper limit of the yield strength of reinforcing bars which will be used in seismic structures was specified in various specifications and codes [18][19][20][21] as, "the actual yield strength of the longitudinal reinforcements based on mill tests should not exceed the specified minimum yield strength by more than 18,000 psi (124Mpa, 12.7 kgf/mm<sup>2</sup>)". Fig.17 shows the yield strength distributions of reinforcing bars of various countries [15][22][23], which indicates the above limitation is generally met. But whether this limitation is the enough safeguard against that premature failure or not is another question.

#### 4.2. Rotation Capacity of Reinforced Concrete Members

In the reinforced concrete sections which meet the requirements described in the preceding section and thus compressive concrete of which will not crush until the longitudinal steel bars develop substantial plastic elongation, the move of the neutral axis  $x$  from the initial yield of tensile steel bars to the ultimate strength state is within the range of  $x = 0.73d \sim 0.78d$  according to the calculation on the typical member section such as shown in Fig.16, where  $d$  is the distance from the compressive extreme fibre to the tensile reinforcements. If it is assumed, for simplicity, that the neutral axis remains constant  $x = 0.75d$  during this inelastic excursion, the curvature  $\phi$  can be expressed as

$$\phi = \epsilon_s / 0.75d$$

indicating that  $\phi$  is proportional to the plastic strain of the tensile steel bars  $\epsilon_s$ . Also since it indicates that bending moment is simply decided by the  $\epsilon_s$  (or  $\sigma_s$ ), and that the maximum bending moment  $M_u$  can be expressed as  $M_u = M_y / Y$  ( $Y = \sigma_y / \sigma_T$  : the yield ratio of tensile steel bars), the moment-curvature relationship ( $M$ - $\phi$  relationship) can be depicted as shown in Fig.18(b) corresponding to the  $\sigma$ - $\epsilon$  relationship of the tensile steel bars as shown in Fig.18(a).

If  $\sigma$ - $\epsilon$  relationship has a well defined plastic plateau as shown by the solid line in Fig.18(a), the  $M$ - $\phi$  relationship can be written as

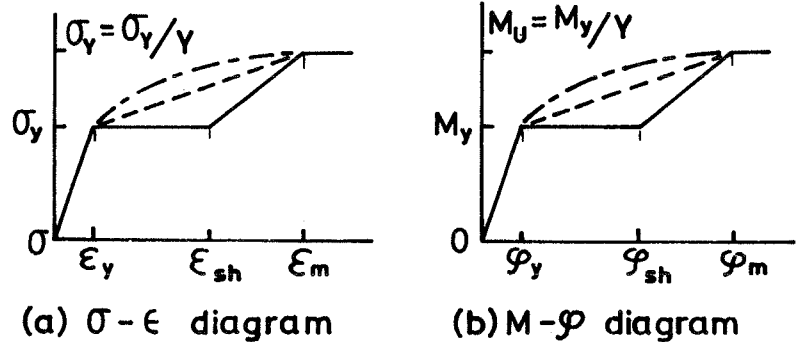
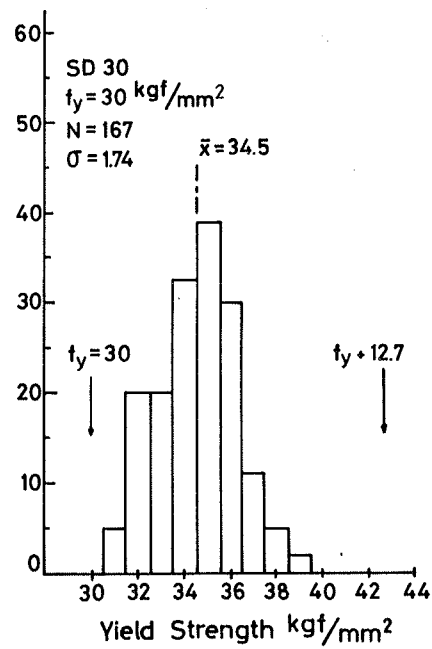
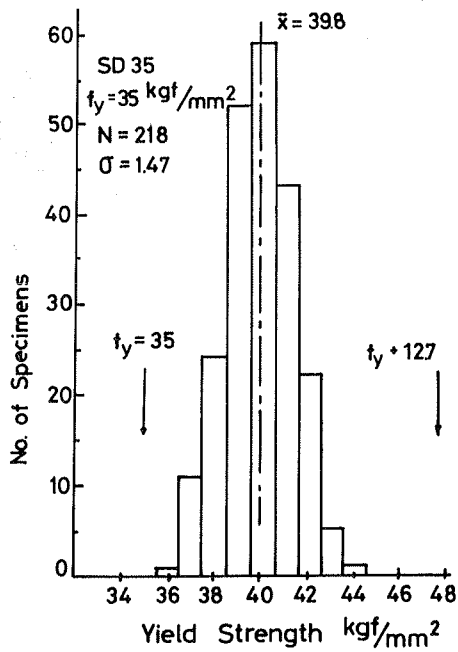


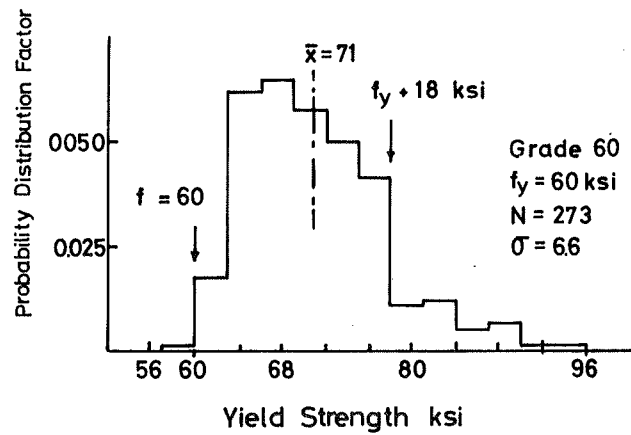
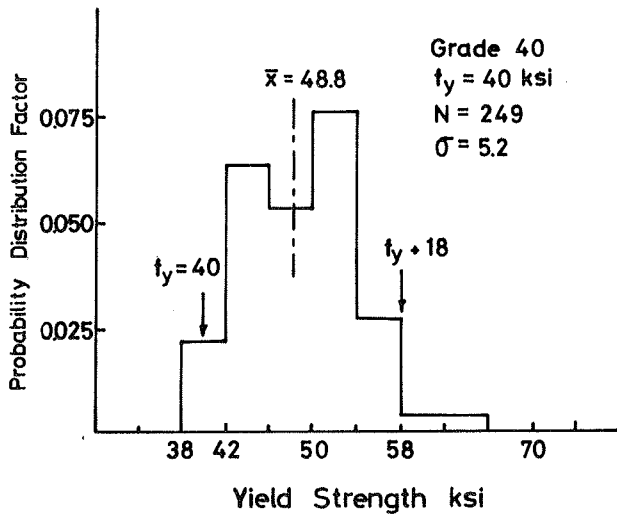
FIG.18.  $\sigma$ - $\epsilon$  Diagram and  $M$ - $\phi$  Diagram

$$\left. \begin{aligned} M &= M_y & \text{for } \phi_y \leq \phi \leq \phi_{sh} \\ M &= M_y + \frac{(1/Y - 1)M_y}{\phi_m - \phi_{sh}} (\phi - \phi_{sh}) & \phi > \phi_{sh} \end{aligned} \right\} \quad (9)$$

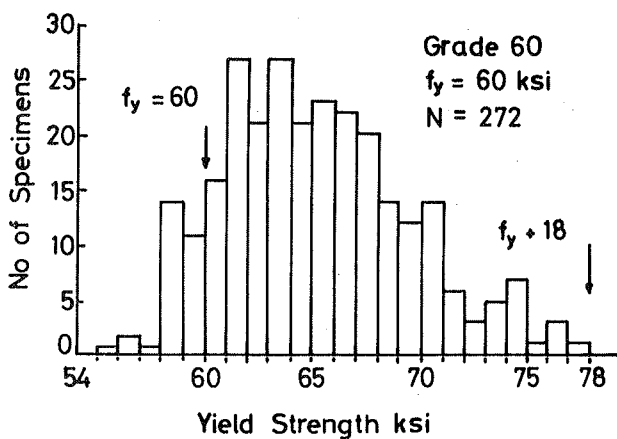
On the other hand, if the bending moment diagram of a beam of a rigid frame subjected to earthquake loading is given as shown in Fig.19 at the ultimate



JAPAN [ 22 ]



CANADA [ 23 ]



U.S.A. [ 15 ]

$$1 \text{ ksi} = 0.703 \text{ kgf/mm}^2 = 6.895 \text{ Mpa}$$

$$18 \text{ ksi} = 12.7 \text{ kgf/mm}^2$$

FIG.17. Distribution of Measured Yield Strength of Reinforcing Steel

state, and if the spread of the plastic region along the span length is denoted by  $\tau\ell$  at this ultimate stage,  $\tau$  is expressed as

$$\tau = 1 - \frac{M_y}{M_u} = 1 - Y. \quad (10)$$

Note that  $\tau$  is only the function of the yield ratio of the material and independent of the span of the beam and the moment gradient. Taking a local coordinate  $x$  from the point of initial yield A, the moment at  $x$  is expressed as

$$M = M_y + \frac{(1/Y - 1)M_y}{\tau\ell} x. \quad (11)$$

From eqs.(9) through (11), and introducing the relation of  $\tau = \epsilon/0.75d$ , the curvature  $\phi$  is expressed as

$$\phi = y'' = \frac{1}{0.75d} \left[ \frac{\epsilon_m - \epsilon_{sh}}{(1 - Y)\ell} x + \epsilon_{sh} \right].$$

Then the rotation  $\theta_1$  developed in the plastic region is

$$\theta_1 = \int_0^{\tau\ell} \phi dx = \left( \frac{\epsilon_m + \epsilon_{sh}}{1.5d} \right) (1 - Y)\ell \quad (12)$$

For defferent  $\sigma$ - $\epsilon$  relationships such as bi-linear (dashed line in Fig.18(a)) and round-house (dashed and dotted line in Fig.18(a)), the corresponding rotations can be obtained similarly as

For bi-linear  $\sigma$ - $\epsilon$  relationship:

$$\theta_2 = \left( \frac{\epsilon_m + \epsilon_y}{1.5d} \right) (1 - Y)\ell \quad (13)$$

For round-house  $\sigma$ - $\epsilon$  relationship:

$$\theta_3 = \left( \frac{\epsilon_m + \epsilon_y}{1.5\alpha d} \right) (1 - Y)\ell, \quad \alpha > 1. \quad (14)$$

From eqs.(12),(13),(14), it can be seen that a plastic plateau type of  $\sigma$ - $\epsilon$  curve is preferable to a round-house type of  $\sigma$ - $\epsilon$  curve for maximizing the plastic-hinge rotation capacity. But it should be noted that plastic plateau will disapear when the beam is subjected to cyclic or hysteretic loading due to the Bauschinger effect.

The most important is the fact that the rotation capacity is directly and heavily influenced by the yield ratio of the steel material  $Y$ . The rotation capacity will be much impaired if the yield ratio is excessively high.

In this connection, the A.T.C. of U.S.A.[20] requires that "the ratio of the actual ultimate tensile stress to the actual yield stress (the inverse of the yield ratio) should not be less than 1.25 (or  $Y$  should not larger than 0.8)", and the SEAOC [18] and the Uniform Building Code [19]

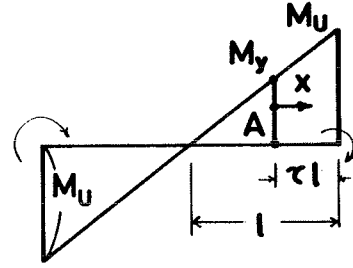


FIG.19. Moment Diagram of a Beam

of U.S.A. specify the ratio as 1.33 (0.75 in terms of Y) rather conservatively.

#### 4.3. Evaluation of Prestressed Concrete

There has been considerable discussion about the suitability of prestressed concrete members in seismic structures, but no extensive researches have been aimed at evaluating the optimum characteristics of prestressing steel for that application. Internationally, the specified minimum elongations for prestressing bars are about 4% or less, and which have been considered adequate by experts [24],[25]. It has been noted that the basic reason is that under seismic loadings the concrete member will rotate extensively without cracking or crushing and without a great increase in the steel strain, yet with a significant increase in moment. However, since the yield ratio of the prestressing bars is considerably high compared with that of regular reinforcing bars and the  $\sigma$ - $\epsilon$  curve of the prestressing bars is round-house as illustrated in Fig.1, these properties will give some adverse effects on the deformability of the prestressed concrete members especially in the severely plastified ultimate stage.

Twisted bars (Rippen Torstahl, Tentorsteel) are also have higher yield ratio, smaller percentage elongation and round-house  $\sigma$ - $\epsilon$  curve, and will give simillar disadvantage on the deformability. Because no pre-compressive strains are given in the concrete in this case, the adverse effect must be much more pronounced compared with the plastic behavior of the prestressed concrete members.

#### 4.4. Effect of The Strain Rate on The Yield Strength of Steel

To estimate the strain rate which structural members will undergo by severe earthquakes, a dynamic response analysis [26] was carried out for seven and three story office buildings and a four story school building under the conditions that;

- a) earthquake wave motions, ElCentro, NS, EW, May 1940, Taft, EW, July 1952, Hachinohe Harber, NS,EW, May 1968.
- b) Damping coefficient,  $h = 0.02$ .

The result of this study had shown the maximum response strain rate was  $\dot{\epsilon} = 0.1\text{sec}^{-1}$ .

While the results of coupon tests with various strain rates had shown that the increase of the yield stress by the comparable magnitude of strain rate is about 1.1 time that obtained from the regular coupon test with the strain rate of  $\dot{\epsilon} = 0.0002$ . Another test result [27] had shown the increase of the yield stress in the same sense is 1.16 for Grade 60 steel and 1.19 for Grade 40 steel.

Such amount of increase seems to be not substantial considering the possible scattering of the yield stress of as-furnished reinforcing bars such as shown in Fig.17.

The influence of the strain rate on the shape of the softened part under hysteretic loading is another interesting problem of which no information is available at present time.

#### 4.5. Buckling of The Longitudinal Reinforcements

As long as a steel bar is embeded in concrete, the concrete will restrain the buckling of the steel bar by serving as an elastic foundation. Though the occurence of the buckling of steel bar is possible even in such a confined state, the drop of the load carrying capacity is negligible since the concrete can prevent the excessive bending of the bar. But if a reinforced concrete section is damaged severely, concrete crushed and spalled-off, due to a severe earthquake, the longitudinal reinforcements must resist against buckling by themselves. Of course such a situation

falls in the failed category and will not be received any interest in the usual field of structural engineering, but if the longitudinal reinforcements could support the gravity load of the structure by themselves after the major quake is over, the structure may escape from the catastrophic collapse and may protect the human lives. The compression members can develop some ductility keeping their axial yield load in post-buckling stage if their effective slenderness ratio is less than about 30, and if the hoops are strong enough to provide the nodal points of the longitudinal reinforcements. The spacing of the hoops which satisfies the above condition becomes  $15d$  under the assumption that the fixed end condition is satisfied at each location of the hoop, where  $d$  is the diameter of the longitudinal steel bar.

#### REFERENCES

- [ 1] Kato,B., Aoki,H. and Yamanouchi,H., Experimental study of Structural Steel Subjected to Tensile and Compressive Cyclic Loads,Proc. 14th Japan Congress on Materials Research, March 1971.
- [ 2] Kato,B., Akiyama,H. and Yamanouchi,H., Predictable Properties of Material under Incremental Cyclic Loading, Symposium on Resistance and Ultimate Deformability of Structures Acted on by Well-Defined Repeated Loads, IABSE, Lisbon 1973.
- [ 3] Yamanouchi,H., Hysteretic Behavior of Steel Materials under Repeated and Reversed Loadings, Dr.-Eng. Dissertation, The Univ. of Tokyo, 1973 (in Japanese).
- [ 4] Dafalias,Yok. and Popov,E.P., A model of Nonlinearly Hardening Materials for Complex Loadings, Acta Mechanica, Vol.21, 1975.
- [ 5] Petersson,H. and Popov,E.P., Constitutive Relations for Generalized loadings, J.Engineering Division Journal, ASCE., August 1977.
- [ 6] Aktan,A.E., Karlsson,B.I. and Sozen,M.A., Stress-Strain Relationships of Reinforcing Bars Subjected to Large Strain Reversals, Civil Engineering Studies, Structural Research Series No.397, Univ. of Illinois, 1973.
- [ 7] Ramberg,R. and Osgood,W.R., Description of Stress-Strain Curve by Three Parameters, Technical Note.902, NACA july 1943.
- [ 8] Masing,G., Eigenspannungen und Verfestigung beim Messing, Proc. of the 2nd International Congress for Applied Mechanics, Zurich, Sept. 1926.
- [ 9] Morrow,J., Cyclic Plastic Strain Ennergy and Fatigue of Metals, Special Technical Publication 378, ASTM, 1965.
- [10] Ma,S.Y., Bertero,V.V. and Popov,E.P., Experimental and Analytical Studies on the Hysteretic Behavior of Reinforced Concrete Rectangular and T-Beams, Report No.EERC 76-2, Earthquake Engineering Research Center, Univ. of California, Berkeley, May 1976.
- [11] Popov,E.P., Bertero,V.V. and Ma,S.M., Model of Cyclic Inelastic Flexural Behavior of Reinforced Concrete Members, Proc. 4th International Conference on Structural Mechanics in Reactor Technology (SMIRT), August 1977, Paper K 6/h.
- [12] Yokoo,Y. and Nakamura,T., Nonstationary Hysteretic Uniaxial Stress-Strain Relations of A Wide-Flange Steel, Trans. of Architectural Institute of Japan, No.260, Oct. 1977.
- [13] Kent,D.C. and Park,R., Cyclic load Behavior of Reinforcing Steel, Strain, vol.9, No.3, July 1973.
- [14] ACI Committee Report 439, Effect of Steel strength and Reinforcement Ratio on the Mode of Failure and Strain Energy Capacity of Reinforced Concrete Beams, ACI Journal, March 1969.
- [15] McDermott,J.F., Mechanical Characteristics and Performance of Reinforcing Steel under Seismic Conditions, Workshop on Earthquake-Resistant R/C Building Construction, Univ. of California, Berkeley,



july 1977.

- [16] Hanson, N.W. and Conner, H.W., Seismic Resistance of Reinforced Concrete Beam-Column Joints, Paper No. 5537, Journal of the STD, Proc. ASCE. Oct. 1967.
- [17] Hanson, N.W., Seismic Resistance of Concrete Frames with Grade 60 Reinforcement, Paper No. 8180, Journal of the STD, Proc. ASCE, June 1971.
- [18] Recommended lateral Force Requirements and Commentary, Seismology Committee, Structural Engineers Association of California (SEAOC), 1975.
- [19] Uniform Building Code, International Conference of Building Officials, 1976.
- [20] Tentative Provisions for the Development of Seismic Regulations for Buildings, Applied Technology Council (ATC), USA, June 1978.
- [21] Code for the Design of Concrete Structures for Buildings, CSA Standard A23.3-1973 including Supplement No. 1, Canadian Standards Association 1973.
- [22] Nishimaki, J., 1978, Nippon Steel Co., Private Communication to Kato.
- [23] Uzumeri, S.M., Otani, S. and Collins, M.P., An Overview of the State-of-the-Art in Earthquake Resistant Concrete Building Construction in Canada, Univ. of Toronto, Dept. of Civil Engineering, ISSN 0316-7968, May 1977.
- [24] Lin, T.Y., Design of Prestressed Concrete Buildings for Earthquake Resistance, Journal of the Prestressed Concrete Institute, Dec. 1964.
- [25] Zavries, K.S., The Design and Construction of Prestressed Concrete Structures for Earthquake Zones, -Designs and Standards, Report Presented at the F.I.P. Symposium on Seismic Structures, Tbilisi, 1972, London.
- [26] Japan Centre of Testing Materials for Buildings, Research Report on the Structural Safety, March 1978 (in Japanese).
- [27] ACI, Committee Report 439, Journal of ACI, vol. 66, No. 3, March 1967.

#### ACKNOWLEDGEMENT

The author acknowledges with gratitude the assistance of Miss M. Nakahara who prepared a number of drawings used.



THEME I b

MECHANICAL PROPERTIES OF CONCRETE UNDER LOAD CYCLES  
IDEALIZING SEISMIC ACTIONS

PROPRIETES MECANIKES DU BETON SOUS CYCLES DE CHARGE REPRESENTATIFS DES ACTIONS SISMQUES

Reporter  
Rapporteur

Hiroyuki AOYAMA  
University of Tokyo  
Tokyo, Japan



MECHANICAL PROPERTIES OF CONCRETE UNDER LOAD CYCLES  
IDEALIZING SEISMIC ACTIONS

PROPRIETES MECANQUES DU BETON SOUS CYCLES DE CHARGE  
REPRESENTATIFS DES ACTIONS SISMQUES

HiroYuki AOYAMA  
University of Tokyo  
Tokyo, Japan

Hiroshi NOGUCHI  
Chiba University  
Chiba, Japan

SUMMARY

The state-of-the-art of the uniaxial cyclic loading tests and multi-axial loading tests of concrete is reported. Method of testing, loading history, envelope curve, unloading and reloading curves are reviewed for concrete under uniaxial cyclic loading, and the proposed analytical models are summarized and compared with tests. Studies on the strength, deformation and failure criterion of concrete under multi-axial stresses, including some multi-axial cyclic loading tests, are reviewed and the proposed analytical models are summarized.

RESUME

On présente l'état des connaissances sur le comportement du béton soumis à des cycles de charge uniaxiale et à des charges multiaxiales. Les méthodes d'essais, les modalités de mise en charge, les courbes enveloppes, ainsi que celles de décharge et de recharge, sont décrites en comparant les résultats expérimentaux avec les modèles théoriques disponibles. Les études théoriques et expérimentales sur la résistance, la déformabilité et les critères de rupture du béton en état de contrainte multiaxiale, y compris quelques essais avec cycles de charge multiaxiale, sont aussi présentés.

PART I UNIAXIAL CYCLIC LOADING TESTS

1. Method of Testing

Methods to measure monotonic or cyclic stress-strain relation of concrete including falling branch can be classified into the following five groups.

- (1) Use of regular testing machine, mostly applied to low-strength concrete or small-size specimens (e.g. Hamada, 1951; Kokusho, 1966).
- (2) Use of elastic body such as PC bars, disk springs, or steel beams in parallel with concrete specimen to compensate for the energy release from falling branch (e.g. Blanks, 1949; Aoyama, 1967; Sargin, 1971; Watanabe, 1971; Muguruma, 1973; Okushima, 1974; Suzuki, 1977).
- (3) Eccentric compression tests (e.g. Hognestad, 1951; Rüsçh, 1955; Smith, 1955; Morita, 1971).
- (4) Use of hydraulic servo-control or micro-control stiff testing machine (e.g. Rüsçh, 1960; Barnard, 1964; Nakano, 1969; Hiramatsu, 1975; Koyanagi, 1975).
- (5) Use of mechanically controlled stiff testing machine (e.g. Tanigawa, 1977).

Previous cyclic loading tests have been conducted using methods (1), (2), (4) and (5). Recent trend is to use methods (4) and (5) more frequently, in addition to the persistent use of the simple and inexpensive method (2).

## 2. Loading History

Table 1 summarizes the patterns of loading history in the previous studies involving cyclic loading.

## 3. Envelope Curve

### 3.1. Relation to Monotonic Loading

Envelope curve of the stress-strain relation is defined as a curve connecting the starting points of unloading curves as well as ends of reloading curves. Whether a unique envelope curve exists, and whether such an envelope curve coincides with the monotonic stress-strain curve, were the problems which have attracted attention of many researchers, leading to an almost unanimously affirmative conclusion. Sinha (1964), Horishima (1966), Yamada (1967, 1976), Karsan (1969), Muguruma (1970), Okada (1972), Tanigawa (1976, 1978) admitted that a unique envelope curve was able to be defined, and that it coincided with the monotonic curve, within the data scattering of the falling branch, no matter what loading history was applied within that envelope curve.

### 3.2. Equations for Envelope Curve

The envelope curve, or monotonic stress-strain curve, consists of three parts as shown in Fig. 1; initial linear part, the second part of gradually reducing stiffness up to maximum stress  $\sigma_0$  and associated strain  $\epsilon_0$ , and the third part of gradually decreasing stress, usually referred to as the falling branch, terminated rather arbitrarily by the maximum usable strain  $\epsilon_u$ .

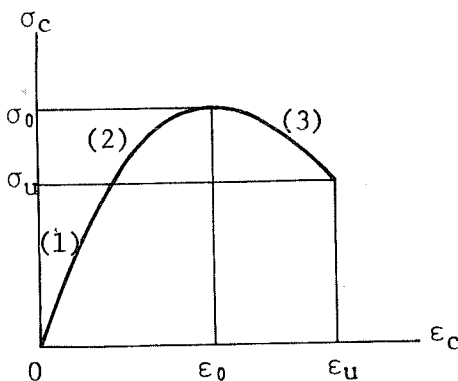


Fig. 1 Stress-Strain Curve of Concrete

Strain-softening characteristics of Fig. 1 is due, first, to bond cracks at the surface of aggregate to the mortar caused by the different stiffness of aggregate and mortar, and second, to micro-cracks in the mortar caused by stress concentration near the bond cracks. Recently efforts have been made by Buyukozturk (1971), Shiire (1972), Kosaka (1974) and Alam (1977), to derive the stress-

strain curve theoretically, idealizing the above-mentioned bond phenomena between aggregate and mortar. However, it will be some time before this kind of microscopic approach succeeds in deriving complete stress-strain relation.

On the other hand, many mathematical expressions were proposed to simulate observed envelope curve. Following the Popovics's summary (1970) and more recent researchers, these expressions are shown in two Tables. Table 2 is for the ascending branch only. Table 3 shows expressions for complete curve, including the falling branch.

Table 1. Loading History

U:Upper, L:Lower

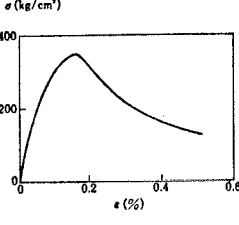
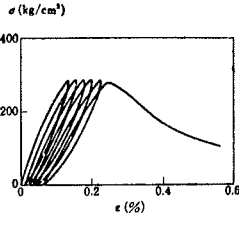
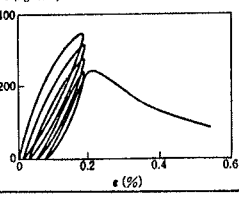
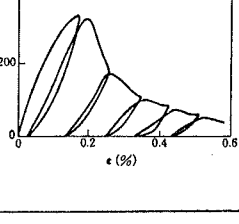
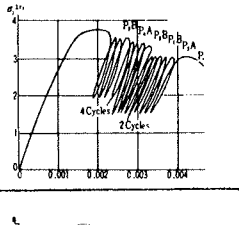
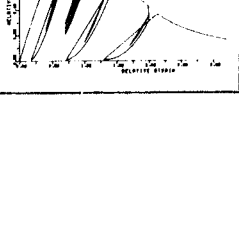
Loading	Loading History	Researchers	Year	Loading Level	Loading Rate
Monotonic		Sinha Horishima Yamada Karsan Okamoto Okada Ogawa Bresler Koyanagi Tanigawa Wakabayashi	'64 '66 '67,76 '69 '71 '72 '75 '75 '75 '77,78 '78		30μϵ/sec 2-3kg/cm²/sec 30sec/1cycle 1000-2000μϵ/min  1-25mm/min  10-100000μϵ/sec  2-3kg/cm²/sec 20-100000μϵ/sec
Sinusoidal		Ban	'60	U.0.6-0.9σ <sub>0</sub> L.0	1.2cycle/sec
Constant stress cyclic		Karsan Yamada Okamoto Ogawa  Bresler  Tanigawa  Yamada	'69 '67 '71 '75  '75  '77,78  '76	  U.0.90σ <sub>0</sub> , L.0 U.1/3σ <sub>0</sub> , 2/3σ <sub>0</sub> L.1kg/cm²  U.0.5-0.9σ <sub>0</sub> L.0.1σ <sub>0</sub> U.0.8, 0.85, 0.9 0.95σ <sub>0</sub> , L.0 U.0.8, 0.9σ <sub>0</sub>	1000-2000μϵ/min   0.53-215 kg/cm²/sec 20000μϵ/sec  2-3kg/cm²/sec  30sec/1cycle
Constant strain cyclic		Yamada  Okamoto Ogawa  Tanigawa	'67  '71 '75  '77,78	2600, 2800, 3500μ 1.0, 1.5, 2.0ε <sub>0</sub> U.1/3σ <sub>0</sub> , 2/3σ <sub>0</sub> L.1kg/cm²	  0.53-215kg/cm²
Gradually increasing strain cyclic (constant increment)		Sinha Horishima Yamada Karsan Okamoto  Okada Tanigawa Yamada	'64 '66 '67 '69 '71  '72 '77,78 '76	800μ×10cycles 300, 1000μ  1.0, 1.5, 2.0, 3.0ε <sub>0</sub>  250μ 200μ	2-3kg/cm²/sec  1000-2000μϵ/min    2-3kg/cm²/sec 30sec/1cycle
Ditto (variable increment)		Karsan Koyanagi Wakabayashi	'69 '75 '78		1000-2000μϵ/min  50-50000μϵ/sec
Ditto (shake down)		Sinha	'64	minimum stress as variable in falling branch	
Random cyclic		Tanigawa	'78		

Table 2. Equations Suggested for Uniaxial Compression Stress-Strain Curve for Concrete (for Ascending Branch Only)

Author	Equation	Comment
Bach	$\sigma = A\epsilon^n$	Implies E infinite
Saenz	$\sigma = E\epsilon [1 + (3E_0/E - 2)(\epsilon/\epsilon_0) + (1 - 2E_0/E)(\epsilon/\epsilon_0)^2]$	
Saenz	$\sigma = E\epsilon / [1 + (E/E_0 - 2)(\epsilon/\epsilon_0)^2 + (\epsilon/\epsilon_0)^2]$	
Sturman	$\sigma = A\epsilon(1 + B\epsilon^{n-1})$	Implies $E/E_0 = n/(n-1)$
Desai	$\sigma = E\epsilon / [A + (\epsilon/\epsilon_0)^2]$	Implies $E/E_0 = 2$
Terzaghi	$\epsilon = \sigma/E + A\sigma^n$	
Ros	$\epsilon = \sigma/E + A\sigma/(B - \sigma)$	
Kritz and Lee	$\sigma^2 + A\epsilon^2 + B\sigma\epsilon + C\sigma + D\epsilon = 0$	In flexure
Ban	$\sigma = A\epsilon^3 + B\epsilon^2 + C\epsilon$	
Hamada	$1 - \eta = (1 - \xi)^k$	$\eta = \sigma/\sigma_0, \xi = \epsilon/\epsilon_0$

The falling branch plays an important role when the strain gradient exists in the section. The fact that concrete strain at the compressive surface of a flexural member could exceed the strain associated with the maximum stress,  $\epsilon_0$ , was discovered as early as 1904 by A.N. Talbot, and was confirmed by O. Baumann in 1934 (Hognestad, 1951). Any theory dealing with flexure of reinforced concrete members had to incorporate stress-strain relation including the falling branch. For this reason much efforts have been made in the loading methods of concrete cylinders under uniaxial compression into the falling branch, as mentioned before.

Empirical expressions were also developed, as shown in Table 3. Among them, Umemura's e-function (1951) was a pioneering work with emphasis in the simulation of falling branch, which was measured by Hamada (1951).

### 3.3. Effect of Concrete Strength, Strain Rate, and End Restraint

Shape of normalized stress-strain curve varies according to the compressive strength of concrete. Generally speaking, high-strength concrete results in a steeper curve, both in the ascending and descending branches. This effect was incorporated in the works by Popovics (1971), Sargin (1971), and Cohn (1972). Okushima (1974) confirmed Popovics's theory for his parameter  $\underline{n}$  that it increases linearly with concrete strength, and further investigated the effect of strain rate and end-plate restraint. Okushima pointed out that the behavior in the falling branch was not affected by variation of strain rate between 10 and 1000 sec/10<sup>-3</sup>, but that the negative gradient in the falling branch increased as the end-surface restraint of the concrete cylinder was removed.

Among recent studies utilizing high-rigidity loading equipments, Suzuki (1978) compared several available expressions including his own



Table 3. Equations Suggested for Complete Uniaxial Compression Stress-Strain Curve for Concrete

Author	Equation	Comment
Umemura(1951)	$\eta = K(e^{-\alpha\xi} - e^{-\beta\xi})$	
Hognestad(1951)	$\sigma = \sigma_0(2\xi - \xi^2) : 0 \leq \xi \leq 1$ falling branch is linear	$\sigma_0 = 0.85f'_c, \epsilon_0 = 2\sigma_0/E$ $\sigma_u = 0.85\sigma_0, \epsilon_u = -0.38\%$
Smith and Young (1955)	$\sigma = E_c \cdot e \cdot e^{-(\epsilon/\epsilon_0)}$	Implies $E/E_0 = e$
Tulin(1964)	$\sigma = E\epsilon / [A + (\epsilon/\epsilon_0)^n]$	Implies $E/E_0 = A+1$
Alexander(1965)	$\sigma = A\epsilon / [(\epsilon+B)^2 + C] - D\epsilon$	
Shah(1966)	$\sigma = E\epsilon \cdot e^{-[(E\epsilon^{-2})/A]^m}$	
Kokusho(1966)	$\eta = \sin(\pi/2)(A \xi-1  + B\xi + C) : 0 \leq \xi < 2$ $\eta = D\xi + E : 2 \leq \xi \leq 4$	Artificial lightweight concrete
CEB/FIP(1970)	$\sigma = \sigma_0(2\xi - \xi^2) : 0 \leq \epsilon \leq \epsilon_0$	
BSI	$\sigma = \sigma_0 : \epsilon_0 \leq \epsilon \leq \epsilon_w$	
Popovics(1971)	$\eta = \xi n / [(n-1) + \xi^n]$ $n = (0.57 \times 10^{-2} \times f'_c) + 1$ $\epsilon_0 = 1.95 \times 10^{-4} \times k \times 4 \sqrt{f'_c}$ $n = 1 + 0.0125(f'_c - 100)$	Include compressive strength as parameter $k = 2.2$ : normal concrete $f'_c$ (kg/cm <sup>2</sup> )
Okushima(1974)	$\sigma = k_3 f'_c [A\xi + (D-1)\xi^2] / [1 + (A-2)\xi + D\xi^2]$	$k_3$ : Maximum stress ratio
Sargin(1971)	$A = E_c \epsilon_0 / k_3 f'_c$	$D$ : Control slope of falling branch
(Wang 1978)		
Kent(1971)	$\sigma = \sigma_0(2\xi - \xi^2) : 0 \leq \epsilon < \epsilon_0$ $\sigma = \sigma_0 [1 - Z(\epsilon - \epsilon_0)] : \epsilon_0 \leq \epsilon \leq \epsilon_{20c}$ $Z = 0.5 / (\epsilon_{50c} - \epsilon_0)$ $\epsilon_{50c} = (0.21 + 0.002f'_c) / (f'_c - 70) + (3/4)\rho'' \sqrt{b''/S}$	Confined concrete $f'_c$ (kg/cm <sup>2</sup> )
Cohn(1972)	$\sigma = k f'_c [A\xi + (D-1)\xi^2] / [1 + (A-2)\xi + D\xi^2]$ $A = E\epsilon_0 / k f'_c$	$E, k, \epsilon_0, D$ are given according to concrete strength
Muguruma(1976)	$\sigma = E\epsilon + (f'_c - E\epsilon_0)\xi^2 : 0 \leq \xi \leq 1$ $\sigma = [(f'_c - 100) / (\epsilon'_{cu} - 0.004)]\epsilon$ $+ (100\epsilon'_{cu} + 0.004f'_c) / (\epsilon'_{cu} - 0.004) : 1 \leq \xi \leq 4$ $\epsilon'_{cu} = (0.0013f'_c + 1.299) \times 10^{-3}$	In flexure $f'_c$ (kg/cm <sup>2</sup> )
Suzuki(1978)	$\eta = 2\xi - \xi^2 : 0 \leq \xi \leq 1, \eta = -\tan\theta \cdot \xi + (\tan\theta + 1) : 1 \leq \xi$ $\epsilon_0 = 0.468 \sqrt{f'_c} \times 10^{-3}, \tan\theta = 1.33 \times 10^{-3} f'_c + 0.1002$	$f'_c$ (kg/cm <sup>2</sup> )

with his test data, and pointed out that the strain associated with the maximum stress and the negative slope must be expressed as the function of concrete strength. Kiyama (1975) studied the effect of the type of aggregate (rock or lightweight).

Muguruma (1976) redefined the ultimate strain  $\epsilon_{cu}$  to be the strain at which stress block coefficient  $k_1 k_2$  becomes maximum, and proposed empirical expression to cover concrete strength ranging from 150 to 700 kg/cm<sup>2</sup>, as shown in Table 3. According to his study, ultimate strain increased slightly with the increase of concrete strength.

### 3.4. Effect of Strain Gradient

Morita (1971) made eccentric compression tests and obtained stress-strain curves under strain gradient by a method similar to Hognestad's one. Comparing these with concentric compression tests he concluded that they coincided fairly well except that eccentric tests show greater strength for high-strength concrete.

Suzuki (1976) criticized the prevalent eccentric test method (after Hognestad) for not representing the variation of neutral axis depth due to discrete cracking, and proposed beam-type tests. Comparing these with simple beam tests he pointed out the expansion of failure zone which is directly related to ultimate rotation capacity. He concluded that the falling branch of the apparent stress-strain curve within the failure zone had more flat descending slope.

### 3.5. Effect of Confinement

Effect of confinement by hoops or spirals was summarized by Sargin in 1971, by Park in 1975, and by Bertero in 1977. They reviewed works by King (1946), Chan (1955), Blume (1961), Bresler (1961), Szulczynski (1961), Rüsch (1963), Baker (1964), Pfister (1964), Roy (1964), Soliman (1967), Sargin (1971), Kent (1971), Uzumeri (1976) and Vallenias (1977).

Not very much works are found on the effect of strain rate and cyclic loading on confined concrete. Bresler (1975) made cyclic loading tests of normal and lightweight concrete with spirals under strain rate of  $20,000 \times 10^{-6}$ /sec, and indicated that confinement substantially improves the deformability of all concrete, and effectiveness of confinement in improving strength is much greater for normal concrete than lightweight one. Tanigawa (1977) tested normal and lightweight concrete prism with rectangular hoops under monotonic and different loading histories. He pointed out that effectiveness of hoops is much greater in improving ductility than strength, and that an envelope curve under gradually increasing cyclic loading coincides with the monotonic stress-strain curve for the strain below  $3000 - 4000 \times 10^{-6}$ , but lies a little lower than the monotonic stress-strain curve for large strain, indicating that the deterioration by cyclic loading is observed.

## 4. Unloading and Reloading Curves

### 4.1. Review of Test Results

A pioneer in testing concrete under cyclic load, Ban (1960) made sinusoidal loading test at the strain rate roughly corresponding to seismic

excitation to the building. Unloading curves in his tests were concave from the unloading point, and had very flat slope in the small stress range. Sinha (1964) showed that the family of unloading curves from various unloading points could be represented by quadratic expressions.

According to Horishima (1966), relation between unloading strain and residual strain was greatly affected by concrete strength. Stronger concrete had less residual strain, particularly for unloading strain near the maximum stress point. He proposed this relation separately for high-strength and regular strength concrete. Karsan (1969) pointed out that residual (plastic) strain was a principal parameter to determine shape of unloading curve.

Ban's work in 1960 showed reloading curves to change from convex to concave with respect to stress axis, more conspicuously as unloading stress increases. He also showed that conspicuous concave indicates a notice of approaching failure, and that cyclic failure is more likely to occur for unloading strain greater than  $1000 \times 10^{-6}$ .

Sinha (1964) expressed the observed pattern of reloading curves by a family of straight lines converging to a point. He also defined shake-down and incremental deformation; the former is for residual strain to converge to a constant, while the latter is literally ever-increasing deformation leading to a collapse. A locus of intersection of unloading and reloading curves was defined as "shake-down limit," which is dependent to the minimum stress in the cyclic loading; for complete unloading, the shake-down limit is closer to the envelope curve, whereas for partial unloading, the limit occurs at a lower value of stress.

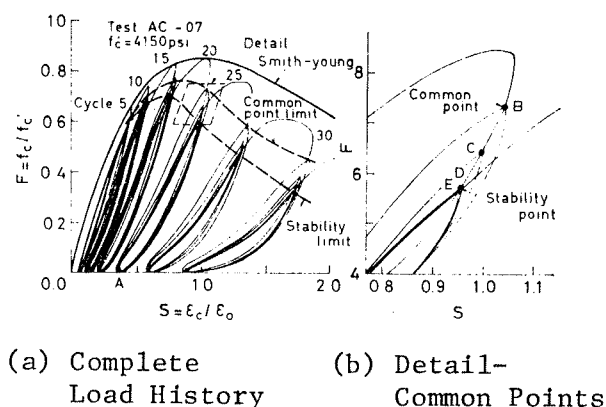


Fig. 2 Variation of Common Points. Karsan (1969)

Horishima's findings (1966) generally followed those by Ban and Sinha. However Karsan (1969) made a new definition of "common point," to be the intersection of unloading and reloading curves (Fig.2), and pointed out that this point is not affected by the minimum stress, which does not confirm to Sinha's observation. For cycling within common point up to the first unloading curve as shown in Fig.2, the maximum stress decreases and reaches to a convergence which he called the "stability limit."

Muguruma (1970) reviewed the studies on the concrete subjected to the repeated overload, and compared the shake-down limit and common point with the critical point for microcrack increase or fatigue limit, as shown in Fig.3. Shake-down limit under constant stress cycling lies between the envelope curve and common point, and forms the upper bound of critical load, indicating that the microcracking has negligible effect on the deformation of concrete under the repeated overload. This was also shown by Shah's test (1966). Further, the fatigue limit lies lower than shake-down limit and critical load, and corresponds to the upper bound of stability limit.

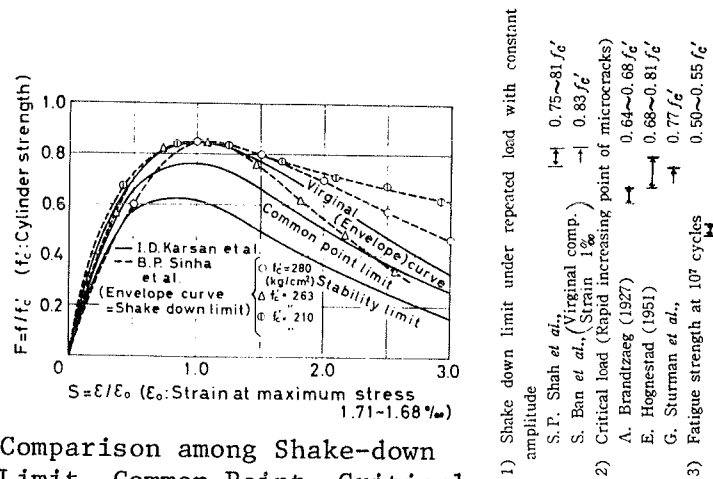


Fig. 3 Comparison among Shake-down Limit, Common Point, Critical Load and Fatigue Strength of Concrete. Muguruma (1970)

#### 4.2. Equations for Unloading and Reloading Curves

Table 4 contains proposed equations for uniaxial unloading and reloading stress-strain curves for concrete.

#### 4.3. Effect of Strain Rate

Bresler (1975) made loading tests under wide range of strain rate, namely, monotonic loading under strain rate from  $10 \times 10^{-6}/\text{sec}$  to  $100,000 \times 10^{-6}/\text{sec}$ , and cyclic loading under strain rate of  $20,000 \times 10^{-6}/\text{sec}$ , and pointed out that cyclic loading at maximum stress below one half the dynamic monotonic strength does not produce any change, while cyclic loading at maximum stress exceeding 85% of dynamic strength produces considerable strength and stiffness reduction, and accumulation of plastic strain.

Ogawa (1975) made constant strain and constant stress tests using hydraulic actuator, and showed the followings. The hysteresis loop under cyclic load below one-thirds the compressive strength is almost linear without strength reduction, while the constant stress cyclic load at two-thirds the compressive strength produces hysteretic loop of thin J shape with remarkable decrease in equivalent elastic modulus along with the number of cycles. Wakabayashi (1978) also made the tests under four different strain rates ranging from  $20 \times 10^{-6}/\text{sec}$  to  $100,000 \times 10^{-6}/\text{sec}$ , and observed similar results as above, but he did not observe conspicuous effect of strain rate.

Tanigawa (1978) tested normal and lightweight concrete under different loading histories, and obtained empirical expressions between Karsan's common point strain and residual strain, variation of upper bound stress under constant strain loading or that of upper bound strain under constant stress loading, S-N curve under constant stress loading (ref. 4.2).

#### 4.4. Effect of Confinement

The change of shape of unloading and reloading curves for confined concrete has only been studied very recently, and such studies are few in number. Therefore researchers assume that unloading and reloading curves for confined concrete is represented in the same way as plain concrete.

Table 4 - 1. Equations Suggested for Uniaxial Unloading and Reloading Stress-Strain Curves for Concrete

Researchers	Envelope Curve	Unloading Curve	Reloading Curve	Comment
Sinha (1964)	Polynomial $Q_1\sigma^2 + Q_2\sigma + Q_3 = 0$ $Q_1 = 1 + E\epsilon_e + G\epsilon_e^2$ $Q_2 = C + B_1\epsilon_e + F\epsilon_e^2$ $Q_3 = D\epsilon_e + A_1\epsilon_e^2$ $\epsilon_e = \epsilon / (1 - \alpha\epsilon)$ $\epsilon$ : strain under monotonic loading	Second order curves $\sigma + H = (J/X)(\epsilon - X)^2$ $X$ : parameter	Converging straight lines $\sigma = K + Y(\epsilon + L)$ $Y$ : parameter	
Horishima (1966)	Polynomial Normal concrete (NC) $\eta = 0.4\xi^3 - 1.8\xi^2 + 2.4\xi : 0 \leq \xi \leq 2$ $\eta = -0.25\xi + 1.3 : 2 < \xi$ High-strength concrete (HC) $\eta = -0.5\xi^2 + 1.5\xi : 0 \leq \xi \leq 1$	Second order curves $\eta = (\xi - \xi_0)[A(\xi - \xi_a) + \eta_a / (\xi_a - \xi_0)]$ $\eta_a$ : stress ratio at unloading point $\xi_a$ : strain ratio at unloading point $\xi_0$ : residual strain ratio NC: $\xi_0 = 0.18\xi_a^2$ A = $0.225\xi_a^2 - 1.225\xi_a + 1.85$ HC: $\xi_0 = 0.05\xi_a^2$ A = $-0.44\xi_a + 0.7$	Converging straight lines $\eta = [\beta / (\alpha + \xi_0)](\xi + \alpha) - \beta$ NC: $\alpha = 0.3, \beta = 0.57$ HC: $\alpha = 0.12, \beta = 0.17$	
Karsan (1969)	e-function $\eta = 0.85\xi_e(1 - \xi)$	Second degree parabola curves passing through three points: $(\eta_E, \xi_E)$ : unloading point on envelope curve $(\eta_C, \xi_C)$ : common point $(\eta_p, 0)$ : plastic strain point	Second degree parabola curves passing through three points: $(\eta_p, 0)$ , $(\eta_C, \xi_C)$ , $(\eta_E, \xi_E)$ : point at which reloading curve or its extension reaches envelope curve	Common points: $\eta_C = \beta[\xi_C / (0.315 + 0.77\beta)]$ $\times_e \{1 - [\xi / (0.315 + 0.77\beta)]\}$ $\beta = 0.76$ : common point limit $\beta = 0.63$ : stability limit $\xi_p = (1.76 - \beta)(0.160\xi_C^2 + 0.133\xi_C) : 0.63 \leq \beta \leq 0.76$ loading: $\xi_p = 0.093\xi_E^2 + 0.91\xi_E$ unloading: $\xi_p = 0.145\xi_E^2 + 0.13\xi_E$

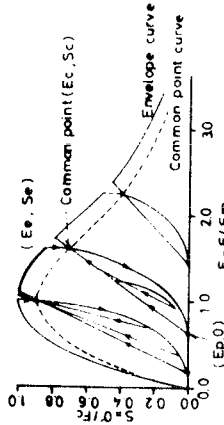
Table 4 - 2. Equations Suggested for Uniaxial Unloading and Reloading Stress-Strain Curves for Concrete

Researchers	Envelope Curve	Unloading Curve	Reloading Curve	Comment
Blakeley (1973)	Ref. Table 3 Kent (1971)			$F_c = 0.8 - [(\epsilon_{cm} - \epsilon_0) / (\epsilon_{20c} - \epsilon_0)] \geq 0.1$
Aoyama (1973)	$0 \leq \epsilon \leq \epsilon_0$ : $(\sigma_0 - \sigma) / \sigma_0 = [(\epsilon_0 - \epsilon) / \epsilon_0]^\alpha$ $\alpha = E\epsilon_0 / \sigma_0$ $\epsilon_0 < \epsilon$ : straight line passing through two points, $(\sigma_0, \epsilon_0)$ , $(0.7\sigma_0, \epsilon_u)$ , $\epsilon_u = 4000 \times 10^{-6}$			$R(\sigma_r, \epsilon_r), \epsilon_r = \sigma_0 / E$ $\epsilon_p \geq \epsilon_r$ : reloading from $(0, \epsilon_y)$ ; $\epsilon_y = (\epsilon_p + 2\epsilon_r) / 3$ to $(\epsilon_p, \sigma_p)$ $\epsilon_p < \epsilon_r$ : $\epsilon_{MIN} > \epsilon_{cr}$ : from $(0, \epsilon_p)$ to $(\sigma_p, \epsilon_p)$ , $\epsilon_{MIN} < \epsilon_{cr}$ : from $(0, \epsilon_y)$ to R when $\alpha = 2, \epsilon_{cr} = -0.33\sigma_0 / E$
Omote (1974)	$0 \leq \xi \leq 1$ : $\eta = 2\xi - \xi^2$ $1 \leq \xi \leq \xi_u$ : $\xi_u = \epsilon_u / \epsilon_0$ Umemura's e-function $\eta = K(e^{-\alpha\xi} - e^{-\beta\xi})$ $K = 6.75, \alpha = 0.812, \beta = 1.218$ $\xi_u \leq \xi$ : $\eta = 0.2$			Model under biaxial cyclic stresses using simplified Karsan's model as principal stress-equivalent uniaxial strain relation.
Darwin (1974)	Ascending branch: Saenz's equation (ref. Table 3), Falling branch: straight line passing through two points, $(\sigma_{ic}, \epsilon_{ic}), (0.2\sigma_0, 4\epsilon_0)$ $\sigma_{ic}$ : strength under biaxial stress			

Table 4 - 3. Equations Suggested for Uniaxial Unloading and Reloading Stress-Strain Curves for Concrete

Researchers	Envelope Curve	Unloading Curve	Reloading Curve	Comment
Kokusho (1975)	Umemura's e-function $\eta = K(e^{-\alpha\xi} - e^{-\beta\xi})$ $K=6.75, \alpha=0.812, \beta=1.218$	$\sigma = (\epsilon - \epsilon_p) [A(\epsilon - \epsilon_p) + \sigma_a / (\epsilon_a - \epsilon_p)]$ $\epsilon = 0.338\epsilon_a^2 / \epsilon_0$ $A = [\alpha_c E - \sigma_a / (\epsilon_a - \epsilon_p)]$ $\alpha = 1.2$		
Okamoto (1976)	Modified Park's equation Ascending branch: $\eta = A\xi - B\xi^2$ $A = 2.4 - 0.001 \cdot \sigma_0$ $B = 1.4 - 0.001 \cdot \sigma_0$ $\epsilon_0 = 1.34 + 0.00116\sigma_0 (\%)$ Falling branch: $\sigma = \sigma_0 [1 - Z(\epsilon - \epsilon_0)]$ $Z = 0.5 / (\epsilon_{50u} - \epsilon_0)$ $\epsilon_{50u} = (0.3 + 0.0021\sigma_0) / (\sigma_0 - 90)$ same as Park's equation on confinement. $\sigma_0$ (kg/cm <sup>2</sup> )		Stiffness for unloading curves, $G \rightarrow H(f_{cm}/2) : E_c F_{cm}$ $H \rightarrow K : E_c F_{c2}/2$ Stiffness for reloading curve: $E_c F_{c2}$ $F_{c2} = 0.76 / \{1 + 2[(\epsilon_{cm} - \epsilon_0) / (\epsilon_{20c} - \epsilon_0)]\}$ $F_{cm} = [(\epsilon_{cm} - \epsilon_{cm}') / 2] / f_{cm}$ $\epsilon_{cm}' = \epsilon_{cm} - f_{cm} / E_c F_{c2}$	
Takiguchi (1976)	Umemura's e-function Same as Kokusho's (1975)	Modified Horishima's equation $\eta = (\xi - \xi_0) [A(\xi - \xi_a + \eta_a / (\xi_a - \xi_0))]$ $A = 0.225\xi_a^2 - 1.225\xi_a + 1.85$ $\xi_0 = \xi_a - \eta_a(\xi_a + \alpha) / (\eta_a + E\alpha)$ $\alpha = 0.1175\sqrt{\xi_a}$ $\xi_0$ : plastic strain ratio	Straight line: $\eta = E \cdot \beta (\xi - \xi_0) / (\xi_0 + \beta)$ $\beta = 0.1002\sqrt{\xi_a}$	

Table 4 - 4. Equations Suggested for Uniaxial Unloading and Reloading Stress-Strain Curves for Concrete

Researchers	Envelope Curve	Unloading Curve	Reloading Curve	Comment
Tanigawa (1978)	<p>Modified Popovics's equation</p> <p>Ascending branch:  <math>\eta = n_a X / [(n_a - 1) + X^{n_a}]</math>  <math>X = \log(\xi + 1) / \log 2</math></p> <p>Falling branch:  <math>\eta = (n_f - 1) \cdot X / [(n_f - 1) + X^{n_f}]</math>  <math>+ (7 - \xi) / 6n_f</math>  <math>X = \log(\xi + 1) / \log 2</math> (normal)  <math>X = \log(\xi + 1) / \log 2 + 1</math> (lightweight)</p>	<p>Straight line parallel with stress axis to common point <math>(\sigma_c, \epsilon_c)</math>, then:</p> $\sigma = \sigma_c \left( \frac{\epsilon - \epsilon_p}{\epsilon_c - \epsilon_p} \right)^{\frac{E_c(\epsilon_c - \epsilon_p)}{\sigma_c}}$	<p>Straight line passing through reloading point and common point</p>	
	<p>(1) common point curve: shrinking envelope curve to constant ratio (0.9) around the origin</p> <p>(2) <math>\epsilon_p / \epsilon_0 = (\epsilon_c / \epsilon_0) \cdot \{1 - \exp[-(\epsilon_c / \epsilon_0)^m / \alpha]\}</math></p> <p><math>E_c / E_0 = 10^{[E_1 + E_2(\epsilon_c / \epsilon_m)]}</math></p> <p><math>E_c</math>: tangent modulus of unloading curve, <math>E_0 = \sigma_0 / \epsilon_0</math></p> <p>(3) upper bound stress under constant strain <math>\sigma_n</math>-number of cycle N:  <math>\sigma_n / \sigma_1 = 1.0 - d \cdot \log N</math>, <math>d = P_1 + P_2(\epsilon_1 / \epsilon_0)</math> (<math>0 \leq \epsilon_1 / \epsilon_0 \leq 2.0</math>)  <math>d = P_1 + 2 \cdot P_2</math> (<math>\epsilon_1 / \epsilon_0 &gt; 2.0</math>)</p> <p><math>\sigma_1</math>: first upper bound stress, <math>\epsilon_1</math>: specified upper bound strain</p> <p>(4) upper bound strain under constant stress <math>\epsilon_n</math>  <math>v = 1 - \int_{-\infty}^X [1 / (S\sqrt{2\pi})] \exp\{-1/2 \cdot [(X - \bar{X}) / S]^2\} dx</math> <math>X = \log[D / (1 - D)]</math></p> <p><math>D = (\epsilon_n - \epsilon_1) / (\epsilon_{nf} - \epsilon_1)</math> <math>\epsilon_{nf}</math>: failure strain <math>\bar{X}</math>: average of X  <math>v = (N - 1) / (N_f - 1)</math> <math>N_f</math>: N at failure <math>S</math>: standard deviation of X</p> <p>(5) S-N curve: stress amplitude under constant stress <math>S</math> (<math>= \sigma_{ck} / F_{cs}</math>) - <math>N_f</math>  <math>S = 1.0 - 0.083 \cdot \log N_f</math> (<math>\sigma_{ck}</math>: specified upper bound stress, <math>F_{cs}</math>: monotonic compressive strength)</p>			



Among recent studies Tanigawa (1977) studied the effect of hoop spacing and cover thickness on the relation between residual strain and unloading point strain, stiffness at unloading point, averaging stiffness of reloading curve, strain increasing rate - N curve under constant stress loading and stress decreasing rate - N curve under constant strain loading. (ref. 3.5.) He pointed out that the effect of confinement on the shape of unloading and reloading curves is fairly great.

## 5. Comparison of Tests and Analytical Models

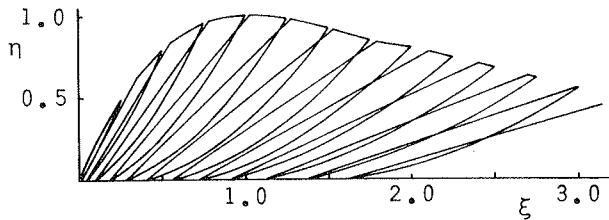
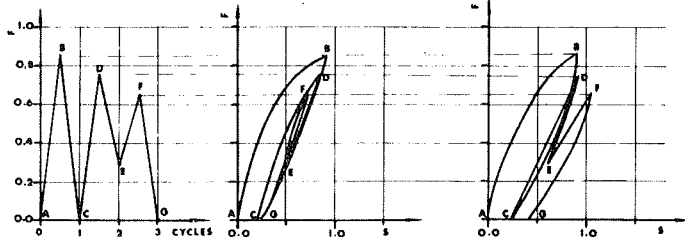


Fig. 4 Computed Curves by Model of Horishima (1966)

Figures 4 - 10 show computed results by proposed models for uni-axial unloading and reloading stress-strain curves for concrete, including some comparisons of analytical and experimental curves.



(a) Load History (b) Computed by Karsan (c) Computed by Sinha

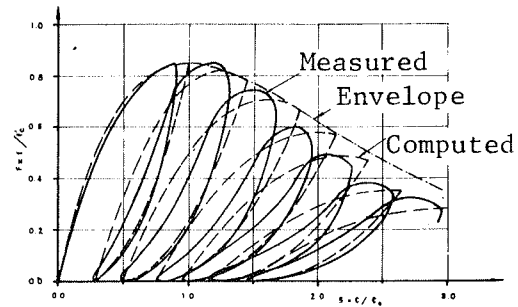


Fig. 5 Computed and Measured Curves. Karsan (1969), Sinha (1964)

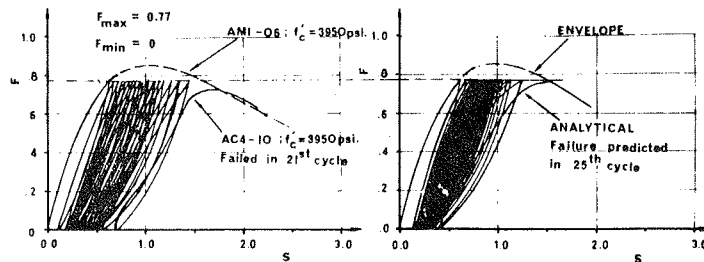


Fig. 7 Computed and Measured Curves. Karsan (1969)

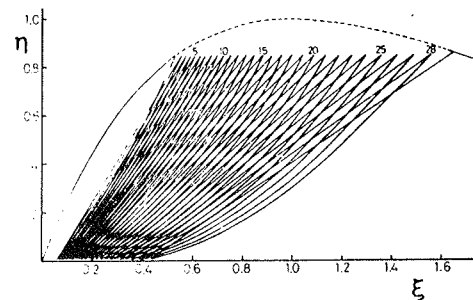


Fig. 8 Computed Curves. Takiguchi (1976)

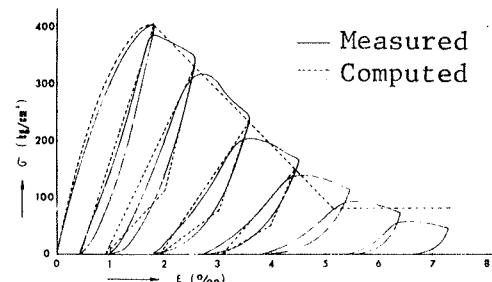
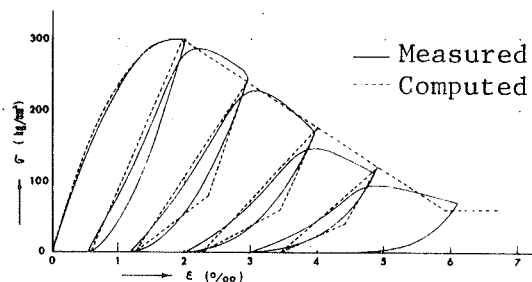


Fig. 9 Computed and Measured Curves. Okamoto (1976)

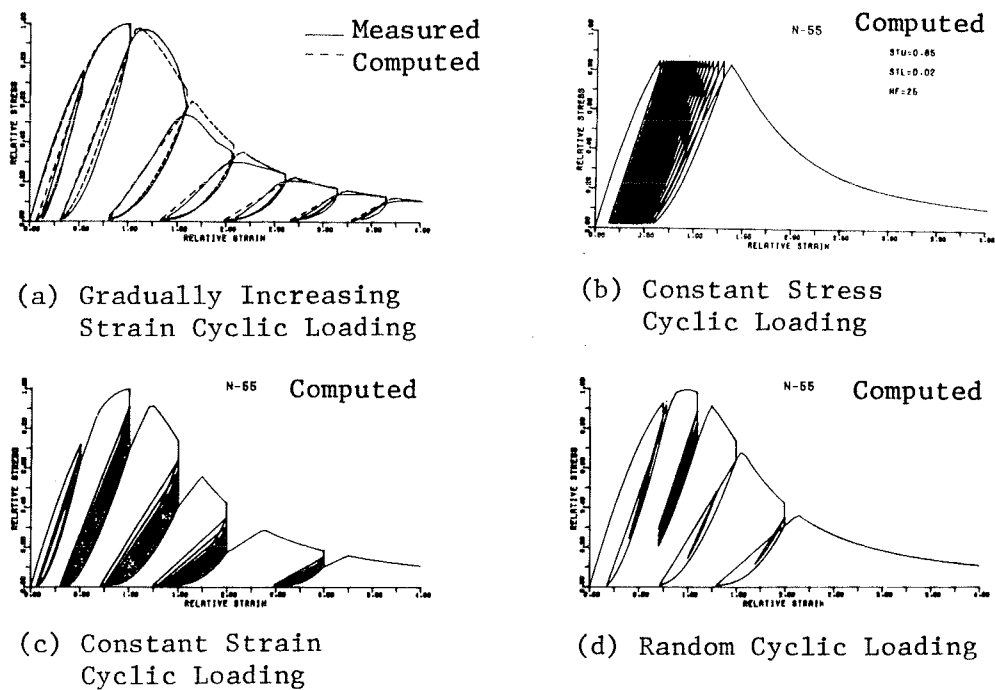


Fig. 10 Computed and Measured Curves. Tanigawa (1978)

## PART II BIAXIAL AND TRIAXIAL LOADING TESTS

### 1. Strength under Multi-axial Stresses

The earliest tests of mortar and concrete under multi-axial stresses were reported by Considere in 1903 and 1906. In 1928 Ros and Eichinger pointed out the existence of the inherent failure criterion for mortar, concrete and rock. Richart (1928) reported the test of concrete cylinders under tri-axial stresses.

Okajima (1970) pointed out the following common problems to previous experimental studies.

- (1) Experimental conclusions are not always the same according to researchers for limits of combination of stresses possible to one testing facility.
- (2) An universal failure criterion has not been obtained, reflecting the difference of materials: aggregate and cement, and concrete strength.
- (3) Elastic plastic characteristics of concrete under combined stresses is not so clear.
- (4) There are few tests on dynamic characteristics under combined stresses.
- (5) There are few tests under triaxial stresses, especially on the effect of the intermediate principal stress.
- (6) There are less tests under tension stress system than under compression stress system.

Recently the following researchers made a contribution to each problem above mentioned.

- (1) Okajima (1970), Otani (1973); Effect of confinement due to friction on the shape of failure criterion.
- (2) Smith (1953), Nishizawa (1969); Equations using principal stresses, Suenaga (1969); Unification of failure criterion, Kosaka (1969); Equations using compressive strength and splitting strength.
- (3) Hannant (1966), Gopalakrishnan (1969); Measurement of creep under triaxial stresses, Okajima (1970).
- (4) Suenaga (1969); Failure function on the basis of kinetic analysis.
- (5) Bellamy (1961), Campbell-Allen (1962); Compression tests of hollow cylinders subjected to internal and external pressure, Niwa (1967); Triaxial stress test of cubic specimens, with three degrees of freedom.
- (6) Mchenry (1958), Tsuboi (1964), Nishizawa (1969); Tension-compression test, Kupfer (1969); Biaxial tension, tension-compression, biaxial compression, Okajima (1970).

Hobbs (1977) classified experimental techniques into the following five groups:

- (1) Loading through solid platens - biaxial compression, triaxial compression and tension plus compression.
- (2) Loading through brush platens - biaxial compression and tension.
- (3) Subjecting hollow cylinders to compression and torsion - tension plus compression.
- (4) Subjecting hollow cylinders to axial compression and internal or external pressure - compression plus tension and biaxial compression.
- (5) Combined loading of cylinders through fluid membranes and solid platens - triaxial compression, equal biaxial compression and tension plus equal biaxial compression.

Hobbs pointed out that serious objections can be raised to the use of techniques (1), (3) and (4), and summarized the test results which were obtained using techniques (2) and (5). (ref. Fig. 11) The results are

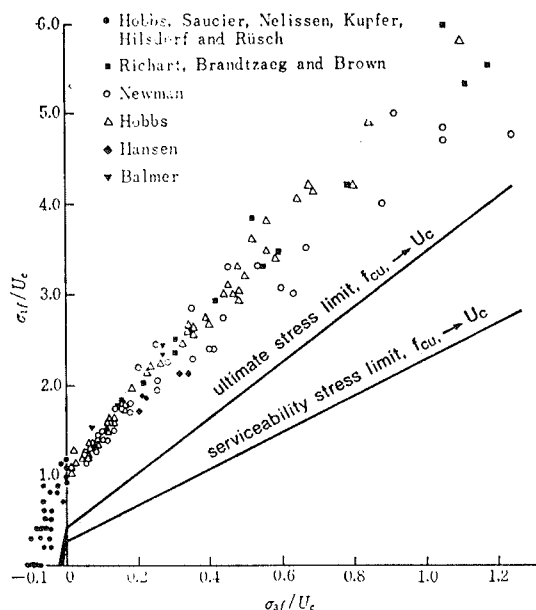


Fig. 11 Strength of Concrete under Multi-axial Stresses. Hobbs (1977)

normalized with respect to the mean uniaxial compressive strength (i.e. cylinder or cube strength). Also shown plotted on Fig. 11 are the ultimate and serviceability stress limits proposed by Hobbs (1977) for the design stresses corresponding to the theory of limit state design in CP110, The structural use of concrete, of BSI (1972). From Fig. 11 and so on the following matters were concluded.

- (1) The application of restraint to concrete increases the compressive strength.
- (2) The magnitude of the intermediate principal stress has no significant influence on the major and minor principal stress at failure.
- (3) When one of the stresses is tensile, there is a marked reduction in the compressive stress which concrete is able to support.

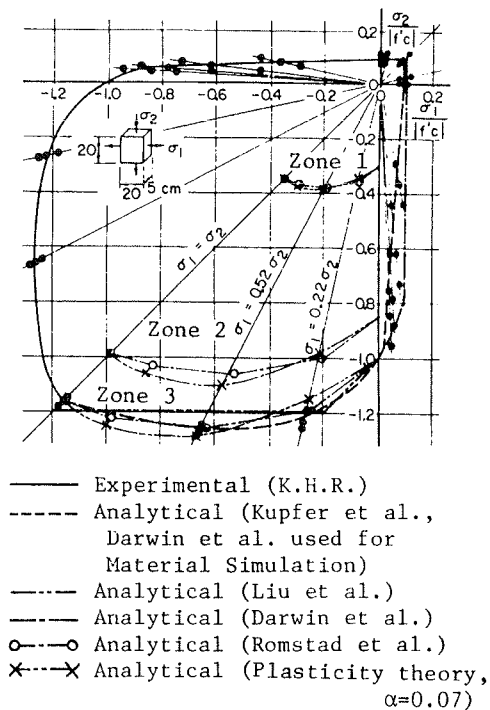


Fig. 12 Biaxial Strength Envelopes

Kupfer's test (1969) covered a full area of biaxial stresses using brush platens and it appears to be the most reliable. Biaxial strength envelope obtained from this test is shown in Fig. 12.

From the recent biaxial test by Tasuji (1978), in which all combinations of compressive and tensile loadings were also included, the ultimate strength behavior was generally similar to Kupfer's (1969), Liu's (1972) and Nelissen's (1972), and the difference between the results of Liu and Tasuji seem to indicate that the increase in biaxial compression strength for concrete is higher for concrete with a lower uniaxial compressive strength.

## 2. Deformation under Multi-axial Stresses

Very few experimental results are available regarding the deformation behavior under multi-axial stresses, and this trend is remarkable in the case of triaxial tension plus compression.

The experimental investigations on the stress-strain relation under triaxial stresses were summarized by Cedolin (1977). He reviewed works by Richart (1928), Balmer (1952), Gardner (1969), Palaniswamy (1974), Mills (1970), Launay (1970) and Linse (1973), and proposed an analytical model expressed by bulk and shear moduli, variable with the strain rate.

Fig. 13 shows the stress-strain relation under triaxial stresses illustrated by Hobbs (1977). From Fig. 13 it can be stated that under triaxial compression the strains sustained by concrete greatly exceed those for uniaxial compression, and increase with the increase of the lateral pressure. These phenomena were shown in tests by many researchers; Richart (1928), Ito (1957), Krah1 (1965), Gardner (1969) and Okajima (1971).

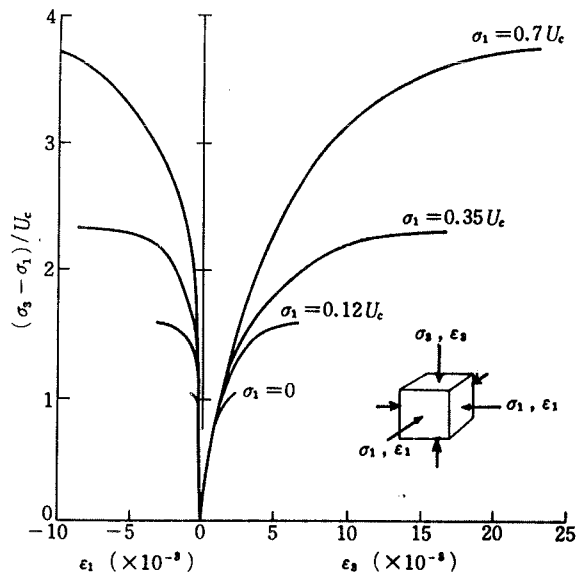


Fig. 13 Stress-Strain Curves for Concrete under Triaxial Compression. Hobbs (1977)

Palaniswamy (1974) pointed out that axial and lateral strain at maximum axial stress increases at first with increasing confining pressure, but for lateral stress beyond the uniaxial compressive strength, increasing lateral stress decreases the value of axial and lateral strains at failure.

In Fig. 13 it is assumed that concrete stiffness,  $E$ , at a relatively low different stress,  $(\sigma_3 - \sigma_1)/U_c$  is essentially independent of the level of restraint,  $\sigma_1$ . However, Hobbs pointed out that concrete stiffness,  $E$ , under triaxial compression decreases, when  $|\sigma_1| > 0.3|U_c|$ , reaching value roughly 50 per cent of the uniaxial value at  $\sigma_1 = U_c$ . Poisson's ratio,  $\nu$ , is similarly affected by restraint falling from approximately 0.1 to 0.15 at  $0 < |\sigma_1| < 0.3|U_c|$  to approximately 0.05 at  $\sigma_1 = U_c$ . But the ratio,  $\nu/E$  appears to be essentially independent of the level of restraint,  $\sigma_1$ .

### 3. Failure Criterion under Multi-axial Stresses

Suenaga (1969) and Koyanagi (1972) reviewed the failure criterions of concrete. Formerly the maximum principal stress (or strain) theory, Mohr's criterion, Octahedral shear stress theory, the expression by failure curved surface and so on were proposed as the macroscopic failure criterion. As the microscopic failure criterion, Griffith criterion and modified Griffith criterion were suggested. However they are insufficient for explaining all test results generally.

The recent studies on the failure criterion were reviewed by Nagamatsu (1976). It is necessary for establishing the general view of failure criterion to study test results, estimating combined stresses by the concept of 'Limit stress curved surface' proposed by Niwa (1967). The dual fracture theory, in which failure is separated into tension failure and compression failure, was proposed by Cowan (1953) and it is getting firmly fixed by recent studies by Suenaga (1969) and Han-Chin (1974). Sakurai (1968) suggested the failure criterion in function of the maximum principal stress, considering the semi-macroscopic failure mechanism. Fujimatsu (1974) showed a physical approach to the failure criterion based on 'The phased plane-moment fracture hypothesis.'

Nagamatsu (1976) proposed a new dual fracture criterion which is separated into two fracture types: brittle and quasi-ductile. For the former the Griffith theory was extended to the overall collapse criterion and for the latter the theory of elastic shear strain energy was extended including the maximum principal stress as a variable in the function. He verified that these failure criterions agree most closely with the previous tests in comparison with other criterions. Four constants involved in his criterion have been decided by the least square method from as many test data as he can collect in literature.

The above-stated studies are trials to express the failure criterion only by stress state. Tsuboi (1964) pointed out that the maximum principal strain theory is effective as the failure criterion in the case of biaxial tension or tension plus shear from his test. Hatano (1967) paid his attention to failure strain under triaxial compression and confirmed that when shear strain strength,  $S$ , reaches the value given by the equation,  $S = f(\epsilon) = a + b\epsilon$ , failure occurs. Okajima (1973) proposed the critical tensile strain theory expressed by the following simple linear equation with octahedral normal stress,  $\sigma_{oct}$ , at failure.  $\epsilon_{cr} = a\sigma_{oct} + b$  Where 'a' and 'b' are the constants obtainable from strength and critical

tensile strain in uniaxial compression and tension tests. And he confirmed that this theory is applicable for the strength of concrete under biaxial tension and tension plus compression. Carino (1976) also proposed the critical tensile principal strain theory in the linear function of the mean normal stress for the failure criterion under tension plus compression.

#### 4. Multi-axial Cyclic Loading Tests

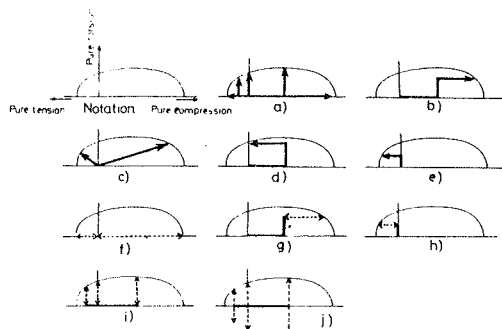


Fig. 14 Loading Procedure.  
Okajima (1972)

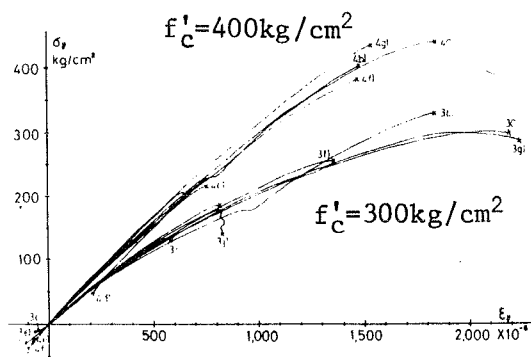


Fig. 15 Axial Stress-Strain Curves  
under Biaxial Monotonic  
Loading. Okajima (1972)

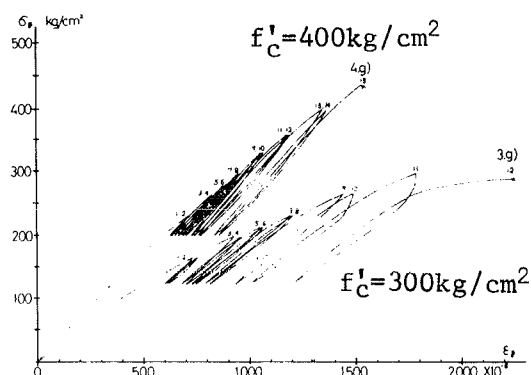


Fig. 16 Axial Stress-Strain Curves  
under Biaxial Cyclic  
Loading. Okajima (1972)

Okajima (1972) studied the effect of loading path and cyclic biaxial loading on the elastic plastic characteristics of concrete using the hollow cylinder specimens. He pointed out the following matters. In the case of tension plus torsional moment, the axial stiffness deteriorates to some extent for the existence of torsional moment. But shear stiffness is almost constant for all loading procedure. Under cyclic loading, the envelope curves of both axial and shear stress-strain relations are almost the same as under monotonic loading, as shown in Figures 14, 15, 16. Residual axial and shear strain are larger for lower-strength, as shown in Fig. 16.

Ito (1972) developed the high-pressure triaxial cyclic testing machine and Endo (1978) reported the tests using this machine with emphasis on the vertical and lateral strain measurement. From his test results under gradually increasing strain cyclic loading, the vertical stress-strain curve, under restraint pressure  $30\text{kg/cm}^2$ , is higher in strength and more ductile as compared with under no restraint pressure, but the shape of curves is much the same.

Being not so much other works are found in the Japanese literature on this subject, more comprehensive studies are needed hereafter.

## 5. Analytical Model for Concrete under Multi-axial Stresses

Various analytical models under multi-axial stresses have been proposed with the recent advance of finite element method, and these were reviewed by Scordelis (1972), Kawamata (1974), Schnoblich (1976), Noguchi (1976) and Wegner (1976). Here the stress-strain relation and cracking are discussed and then the typical models are summarized.

### 5.1. Stress-Strain Relation

The model based on the theory of plasticity for the compressible materials, using Drucker-Prager's yield criterion, has been used by many investigators. Noguchi (1977) compared this model and four other biaxial models with the tests by Kupfer (1969) and Nelissen (1972), and concluded that the plasticity model can not represent the nonlinear behavior of concrete adequately. At high stresses this model is unreasonably hard in both principal directions. This tendency is more remarkable, as the ratio of  $\sigma_1$  to  $\sigma_2$ ,  $\alpha$ , becomes more positive for biaxial compression. And the orthotropic material model of Darwin (1976) gives the best result in both principal direction.

Triaxial models have been proposed by Palaniswamy (1974), Imoto (1975), Muto (1976), Bažant (1976), Cedolin (1977), Kotsovos (1978) and others. The endochronic theory, which had been originally developed for metals, was extended to concrete by Bažant, including the inelastic dilatancy, strain-softening and others. Good agreements with biaxial and triaxial tests were reported, but the adequacy to cyclic loading and strain-softening is not so clear from the lack of test data as well as Darwin's model.

### 5.2. Cracking

Analytical models for cracking are divided broadly into two groups. One is the method to separate nodes by setting up cracking surface between neighboring elements and the other is to change the element into orthogonal anisotropic. For the former, Taylor (1972) and Noguchi (1977) proposed the model for crack initiation and propagation without predefining crack pathes. In this case, there is a tendency for the calculation method to be complicated and it requires a lot of computing time. For the latter, it is rather easy even for cyclic loading without the movement and separation of nodes. But it becomes difficult to evaluate the stiffness of cracked element and express the crack spacing. Hence it is necessary to use cracking models properly in accordance with the object, e.g. the former for the shear resistant mechanism of reinforced concrete members and the latter for the nuclear reactor vessels.

### 5.3. Summaries and Comparisons of Analytical Models under Biaxial and Triaxial Stresses

Proposed analytical models under biaxial and triaxial stresses are summarized on the following items. When some items are omitted, it means that the model does not take account of them.

- A: Stress-strain relation
- B: Yield or failure criterion
- C: Nonlinear analysis method
- D: Cracking
- E: Aggregate interlock
- F: Compressive failure

(1) Nilson (1967)

- A: Biaxial stress-strain relation is transformed to uniaxial one. Saenz's equation in uniaxial compression and linear in tension.  
 $E_1 v_2 = E_2 v_1$
- C: Load incremental method.  $E_1$  and  $E_2$  are obtained from  $\epsilon_1$  and  $\epsilon_2$ , according to Saenz's equation.
- D: When the average value of principal tensile stress in two adjacent elements exceeds the tensile strength, the elements are disconnected at their common corners.
- F: When the principal compression strain exceeds the ultimate strain under uniaxial compression, the element fails.

(2) Iwashita (1967)

- A: Linear-quadratic curve in compression and linear in tension for no cracked rectangular truss element with two diagonal members.
- B: Maximum principal theory is assumed in tension yield and compression yield is caused on the minimum principal stress.
- C: Load incremental iterative method.
- D: When the maximum principal stress at the center of the element is over a limit value, a crack occurs and is expressed by the orthogonal anisotropic rectangular element.

(3) Franklin (1970)

- A: Same as Nilson's (1). Multilinear in compression and plateau after the maximum stress, and linear in tension. The smaller of  $E_1$  and  $E_2$  is adopted as  $E$ , and  $v$  is constant.
- B: Compressive and tensile strength are constant. Linear approximation of Bresler-Pister's curve. (Fig. 17)
- C: Incremental iterative method.
- D: When the principal tensile stress exceeds the failure criterion, the stiffness in the principal direction is set at zero and crack is formed perpendicularly to that direction.

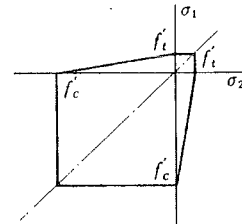


Fig. 17 Failure Criterion. (Franklin)

$$\begin{Bmatrix} \Delta \sigma_1 \\ \Delta \sigma_2 \\ \Delta \tau_{12} \end{Bmatrix} = \mathbb{D} \begin{Bmatrix} \Delta \epsilon_1 \\ \Delta \epsilon_2 \\ \Delta \gamma_{12} \end{Bmatrix} \quad \mathbb{D} = \begin{bmatrix} 0 & 0 & 0 \\ 0 & E_2 & 0 \\ 0 & 0 & E_2/4 \end{bmatrix}$$

- E: Shear transfer by aggregate interlock is considered by setting  $G_{12}$  of cracked concrete at  $E_2/4$ .
- F: 1) When the final effective strain  $\epsilon_1^*$  exceeds the ultimate strain, failure occurs.  
 2) If failure has not occurred on the criterion 1), the biaxial stress failure criterion is used.

(4) Ngo (1970)

- A: Linear Elastic.
- D: The shape and location of cracks are preformed. Two adjacent nodes



are connected by linkage element. Crack is formed by setting the stiffness in the perpendicular direction of the crack at zero.

E: The stiffness of crack linkage element parallel to the crack is set at a constant value to represent the aggregate interlock.

(5) Liu (1971)

A: Biaxial compressive stress-strain relations were obtained from his experiments and linear elastic,  $E$  in biaxial tension.  $E$  and  $E_2$  (obtained from uniaxial compression tests) are used in tension-compression.  $E_1\nu_2 = E_2\nu_1$ ,  $\nu_1 = 0.2$

B: Simplified biaxial compression test results. (ref. Fig. 12)

C: Incremental method.

D: Same as Franklin's except that  $G_{12}$  is zero. (ref. Franklin (3))

F: Ultimate strain under biaxial stresses,  $\epsilon_p = 0.0025$  ( $\alpha \leq 1$ ),  $\epsilon_p = (-500 + 0.039\sigma_p) \times 10^{-6}$  ( $\alpha > 1$ ),  $\alpha$ : principal stress ratio. After compressive failure, all terms of the constitutive matrix are equal to zero.

(6) Takiguchi (1971)

A: Biaxial stress-strain relation is transformed to uniaxial one.

Trilinear in compression and linear elastic in tension.  $E_1\nu_2 = E_2\nu_1$

B: Drucker-Prager's yield criterion (Fig. 18),  $f = \alpha J_1 + \sqrt{J_2}$ ,  $\alpha = 0.07$  (from Kupfer's tests: ref. Fig. 12)

C: Incremental method in which strain-hardening is defined as the function of plastic work, considering the compressibility of plastic deformation.

D: Crack is formed at the brittle fracture surface. Same as Liu's (5).

F: At the ductile fracture surface the internal stresses are replaced to the nodal forces of cracked element and released.

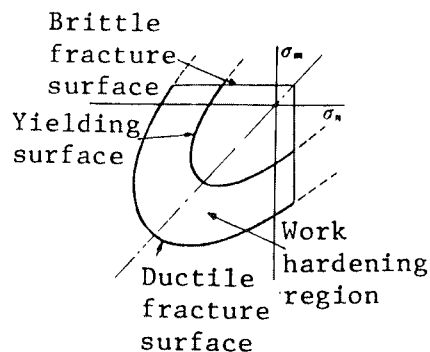


Fig. 18 Yield and Failure Criterion. (Takiguchi)

(7) Isobata (1971)

A: Orthogonally anisotropic elastic plastic body ( $E_p, \nu_p$ ) is assumed corresponding to elastic one ( $E, \nu$ ). Transformation parameters,  $\eta_i, \xi_{ij}$ , ( $E_i = \eta_i E_0$ ,  $\xi_{ij} = \sqrt{\nu_{ij}\nu_{ji}}$ ) and  $G_{31}$  are defined as the function of strain  $\epsilon_i$  and the function is decided from the test results under uniaxial and biaxial compression.

B: 1) Brittle fracture: When at least one principal stress is tension and principal strain  $\epsilon_i$  exceeds limit strain  $\epsilon_{cr}$ , crack is formed perpendicularly to  $\sigma_i$ .

2) Compressive failure:  $\tau_{oct} > n\sigma_{oct} + c$  (the octahedral shear stress theory).

C: Load incremental method.

D: Same as Liu's (5).

F: Same as Takiguchi's (6).

(8) Muto (1971)

- A: Same as Takiguchi's (6).
- B: Effective strains,  $\epsilon_1^*$ ,  $\epsilon_2^*$ , are the same as Franklin's (3).
- C: Incremental method.
- D: Same as Liu's (5).
- F: Same as Takiguchi's (6).

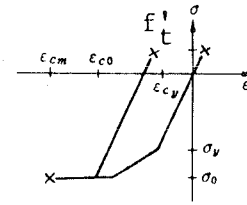


Fig. 19 Stress-Strain Curves. Muto (1972)

(9) Muto (1972)

- A: Biaxial cyclic stress-strain relation is transformed to uniaxial cyclic one. (Fig. 19)
- B: Same as Takiguchi's (6). (Fig. 20, ref. Fig. 12)
- C: Same as Takiguchi's (6).
- D: Same as Liu's except that concrete element goes back to be elastic under compression stress even if tension failure occurred.
- F: Same as Takiguchi's (6).

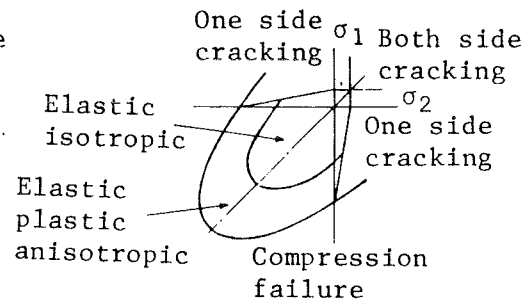


Fig. 20 Yield and Failure Criterion. Muto (1972)

(10) Kawamata (1972)

- A: Linear elastic.
- D: When the tensile strain exceeds the critical value, a crack is formed. A new node is introduced, and the structural system has a continuously changing topology.

(11) Imoto (1973)

- A: Biaxial stress-strain relation is transformed to uniaxial one. Linear approximation of Umemura's e-function (ref. Table 3), including falling branch in compression and linear in tension. (Fig. 21) Afterwards elastic plastic in tension.
- B: Mises's criterion in biaxial compression and the maximum principal stress theory in biaxial tension and tension-compression. Afterwards Drucker-Prager's criterion in the former and the Coulomb-Mohr theory in the latter.
- C: Incremental method.
- D: Same as Liu's (5).
- F: For no cracked element,  $\bar{\epsilon} < \epsilon_{cr}$ : elastic or plastic,  $\bar{\epsilon} > \epsilon_{cr}$ : compressive failure, ( $\bar{\epsilon}$ : equivalent strain), for cracked element,  $\bar{\epsilon} = \epsilon_{y1}$ , ( $\epsilon_{y1}$ : strain parallel to crack). The internal stresses are replaced to the nodal forces of cracked element and replaced step by step. (Fig. 22)

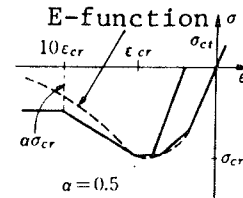


Fig. 21 Stress-Strain Curves. (Imoto)

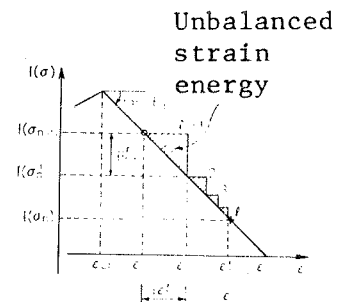


Fig. 22 Model for Strain-softening. (Imoto)

(12) Kupfer (1973)

A: Isotropic model is proposed from his own test results under biaxial stresses.

$$G_s/G_0 = 1 - a(\tau_0/f'_c)^m, \quad K_s/K_0 = G_0/[G_0 e^{-(c\gamma_0)^p}]$$

( $G_s$ : secant shear modulus,  $K_s$ : secant bulk modulus,

$\tau_0$ ,  $\gamma_0$ : octahedral shear stress, strain,

$a$ ,  $m$ ,  $c$ ,  $p$ : constants given according to compressive strength)

B: Stiffness relations above mentioned are effective to the ultimate strength corresponding to principal stress ratio. (ref. Fig. 12)

C: Secant modulus or tangent modulus.

(13) Romstad (1974)

A: Biaxial compression model:

1) The existence of four stages of behavior prior to failure in uniaxial compression.

2) Nearly linear elastic in uniaxial and biaxial tension.

3) The progressive damage concepts described for uniaxial compression are applicable to biaxial response. The strain space is divided into four damage zones and the estimation for the incremental value of  $E$  and  $\nu$  is performed by weighting and summing  $E_i$  and  $\nu_i$ , given from uniaxial compression tests.

B: Ref. Fig. 12.

F: The modulus of falling branch is set as  $E = -0.075E_0$ , in the zone 4. ( $E_0$ : initial modulus)

(14) Palaniswamy (1974)

A: Isotropic model under triaxial compression. The dependence of bulk modulus and Poisson's ratio on the stress invariants were determined from experiments.

B: Not considered. Correlation near failure stresses is not so good.

(15) Sato (1975)

A: Same as Takiguchi's (6).

B: Same as Takiguchi's (6).

C: Load incremental iterative method.

D: Almost the same as Ngo's (4).

E: The stiffness of crack linkage element parallel to the crack is evaluated from crack width.

(16) Imoto (1975)

A: Isotropic model under triaxial stresses. Brittle fracture in tension and elastic plastic for ascending branch and strain-softening for falling branch in compression. Triaxial stress-strain curves are transformed to uniaxial one using the plastic theory.

B: Isotropic hardening according to the Reuss's flow rule using Drucker-Prager's yield criterion.

C: Mixed type of tangent stiffness method and initial stress method.

D: Franklin's (3) and Muto's (9) models has been extended to three dimensional one.

E: Shear stiffness along the crack,  $\mu G$  is evaluated as the function of crack width.

F: When the scholar function,  $f$ , exceeds the maximum strength, compression failure occurs. (ref. Imoto (11) )

(17) Darwin (1976)

- A: Orthogonally anisotropic model with the tangent moduli,  $E_1$ ,  $E_2$ , and the equivalent Poisson's ratio,  $\nu = \sqrt{\nu_1 \nu_2}$ .  $E_1$  and  $E_2$  are determined from a family of uniaxial cyclic stress-strain curves for each principal stress direction with the equivalent uniaxial strains,  $\epsilon_{iu}$ . (ref. Table 4 - 2)
- B: Kupfer's failure criterion except that modulus of rupture is used for members in biaxial tension and tension-compression. Variation of  $\epsilon_{ic}$  at the peak compressive stress,  $\sigma_{ic}$ , has been determined experimentally.
- C: Load or displacement incremental iterative method.
- D: Same as Liu's (5) and Muto's (9).
- E: Same as Franklin's (3).
- F: Same as Imoto's (11), except that falling branch is straight line passing through the two points:  $(\sigma_{ic}, \epsilon_{ic})$ ,  $(0.2f'_c, 4\epsilon_0)$ .

(18) Phillips (1976)

- A: Isotropic model assuming the tangent bulk modulus  $K_t$  and shear modulus  $G_t$  to be functions of the first and second stress invariants from Kupfer's experiments.

$$K_t = f_1(I_1) = f_1(\sigma_1 + \sigma_2 + \sigma_3)$$

$$G_t = f_2(J_2) = f_2[\{(\sigma_1 - \sigma_2)^2 + (\sigma_2 - \sigma_3)^2 + (\sigma_3 - \sigma_1)^2\} / 6]$$

- B: Octahedral shear stress theory in multi-compressive zones and the maximum principal stress and maximum principal strain criterion in tension zones.
- C: Load incremental iterative method.
- D: Almost the same as Franklin's (3) and Muto's (9), except for evaluating cracking at integrating points and using two fracture laws (ref. B).
- E:  $\tau^* = a' G \gamma^*$ , where  $G$  is the initial shear modulus and  $a'$  is a preselected constant such that  $0 \leq a' \leq 1$ .  $\gamma^*$  is the shear strain along the crack.
- F: After peak stress, the stress is held constant to allow local stress redistribution to occur.

(19) Muto (1976)

- A: Same as Imoto's (16), except that falling branch is considered only for cover concrete using uniaxial stress-strain relation as a spring element.
- B: Same as Imoto's (16), except for assuming the Prager's kinematic hardening rule modified by Ziegler.
- C: Incremental method.
- D: Same as Imoto's (16).
- E:  $\beta G$ ,  $\beta$ : constant ( $0 \leq \beta \leq 1$ )
- F: When core concrete fail in compression, all internal stresses are released, but for cover concrete internal stresses are released step by step.

(20) Noguchi (1976)

- A: Linear elastic except that the orthogonally anisotropic theory is used for the internal cracked concrete element around the main bar element to simulate the bond-slip behavior between the deformed bar and concrete.
- C: Load incremental iterative method.
- D: When the principal stress exceeds the modulus of rupture, a crack occurs along a particular grid line. The grid line is relocated

perpendicular to the maximum principal stress and new nodes are introduced to express the new crack along the grid line. Then the cracking release nodal forces are applied at the next iterative step.

(21) Bažant (1976)

- A: Extension of the endochronic theory to concrete. This theory was originally developed for metals which correctly predicts strain-hardening, unloading, contraction of hysteresis loops in cyclic loading and so on. The incremental stress-strain relations may be split into volumetric and deviatoric components and each strain increment is expressed as a sum of elastic and inelastic increments. Three major extensions are considered:
  - 1) The hydrostatic pressure sensitivity of inelastic strain.
  - 2) The inelastic dilatancy.
  - 3) The strain-softening tendency at high stress.Material parameters are identified from test data.
- B: The absence of yield function and normality rule. But material parameters are identified from fit of biaxial failure envelope and so on.
- C: Incremental method.
- D: Tensile failure is accounted by the function equivalent to maximum tensile strain and stress cutoffs in the failure criterion.
- F: Strain-softening is expressed by the function of stress and strain invariants. Material parameters are identified from test data.

(22) Arai (1978)

- A: Biaxial stresses are determined as a function of principal strain similar to Liu's (5), in a state of plane stress on the basis of Kupfer's test data (1969).
- B: Kupfer's failure criterion.
- C: Iterative method.
- D: Same as Liu's (5).

## References

- Alam, M.S., "General Analysis of Reinforced Concrete by Finite Element Method," Doctoral Thesis, Univ. of Tokyo, May 1977.
- Alexander, S., "A Single Equation for the Stress-Strain Curve of Concrete," Indian Conc. Jour., Bombay, Vol. 39, No. 7, July 1965, pp. 274-277.
- Aoyama, H., et al., "Ultimate Strain of Concrete under Compression," Proc. Kanto Dist. Symp., AIJ, No. 38, 1967, pp. 433-436.
- Aoyama, H., et al., "Moment-Curvature Relations of Reinforced Concrete Sections Obtained from Material Characteristics," Proc. Annual Conv., AIJ, Oct. 1973, pp. 1261-1262.
- Arai, Y., "Nonlinear Analysis of a Shear Wall-Frame Systems of Reinforced Concrete," Trans. of AIJ, No. 264, Feb. 1978, pp. 41-49.
- Baker, A.L.L., et al., "Inelastic Hyperstatic Frames Analysis," Proc. of the Internat. Symposium on the Flexural Mechanics of Reinforced Concrete, ASCE-ACI, Nov. 1964, pp. 85-142.
- Balmer, G., "A General Analytic Solution for Mohr's Envelope," Proc., ASTM, Vol. 52, 1952, pp. 1260-1271.
- Ban, S., et al., "Behaviour of Plain Concrete under Dynamic Loading with Straining Rate Comparable to Earthquake Loading," Proc. of the Second World Conference on Earthquake Engrg., Vol. III, 1960, pp. 1979-1993.
- Barnard, P.R., "Researches into the Complete Stress-Strain Curve for Concrete," Mag. of Conc. Res., Vol. 16, No. 49, Dec. 1964, pp. 203-210.
- Bažant, Z.P., et al., "Endochronic Theory of Inelasticity and Failure of Concrete," Jour. Engr. Mech. Div., ASCE, Vol. 102, No. EM4, Aug. 1976, pp. 701-722.
- Bellamy, C.J., "Strength of Concrete under Combined Stresses," ACI J., Vol. 58, Oct. 1961, pp. 367-381.
- Bertero, V.V., et al., "Confined Concrete: Research and Development Needs," Proc. of a Workshop on Earthquake-Resistant Reinforced Concrete Building Construction, Vol. 2, Univ. of Calif., Berkeley, July 1977, pp. 594-610.
- Blakeley, R.W.G., et al., "Prestressed Concrete Sections with Cyclic Flexure," Jour. Struct. Div., ASCE, Vol. 99, No. ST8, Aug. 1973, pp. 1717-1742.
- Blanks, R.F., et al., "Plastic Flow of Concrete Relieves High-Load Stress Concentrations," Civ. Engrg., Vol. 19, No. 5, May 1949, pp. 320-322.
- Blume, J.A., et al., "Design of Multistory Reinforced Concrete Buildings for Earthquake Motions," Portland Cement Association, 1961, 318pp.
- Bresler, B., et al., "Tie Requirements for Reinforced Concrete Columns," ACI J., Vol. 58, No. 5, Nov. 1961, pp. 555-569.
- Bresler, B., et al., "Influence of High Strain Rate and Cyclic Loading on Behavior of Unconfined and Confined Concrete in Compression," Preprint from Second Canadian Conference on Earthquake Engrg., Hamilton, June 1975.
- BSI, "British Standard Code of Practice for the Structural Use of Concrete," CP110, Part 1, Nov. 1972.
- Buyukozturk, O., et al., "Stress-Strain Response and Fracture of a Concrete Model in Biaxial Loading," ACI J., Vol. 68, No. 8, Aug. 1971, pp. 590-599.
- Campbell-Allen, D., "Strength of Concrete under Combined Stresses," Constructional Review, No. 35-4, April 1962.
- Carino, N.J., et al., "Limiting Tensile Strain Criterion for Failure of Concrete," ACI J., Vol. 73, No. 3, March 1976, pp. 160-165.
- CEB-FIP, "Recommendations internationales pour le calcul et l'exécution des ouvrages en béton," 1970.

- Cedolin, L., "Triaxial Stress-Strain Relationship for Concrete," Jour. Engr. Mech., ASCE, Vol. 103, No. EM3, June 1977, pp. 423-439.
- Chan, W.L., "The Ultimate Strength and Deformation of Plastic Hinges in Reinforced Concrete Frameworks," Mag. of Conc. Res., Vol. 7, No. 21, Nov. 1955, pp. 121-132.
- Cohn, M.Z., et al., "The Flexural Ductility of Reinforced Concrete Sections," Publication of IABSE, Vol. 32, Part II, 1972, pp. 53-83.
- Considere, A., "Experimental Researches on Reinforced Concrete," Translation and Introduction by L.L. Moisseiff, 2nd ed., New York, McGraw-Hill, 1906.
- Cowan, H.J., "The Strength of Plain, Reinforced and Prestressed Concrete under the Action of Combined Bending and Torsion of Rectangular Sections," Mag. of Conc. Res., Vol. 5, No. 14, Dec. 1953.
- Darwin, D., et al., "Analysis of R.C. Shear Panels Under Cyclic Loading," Jour. Struct. Div., ASCE, Vol. 102, No. ST2, Feb. 1976, pp. 355-369.
- Darwin, D., et al., "Nonlinear Biaxial Stress-Strain Law for Concrete," Jour. Engrg. Mech., ASCE, Vol. 103, No. EM2, April 1977, pp. 229-241.
- Endo, T., "Test Results of Concrete Using High-Pressure Cyclic Triaxial Testing Machine," Proc. Annual Conv., AIJ, Sept. 1978, pp. 443-444.
- Franklin, H.A., "Nonlinear Analysis of Reinforced Concrete Frames and Panels," Ph.D. Dissertation, Univ. of Calif., Berkeley, March 1970.
- Fujimatsu, S., "A Physical Approach to the Failure Criterion of Concrete, Based on 'The Phased Plane-Moment Fracture Hypothesis'," Trans. of AIJ, No. 219, May 1974, pp. 1-8.
- Gardner, N., "Triaxial Behaviour of Concrete," ACI J., Vol. 66, No. 2, Feb. 1969, pp. 136-146.
- Gopalakrishnan, K.S., et al., "Creep Poisson's Ratio of Concrete under Multiaxial Compression," ACI J., Vol. 66, No. 12, Dec. 1969, pp. 1008-1020.
- Hamada, M., et al., "Stress-Strain Curves Including Strain over the Compressive Strength of Concrete," Trans. of AIJ, No. 42, Feb. 1951, pp. 37-41.
- Han-Chin, W., "Dual Failure Criterion for Plain Concrete," Jour. Engrg. Mech., ASCE, Vol. 100, No. EM6, Dec. 1974, pp. 1167-1181.
- Hannant, D.J., "Equipment for the Measurement of Creep of Concrete under Multiaxial Compressive Stress," Bulletin RILEM, No. 33, Dec. 1966, pp. 421-422.
- Hatano, T., "Deformation and Failure of Concrete under Combined Compressive Loading," Proc. of JSCE, No. 143, July 1967, pp. 22-27.
- Hatano, T., "Theory of Failure of Concrete and Similar Brittle Solid on the Basis of Strain," Proc. of JSCE, No. 153, May 1968, pp. 31-39.
- Hiramatsu, Y., et al., "Design and Production of Stiff Testing Machine and Test Results of Concrete," Jour., The Society of Materials Science, Japan, Vol. 24, No. 260, May 1975, pp. 447-454.
- Hobbs, D.W., et al., "Design Stresses for Concrete Structures Subjected to Multi-Axial Stresses," The Struct. Engrg., Vol. 55, No. 4, April 1977, pp. 151-164.
- Hognestad, E., "A Study of Combined Bending and Axial Load in Reinforced Concrete Members," Bulletin No. 399, Univ. of Illinois Engineering Experiment Station, Urbana, Nov. 1951, 128pp.
- Hognestad, E., et al., "Concrete Stress Distribution in Ultimate Strength Design," ACI J., Proc. Vol. 52, No. 4, Dec. 1955, pp. 455-479.
- Horishima, T. et al., "Study on Characteristics of Concrete under Cyclic Stresses," Report of the Engrg. Research Dept., Taisei Construction Co., Ltd., 1966.
- Imoto, K., "Elastic Plastic Analysis of Reinforced Concrete Members by the Finite Element Method," Proc. Annual Conv., AIJ, Oct. 1973, pp. 505-506.

- Imoto, K., et al., "Non-Linear Analysis of Reinforced Concrete by the Finite Element Method (Part 1)," Report of the Technical Research Inst. Ohbayashi-Gumi, Ltd., Tokyo, No. 11, 1975, pp.1-7.
- Imoto, K., et al., "Non-Linear Analysis of Reinforced Concrete by the Finite Element Method (Part 4)," Report of the Technical Research Inst. Ohbayashi-Gumi, Ltd., Tokyo, No. 16, 1978, pp. 1-7.
- Isobata, O., "Two-Dimensional Elastic-Plastic Analysis of Concrete Structure by the Finite Element Method," Trans. of AIJ, No. 189, Nov. 1971, pp. 43-50.
- Isobata, O., "Elastic-Plastic Analysis of Three-Dimensional Concrete Structure by the Finite Element Method," Trans. of AIJ, No. 211, Sept. 1973, pp. 7-14.
- Isobata, O., "On an Anisotropic Constitutive Model of Concrete for the FEM Nonlinear Stress Analysis," Trans. of AIJ, No. 265, March 1978, pp. 11-18.
- Itoh, K., "Restrained Cyclic Compression Tests of Concrete Cylinders," Proc. Annual Conv., AIJ, Oct. 1972, pp. 49-50.
- Itoh, S., et al., "Strength of Concrete under Combined Stresses," Bulletin of Research Inst. of Civil Engrg., Japan, No. 100, 1957.
- Iwashita, T., "A Calculation Method in Two Dimensional Analysis of Reinforced Concrete Structures," Trans. of AIJ, No. 141, Nov. 1967, pp. 11-18.
- Iyengar, R.K.T.S., et al., "Stress-Strain Characteristics of Concrete Confined in Steel Binders," Mag. of Conc. Res., Vol. 22, No. 72, Sept. 1970.
- Karsan, I.D., et al., "Behavior of Concrete under Compressive Loadings," Jour. Struct. Div., ASCE, Vol. 95, No. ST12, Dec. 1969, pp. 2543-2563.
- Kawamata, S., et al., "Failure Analysis of Concrete Structures by the Finite Element Method," Proc. Annual Conv., AIJ, Oct. 1972, pp. 689-690.
- Kawamata, S., "Finite Element Analysis of Reinforced Concrete Structures," Proc. Annual Conv., Applied Mechanics League, Japan, Nov. 1974, pp. 29-32.
- Kent, D.C., et al., "Flexural Members with Confined Concrete," Jour. Struct. Div., ASCE, Vol. 97, No. ST7, July 1971, pp. 1969-1990.
- King, J.W.H., "The Effect of Lateral Reinforcement in Reinforced Concrete Columns," Struct. Engineer, London, Vol. 24, July 1946, pp. 355-388.
- Kiyama, H., et al., "Stress-Strain Behaviour of Concrete in Pre- and Post-Failure Region," Proc. of JSCE, No. 240, Aug. 1975, pp. 103-111.
- Kobayashi, S., et al., "Failure Criterion of Concrete Subjected to Multi-Axial Compression," Jour., The Society of Materials Science, Japan, Vol. 16, No. 170, Nov. 1967, pp. 897-902.
- Kokusho, S., et al., "Experimental Study on the Flexural Characteristics of Reinforced Concrete Beams with Artificial Lightweight Aggregates," Trans. of AIJ, Extra, Oct. 1966, pp. 226.
- Kokusho, S., et al., "Experimental Study on Flexural Characteristics of Reinforced Concrete Members Subjected to Variable Axial Forces," Proc. Annual Conv., AIJ, Oct. 1975, pp. 1091-1094.
- Kosaka, Y., et al., "Strength of Concrete under Combined Compression and Torsion," Trans. of AIJ, No. 166, Dec. 1969, pp. 29-35.
- Kosaka, Y., et al., "Model Analysis of Mechanical Characteristics of Concrete," Bulletin of Cement Technology, Tokyo, No. 28, 1974, pp. 202-206.
- Kotsovos, M.D., et al., "Generalized Stress-Strain Relations for Concrete," Jour. Engrg. Mech., ASCE, Vol. 104, No. EM4, Aug. 1978, pp. 845-856.
- Koyanagi, W., "Failure of Concrete," Concrete Library, No. 34, JSCE, Aug. 1972, pp. 93-111.



- Koyanagi, W., et al., "Energetic Study on the Process of Compressive Failure of Concrete," Bulletin of Cement Technology, Tokyo, Vol. 29, 1975, pp. 382-385.
- Krahl, N.W., et al., "The Behavior of Plain Mortar and Concrete under Triaxial Stresses," Proc., ASTM, Vol. 65, 1965.
- Kupfer, H.B., et al., "Behavior of Concrete under Biaxial Stresses," ACI J., Vol. 66, No. 8, Aug. 1969, pp. 656-666.
- Kupfer, H.B., et al., "Behavior of Concrete Under Biaxial Stresses," Jour. Engrg. Mech., ASCE, Vol. 99, No. EM4, Aug. 1973, pp. 853-866.
- Launay, P., et al., "Strain and Ultimate Strength of Concrete under Triaxial Stress," SP-34, ACI, Vol. 1, 1970, pp. 269-282.
- Leslie, P.O., "Ductility of Reinforced Concrete Bridge Piers," Master of Engrg. Report, Univ. of Canterbury, New Zealand, 1974.
- Linse, D., "Versuchsanlage zur Ermittlung der dreiachsigen Festigkeit von Beton mit ersten Versuchsergebnissen," Cement and Concrete Research, Vol. 3, No. 4, July 1973, pp. 445-457.
- Liu, T.C.Y., "Stress-Strain Response and Fracture of Concrete in Biaxial Compression," Ph.D. Thesis and Research Report No. 339, Dept. of Struct. Engrg., Cornell Univ., Ithaca, N.Y., Feb. 1971.
- Liu, T.C.Y., et al., "Biaxial Stress-Strain Relations for Concrete," Jour. Struct. Div., ASCE, Vol. 98, No. ST5, May 1972, pp. 291-295.
- McHenry, D., et al., "Strength of Concrete under Combined Tensile and Compressive Stresses," ACI J., Vol. 29, No. 10, April 1958, pp. 829-839.
- Mills, L.L., et al., "Compressive Strength of Plain Concrete under Multi-axial Loading Conditions," ACI J., Vol. 67, No. 10, Oct. 1970, pp. 802-807.
- Morita, S., et al., "Properties of concrete in the Compression Zone of Flexural Members," Jour., The Society of Materials Science, Japan, Vol. 20, No. 208, Jan. 1971, pp. 59-66.
- Muguruma, H., et al., "Stress-Strain Relations of Concrete under Repeated Over-Load," Jour., The Society of Materials Science, Japan, Vol. 19, No. 200, May 1970, pp. 1-10.
- Muguruma, H., et al., "Mechanical Characteristics of High Strength Concrete," Bulletin of Cement Technology, Tokyo, Vol. 27, 1973, pp. 243-247.
- Muguruma, H., et al., "Study on the Compressive Failure Strain of Concrete," Bulletin of Cement Technology, Vol. 30, 1976, pp. 362-365.
- Muto, K., et al., "Elastic Plastic Analysis of Reinforced Concrete Members by the Finite Element Method (Part 1,2)," Proc. Annual Conv., AIJ, Nov. 1971, pp. 735-738.
- Muto, K., et al., "Elastic Plastic Analysis of Reinforced Concrete Members by the Finite Element Method (Part 4)," Proc. Annual Conv., AIJ, Oct. 1972, pp. 685-686.
- Muto, K., et al., "3-Dimensional Non-Linear Analysis of Reinforced Concrete Members by the Finite Element Method (Part 1)," Trans. of AIJ, No. 249, Nov. 1976, pp. 25-34.
- Nagamatsu, S., et al., "Study on Fracture Criterion of Concrete under Combined Stresses (Part I - III)," Trans. of AIJ, No. 246, 247, 254, Aug., Sept. 1976, April 1977, pp. 7-15, 1-10, 11-20.
- Nakano, K., "Stiff Constant Strain Rate Testing Machine," Research Report, No. 37, Building Research Inst., Japan, 1969, 10pp.
- Nelissen, L.J.M., "Biaxial Testing of Normal Concrete," Heron (Delft), Vol. 18, No. 1, 1972, 90pp.
- Ngo, D., et al., "Finite Element Study of Reinforced Concrete Beams with Diagonal Tension Cracks," UCSESM Report No. 70-19, Univ. of Calif., Berkeley, Dec. 1970.

- Nilson, A.H., "Finite Element Analysis of Reinforced Concrete," Ph.D. Dissertation, Univ. of Calif., Berkeley, March 1967.
- Nilson, A.H., "Nonlinear Analysis of Reinforced Concrete by the Finite Element," ACI J., Vol. 65, No. 9, Sept. 1968, pp. 757-766.
- Nishizawa, N., "Strength of Concrete in Combined Tension and Compression Loading," Laboratory Report of Electric Technology, Vol. 11, No. 3,4, June 1969.
- Niwa, Y., et al., "Failure Criterion of Mortar under Triaxial Compression Stresses," Jour., The Society of Materials Science, Japan, Vol. 16, No. 161, Feb. 1967, pp. 108-114.
- Noguchi, H., "Finite Element Nonlinear Analysis of Reinforced Concrete (Part 1: State-of-the-Art)," Proc. Kanto Dist. Symp., AIJ, No. 47, July 1976, pp. 193-196.
- Noguchi, H., "Finite Element Nonlinear Analysis of Reinforced Concrete (Part 1: Stress-Strain Relationships of Concrete under Biaxial Stresses)," Trans. of AIJ, No. 252, Feb. 1977, pp. 1-11.
- Noguchi, H., "Finite Element Nonlinear Analysis of Reinforced Concrete (Part 4: Crack Initiation and Propagation)," Trans. of AIJ, No. 262, Dec. 1977, pp. 43-52.
- Ogawa, J., et al., "Experimental Study on Cyclic Characteristics of Concrete," Proc. Annual Conv., AIJ, Oct. 1975, pp. 10001-10002.
- Okada, T., et al., "Restoring Forces of Reinforced Concrete Members under Cyclic Stresses," Proc. Annual Conv., AIJ, Oct. 1972, pp. 1045-1048.
- Okajima, T., "The Strength of Concrete under Combined Axial Force (Compression and Tension) and Torsional Moment," Trans. of AIJ, No. 178, Dec. 1970, pp. 1-10.
- Okajima, T., "Failure of Plain Concrete under Combined Stresses (Part 1)," Trans. of AIJ, No. 189, Nov. 1971, pp. 15-24.
- Okajima, T., "Elastic Plastic Characteristics of Concrete under Combined Axial Force (Compression and Tension) and Torsional Moment," Proc. Annual Conv., AIJ, Oct. 1972, pp. 41-42.
- Okajima, T., "Failure of Plain Concrete under Combined Stresses," Trans. of AIJ, No. 202, Dec. 1972, pp. 1-10.
- Okajima, T., "Critical Tensile Strain of Plain Concrete under Biaxial Stress," Jour., The Society of Materials Science, Japan, Vol. 22, No. 232, Jan. 1973, pp. 33-37.
- Okamoto, S., et al., "Earthquake Resistance of Prestressed Concrete Structures," Annual Report of BRI, Japan, 1971, pp. 314-323.
- Okamoto, S., et al., "Earthquake Resistance of Prestressed Concrete Structures," Proc. Annual Conv., AIJ, Oct. 1976, pp. 1251-1252.
- Okushima, S., et al., "Experimental Study on Stress-Strain Curve for Concrete," Bulletin of Cement Technology, Tokyo, Vol. 28, 1974, pp. 215-219.
- Omote, Y., et al., "Hysteretic Characteristics of Reinforced Concrete Cylindrical Sections Subjected to Cyclic Loading," Proc. Annual Conv., AIJ, Oct. 1974, pp. 1265-1266.
- Otani, K., et al., "Strength and Strain Characteristics of Concrete under Biaxial Stresses," Bulletin of Cement Technology, Tokyo, Vol. 27, 1973, pp. 261-266.
- Palaniswamy, R., et al., "Fracture and Stress-Strain Relationship of Concrete under Triaxial Compression," Jour. Struct. Div., ASCE, Vol. 100, No. ST5, May 1974, pp. 901-916.
- Park, R., et al., "Reinforced Concrete Members with Cyclic Loading," Jour. Struct. Div., ASCE, Vol. 98, No. ST7, July 1972, pp. 1341-1360.

- Park, K., et al., "Reinforced Concrete Structures," Wiley-Interscience, 1975, pp. 21-30.
- Pfister, J.F., "Influence of Ties on the Behaviour of Reinforced Concrete Columns," ACI J., Vol. 61, No. 5, May 1964, pp. 521-536.
- Phillips, D.V., et al., "Finite Element Non-linear Analysis of Concrete Structures," Proc. Inst. Civ. Engrs., Part 2, March 1976, pp. 59-88.
- Popovics, S., "Stress-Strain Relations for Concrete under Compression," ACI J., Vol. 67, No. 3, March 1970, pp. 243-248.
- Popovics, S., "Factors Affecting the Elastic Deformation of Concrete," Proc. of the Intern. Conference on Mechanical Behaviour of Materials, Vol. IV, Kyoto, Aug. 1971, pp. 172-183.
- Richart, F.E., et al., "A Study of the Failure of Concrete under Combined Compressive Stresses, Bulletin, No. 185, Univ. of Illinois, Engrg. Experiment Station, Nov. 1928.
- Romstad, K.M., et al., "Numerical Biaxial Characterization for Concrete," Jour. Engr. Mech., ASCE, Vol. 100, No. EM5, Oct. 1974, pp. 935-948.
- Roy, H.E.H., et al., "Ductility of Concrete," Proc. of the Internat. Symposium on the Flexural Mechanics of Reinforced Concrete, ASCE-ACI, Nov. 1964, pp. 213-224.
- Rüsch, H., "Versuche zur Festigkeit der Biegedruckzone," Deutscher Ausschuss für Stahlbeton, Heft 120, Berlin, 1955, 94pp.
- Rüsch, H., "Researches Toward a General Flexural Theory for Structural Concrete," ACI J., Vol. 57, No. 1, July 1960, pp. 1-28.
- Rüsch, H., et al., "Der Einfluss von Bügeln und Druckstäben auf das Verhalten der Biegedruckzone Von Stahlbetonbalken," Heft 148, Deutscher Ausschuss für Stahlbeton, Berlin, 1963, 75pp.
- Sakurai, S., "Failure Criterion of Rock under Static Loading," Jour., The Society of Materials Science, Japn, Vol. 17, No. 181, Oct. 1968, pp. 876- 881.
- Sargin, M., et al., "Effects of Lateral Reinforcement upon the Strength and Deformation Properties of Concrete," Mag. of Conc. Res., Vol. 23, No. 75-76, June-Sept. 1971, pp. 99-110.
- Sargin, M., "Stress-Strain Relationships for Concrete and the Analysis of Structural Concrete Sections," Study No. 4, Solid Mech. Div., Univ. of Waterloo, Ont., Canada, 1971, 167pp.
- Sato, N., et al., "Two-Dimensional Nonlinear Analysis of Reinforced Concrete Members," Proc. Kanto Dist. Symp., AIJ, No. 46, July 1975, pp. 161-164.
- Schnobrich, W.C., "Behavior of Reinforced Concrete Structures Predicted by the Finite Element Method," Second National Symposium on Computerized Structural Analysis and Design, George Washington Univ., March 1976.
- Scordelis, A.C., "Finite Element Analysis of Reinforced Concrete Structures," Proc. of the Speciality Conference on FEM in Civil Engrg., McGill Univ., CSCE, EIC, Montreal, 1972, pp. 71-113.
- Shah, S.P., et al., "Inelastic Behavior and Fracture of Concrete," ACI J., Vol. 63, No. 9, Sept. 1966, pp. 925-930.
- Shiire, T., et al., "Behavior of Bond between Aggregates and Mortar at Failure of Concrete," Proc. Annual Conv., AIJ, Oct. 1972, pp. 31-32.
- Shimazu, T., et al., "Confinement Effects of Web Reinforcements on Reinforced Concrete Columns," Proc. of the Sixth World Conference on Earthquake Engrg., Vol. III, India, Jan. 1977, pp. 3120-3126.
- Sinha, B.P., et al., "Stress-Strain Relations for Concrete under Cyclic Loading," ACI J., Vol. 61, No. 2, Feb. 1964, pp. 195-211.
- Smith, G.M., "Failure of Concrete under Combined Tensile and Compressive Stresses," ACI J., Vol. 50, Nov. 1953, pp. 137-140.

- Smith, G.M., et al., "Ultimate Theory in Flexure by Exponential Function," ACI J., Vol. 52, No. 3, Nov. 1955, pp. 349-360.
- Soliman, M.T.M., et al., "The Flexural Stress-Strain Relationship of Concrete Confined by Rectangular Transverse Reinforcement," Mag. of Conc. Res., Vol. 19, No. 61, Dec. 1967, pp. 223-238.
- Suenaga, Y., et al., "Kinetic Analysis of Concrete under Combined Stresses (Part 1)," Trans. of AIJ, No. 165, Nov. 1969, pp. 1-10.
- Suzuki, K., et al., "Testing Method of Concrete under Flexural Compression and a Study on the Mechanical Characteristics," Proc. Annual Conv., AIJ, Oct. 1976, pp. 1363-1364.
- Suzuki, K., et al., "Study on the Mechanical Characteristics of Concrete Subjected to Lateral Confinement," Proc. Annual Conv., AIJ, Oct. 1977, pp. 1737-1738.
- Suzuki, K., et al., "Study on the Stiff Testing Machine and Complete Stress-Strain Relations for Concrete," Proc. Annual Conv., AIJ, Sept. 1978, pp. 1541-1542.
- Szulczynski, T., et al., "Load-Deformation Characteristics of Reinforced Concrete Prisms with Rectilinear Transverse Reinforcement," Structural Research Series No. 224, Civil Engrg. Studies, Univ. of Illinois, Sept. 1961, 54pp.
- Takiguchi, K., et al., "Two-Dimensional Nonlinear Analysis of Concrete Members by the Finite Element Method (Part 1)," Trans. of AIJ, No. 189, Nov. 1971, pp. 51-57.
- Takiguchi, K., et al., "Analysis of Reinforced Concrete Sections Subjected to Bi-axial Bending Moments," Trans. of AIJ, No. 250, Dec. 1976, pp. 1-8.
- Tanigawa, Y., et al., "Plastic Deformation Behavior of Concrete Confined by Rectangular Ties," Proc. Annual Conv., AIJ, Oct. 1977, pp. 1745-1746.
- Tanigawa, Y., et al., "A New Type of Stiff Testing Machine and Complete Stress-Strain Curve of Concrete," Trans. of AIJ, No. 260, Oct. 1977, pp. 9-19.
- Tanigawa, Y., et al., "Hysteretic Characteristics of Concrete in the Domain of High Compressive Strain," Proc. Annual Conv., AIJ, Sept. 1978, pp. 449-450.
- Tasuji, M.E., et al., "Stress-Strain Response and Fracture of Concrete in Biaxial Loading," ACI J., Vol. 75, No. 7, July 1978, pp. 306-312.
- Taylor, M.A., et al., "A Finite Element Computer Program for the Prediction of the Behavior of Reinforced Concrete Structures Subjected to Cracking," Final Report to Naval Civil Engrg. Laboratory, Port Hueneme, Calif., June 1972.
- Tsuboi, Y., et al., "Failure of Concrete under Combined Stresses," Trans. of AIJ, No. 63, Oct. 1964, pp. 637-640.
- Tulin, L.G., et al., Discussion of "Equation for the Stress-Strain Curve of Concrete," by P. Desayi, et al., ACI J., Vol. 61, No. 9, Sept. 1964, pp. 1236-1238.
- Umemura, H., "Plastic Deformation and Ultimate Strength of Reinforced Concrete Beams," Trans. of AIJ, No. 42, Feb. 1951, pp. 59-70.
- Uzumeri, S.M., et al., "Strength and Ductility of Reinforced Concrete Columns with Rectangular Ties," Proc. of a Workshop on Earthquake-Resistant Reinforced Concrete Building Construction, Vol. 2, Univ. of Calif., Berkeley, July 1977, pp. 611-623.
- Vallenas, J., et al., "Concrete Confined by Rectangular Hoops Subjected to Axial Loads," Report No. EERC 77-13, Univ. of Calif., Berkeley, 1977.
- Wakabayashi, M., et al., "Strain Rate Effects on Stress-Strain Relations for Reinforced Concrete Materials," Proc. Annual Conv., AIJ, Sept. 1978, pp. 1547-1548.

- Wang, P.T., "Stress-Strain Curves of Normal and Lightweight Concrete in Compression," ACI J., Vol. 75, No. 11, Nov. 1978, pp. 603-611.
- Watanabe, F., "Complete Stress-Strain Curve for Concrete in Concentric Compression," Proc. of the Intern. Conference on Mechanical Behavior of Materials, Vol. IV, Kyoto, Aug. 1971, pp. 153-161.
- Wegner, R., "Finite Element-Models for Reinforced Concrete," U.S.-Germany Symposium, "Formulation and Computational Methods in Finite Element Analyses," M.I.T., Boston, Aug. 1976.
- Yamada, M., et al., "Study on Plastic Fatigue of Concrete," Trans. of AIJ, Extra, Oct. 1967, pp. 307.
- Yamada, M., et al., "Study on Plastic Fatigue of Concrete," Proc. Annual Conv., AIJ, Oct. 1976, pp. 1255-1256.
- Yoshimoto, A., "Rheological Model of Concrete under Cyclic Loading," Bulletin of Cement Technology, Tokyo, Vol. 27, 1973, pp. 225-228.



THEME I c

PROPERTIES OF BOND BETWEEN CONCRETE AND STEEL UNDER LOAD  
CYCLES IDEALIZING SEISMIC ACTIONS

PROPRIETES DE L'ADHERENCE ENTRE BETON ET ACIER SOUS CYCLES  
DE CHARGE REPRESENTATIFS DES ACTIONS SISMIQUES

Reporter  
Rapporteur

Theodosios P. TASSIOS  
National Technical University  
Athens, Greece





PROPERTIES OF BOND BETWEEN CONCRETE AND STEEL  
UNDER LOAD CYCLES IDEALIZING SEISMIC ACTIONS

PROPRIETES DE L'ADHERENCE ENTRE BETON ET ACIER  
SOUS CYCLES DE CHARGE REPRESENTATIFS DES ACTIONS SISMQUES

Theodosios P. TASSIOS  
National Technical University  
Athens, Greece

1.- P R E A M B L E

"There are extraordinarily many unresolved problems in the general area of bond and slip of reinforcing steel under severe cyclic loading".

E. POPOV, 1977

- 1.1. This was not intended to be a detailed State of the Art Report. One cannot find here a systematic review of all previous papers published on the subject (mainly after 1967).

This Report has rather to be considered as an attempt to serve as a framework of ideas, for a possible rational approach of the mechanisms governing bond, mainly under cyclic loading. Nevertheless, many References, are cited and numerical values are very often presented along this Report, making practical "computing" possible for some design purposes.

- 1.2. One cannot overestimate the fundamental significance of steel-to-concrete bond on every aspect of structural behaviour of R.C., including anchorage and splices, cracking, deformations, damping etc. When cyclic loading enters into the picture, bond deterioration under cyclic straining calls for higher development lengths, better provisions against cracking, measures against larger deflections and dangerous stiffness degradation; finally a problem of low cycle fatigue or desintegration may be raised due to this bond deterioration, especially within joints, in monolithic or pre-casting technology. Compared to this fundamental significance of bond, the amount of research devoted to this topic (both theoretical and experimental) is strangely small, particularly when reversed loading is concerned. As a consequence, the preparation of this Report was not a very easy task: On many occasions, the Reporter felt the obligation to make use of oversimplifications and/or simple assumptions when evidence was missing; otherwise, this Report would be an incoherent alinement of unconnected empirical data. It is hoped, however, that precisely these weak points of the Report will engender the additional research works urgently needed, so that after an extremely short time this Report will be obsolete.

## 2.- FOR A CONCEPTUAL MODEL OF BOND

"A thorough knowledge of the sources of bond would help reduce the amount of required testing and make it possible to predict and understand the influence of variables to which bond is most sensitive".

Stocker + Sozen, 1970

### 2.0. Before loading

- a) Penetration of dissolved components of cement paste in the oxide layer of the steel (physicochemical interlocking), [Martin, 1967].
- b) Interlocking of cement paste on the surface irregularities of the bar (approx. 30  $\mu$  of depth and 300  $\mu$  of width, [Rehm, 1961]), as well as interlocking of mortar on the possible ribs of a (deformed) bar.
- c) Casting of concrete, depending on the position and direction of the steel bar, affects bond due to settlement, bleeding and surrounding pressure of fresh concrete, [e.g. Ferguson, 1966].
- d) Shrinkage of concrete creates compressive stresses " $\sigma_{y0}$ " normal to the lateral surface of the bar. For a shrinkage value of  $3 \cdot 10^{-4}$ ,  $\sigma'_{y0}$  - values of the order of 0,5 MPa have been reported [Lutz + Gergely, 1967]. A linear relationship is found between shrinkage coefficient and  $\sigma_{y0}$  -values, depending on the elasticity moduli of the paste and the "inclusion" [Koufopoulos + Theocaris, 1969].

### 2.1. Loading of bar within uncracked concrete

- a) Extremely small slips are produced (of the order of few microns [ $\mu$ ]) before reaching the level  $\tau_o$  of adhesion (Fig. A2/1). Values of  $\tau_o$  as low as 0,6 MPa are reported for almost zero slip [Mikhailov, 1952]. The same order of magnitude (approx. 0,4 ÷ 1,5 MPa) has been measured for cement-paste and aggregate interface adhesions under tension [Taylor + Broms, 1964]. The corresponding slip may be of the order of 5÷10 $\mu$ (see, e.g., Edwards + Yannopoulos, 1978).
- b) Further loading will mobilize the mechanical interlocking of cement paste on the microscopic irregularities of the bar surface, as well as the interlocking of the mortar on the ribs if any. Increasing bond-stresses  $\tau$  thus induced into the surrounding concrete may create a first internal cracking (at, say,  $\tau = \tau_A$ ) of the concrete. Such cracks will in turn modify the response of this concrete: Its stiffness will be diminished; consequently larger slips will be needed for further  $\tau$  - increments.

## 2.2. First internal cracking

a) Figures 2/1 to 2/3 show several stress distributions around the bar, depending i.a. on the conditions of loading and the subsequent  $\tau$ -distribution, as well as on the boundary conditions. In spite of their variety, the following characteristics may be derived from these examples:

- Relatively large longitudinal tension stresses  $\sigma_x$  are acting on the concrete surrounding the bar, if tensioned.
- Compressive radial stresses  $\sigma_y$  are engendered by the pull-out itself, at least away from the boundaries and/or when separation near the end-face is not taking place. (In this connection, Fig. 2/4 may be instructive: If a tensioning displacement were applied,  $\sigma_y$  would become tension near the end-face, leading to a possible separation). Similar compressive  $\sigma_y$  are shown in Fig. 2/5.

b) Under the combined action of  $\tau$ ,  $\sigma_x$  and  $\sigma_y$ , plus the possible "external" longitudinal and radial stresses (shrinkage- $\sigma_{y0}$  included), large diagonal tension stresses  $\sigma_I$  are produced, leading to diagonal (transversal) cracks along the bar, as found experimentally [Goto, 1971] or by means of finite elements simulation (Fig. 2/5), [Yannopoulos, 1976].

In the meantime, tangential normal tensions  $\sigma_t$  (see i.a. Fig. 2/3), created due to the radial compressions  $\sigma_y$ , tend to produce internal micro-splitting. Nevertheless, for the stage of stresses considered just now,  $\sigma_t$ -values are somehow lower than  $\sigma_I$  values. Consequently,  $\sigma_t$  transversal cracking precedes splitting cracking.

c) The critical  $\tau_A$ -value for the first internal cracking is highly dependant on a large variety of conditions summarized here below.

### • Technological conditions:

- Tension strength ( $f_{ct}$ ) of concrete, plain or as modified (slightly though) by means of both longitudinal and/or transversal reinforcements (stirrups, spirals etc).
- Coefficient of shrinkage.
- Position and direction of steel bar against direction of settlement of fresh concrete.
- Amount of cover and/or free spacings between adjacent bars.

### • Loading conditions:

- External axial and/or radial loading of concrete, produced independently of the bond action. It is worth to note here that this is not always the case with external shear forces: Flexural reinforcements introduce to the concrete just the amount of axial bond-force which is dictated by the external shear force.
- Loading induced by the stressing of the bar itself. This loading is extremely sensitive to actual conditions: Pull-out or push-in, possibilities for

- confinement and wedging (stirrups, cover etc).
- Rate of loading.

Under the actual state of knowledge, it is not possible to quantify the influence of all the above mentioned conditions on the critical local bond-stress  $\tau_A$  which leads to the first local cracking. Nevertheless, Fig. 2/6 offers a first elementary quantification of this nature  $\tau_A = \zeta \cdot f_{ct}$ , where  $\zeta$  depends on  $\sigma_x$  and  $\sigma_y$  values, both of external or internal origin. Empirical corrective factors should complete this equation. However for the limits of variation of  $\sigma_x$  and  $\sigma_y$  shown in Fig. 2/1 to 2/3, one could venture some rough estimations for  $\tau_A$  at points situated at a distance  $l/3$  from the points of severe discontinuity:

Fig. A2/1,  $\sigma_x = +0,55 \tau$ ,  $\sigma_y = 0$   $\therefore \tau_A \approx 0,8 f_{ct}$

Fig. A2/2,  $\sigma_x = +1,0 \tau$ ,  $\sigma_y = 0$   $\therefore \tau_A \approx 0,6 f_{ct}$

Fig. A2/3,  $\sigma_x = +0,8 \tau$ ,  $\sigma_y = -0,6 \tau$   $\therefore \tau_A \approx 0,8 f_{ct}$

Some possible favourable conditions could also be taken into account for many practical cases. Thus, radial compression due to shrinkage, a certain amount of stirrups, as well as a reasonable plastic delay of the phenomenon, may easily rise these figures to the level of  $\tau_A \approx f_{ct}$ , or even higher. (\*) Finally, for the case of

pushed-in bars (Fig. A2/4) a similar rough estimates could lead to:

$\sigma_x = -4,5 \tau$ ,  $\sigma_y = +0,5 \tau$   $\therefore \tau_A \approx 1,5 f_{ct}$

which, in turn, may be raised to approximately  $\tau_A \approx 2f_{ct}$ .

d) Variable as it may be this  $\tau_A$ - value, the small local slips of the bar for  $\tau < \tau_A$  appear to depend only on the extensibility of plain concrete. Consequently, the slope of the first branch of  $\tau$ -s curve illustrated in Fig. 2/7, may reasonably be considered as constant.

### 2.3.- Loading of the bar after the first cracking

a) In the preceding paragraph it is recognized that some splitting cracks may appear just after or simultaneously with the main transversal (diagonal) cracking. As the loading increases, these splitting cracks propagate both longitudinally and radially (see Fig. 2/5). Nevertheless, up to this moment, the surrounding concrete can still offer the following mechanisms for bond development.

- General shear by means of mechanical interlocking on the surface irregularities previously mentioned: A first difference, after the cracks which started at the stress level of  $\tau_A$ , is that the surrounding concrete is now much weaker; consequently, the slope AB (Fig. 2/7) will be comparatively very much smaller. A second difference lies in that, after the diagonal

(\*) E.g. for moderate or pronounced confinement, empirical factors equal to  $1\frac{1}{4}$  and  $1\frac{1}{2}$  may be justified.

microcracking, constant radial stresses  $\sigma_r \approx \tau$  are necessarily introduced at the interface  $\gamma$  (Fig. A2/8) for equilibrium purposes. Consequently, for relatively large slips which have taken place (and have partly destroyed interlocking), a frictional component is entering the picture. Thanks to this friction ( $\tau_f = \mu \cdot \sigma_y$ ) even plain bars are able to replace, partly though, the lost part of interlocking-transfer of bond stresses.

And so it is, up to a certain stress level  $\tau_B$  for which splitting cracks outbreak through the whole cover "c" (see Fig. 2/9). Unless, in the meantime, the frictional resistance is exhausted or becomes insufficient: In such a case, splitting is not generalized but the bar is pulled-out leaving behind it an almost intact hole into the concrete.

- Deformed bars apply their bond shear stresses by means of similar but much more pronounced (macroscaled) mechanisms. The big difference here is that the rib's-interlocking cannot be lost. Consequently, only a generalized splitting can put an end to this stage of bond, for  $\tau = \tau_B$ .

b) An attempt is made here (Fig. 2/10) to illustrate the stress condition at the moment of splitting-outbreak (see also Tepfers [1973]):

$$\sigma_y \cdot \phi = 2 \frac{2}{3} (c - e_{crit}) \cdot f_{ct} + (2 \frac{A_s}{a_s} \cdot \sigma_s) \cdot \gamma$$

where the empirical factor " $\gamma$ " may reflect (very roughly though), the efficiency of the surrounding reinforcement provided against splitting, under the condition, however, that this reinforcement is close to the bar (closer than  $e_{crit}$ ). At the moment of cracking concrete extensibility may be taken as  $\epsilon_{ct} \approx 2 \cdot 10^{-4}$ . Consequently,  $\sigma_s = \epsilon_{ct} \cdot E_s \approx 40$  MPa. Therefore for  $\beta \approx 45^\circ$  i.e.  $\sigma_y = \tau$ , (Fig. 2/8), and for the critical depth of pre-splitting suggested by Tepfers [1973],  $e_{crit} \approx \frac{c}{3} - \frac{\phi}{4}$ , (Fig. 2/9), it follows:

$$\tau_B \approx \left( \frac{2}{3} \frac{c}{\phi} + \frac{1}{3} \right) \cdot f_{ct} + 2\gamma \cdot \epsilon_{ct} \cdot E_s \cdot \frac{A_s}{\phi a_s}, \text{ where } \frac{c}{\phi} \leq 6$$

c) When an external pressure  $p_y$  is acting on the lateral surface of the bar, an additional bond should be taken into account  $\Delta \tau = \mu \cdot p_y$ , where  $\mu$  denotes an appropriate friction(\*) coefficient for small values of slips. On the basis of the data presented in §2.5a, a value of  $\mu \approx \frac{1}{4}$  is used here. So that, finally,

$$\tau_B \approx \left( \frac{2}{3} \frac{c}{\phi} + \frac{1}{3} \right) \cdot f_{ct} + 2\gamma \epsilon_{ct} \cdot E_s \cdot \frac{A_s}{\phi a_s} + \frac{1}{4} p_y$$

$$\text{where } \frac{c}{\phi} \leq 6$$

(\*) For the oversimplified approach of the model we are dealing with here, this external pressure cannot be taken into account in a more elegant way, in a medium with manifold cracks.

d) In the case of plain bars, as mentioned before, this bond level is not practically reached, because of the insufficient friction which should be mobilized in order to replace lost interlocking. As a consequence, for plain bars, a value substantially lower will put an end to this stage-and this will also be the ultimate bond  $\tau_u$  for plain bars. An attempt is made here to estimate a possible upper bound value of  $\tau_u$  for plain bars: Assuming a higher friction coefficient equal to 0,4 (thanks to the uniformity and the low value of normal stresses acting on the interface of plain bars) (see §2.5a),

$$\text{i.e. } \tau = 0,4 \cdot \sigma_y$$

the previously found equation becomes

$$\tau_u < 0,4 \left( \frac{2}{3} \frac{c}{\phi} + \frac{1}{3} \right) f_{ct} + 0,8 \gamma \epsilon_{ct} \cdot E_s \cdot \frac{A_s}{\phi a_s} + 0,4 \cdot p_y$$

However it should always be  $0,4 \left( \frac{2}{3} \frac{c}{\phi} + \frac{1}{3} \right) > \zeta$ , (§2.2.c).

#### 2.4. Loading of deformed bars up to bond failure

a) In this pseudo-quantitative building-up of a simplified physical model, it will be admitted that the main remaining mechanism is ribs' interlocking, combined with considerable destruction of the surrounding concrete. Fig. 2/11 illustrates a possible final stage at bond-failure: The concrete "teeth", between consecutive transversal cracks, are loaded with a compressive stress approximately equal to  $2\tau_u$  (see Fig. 2/8). It is worth to remind here that longitudinal cracks (splitting) have isolated these concrete "teeth", which are now loaded under almost unconfined compression, notwithstanding some shear. Due to this shear, let us consider a reduction of compressive strength, putting

$$\sigma_c (\approx 2\tau_u) = \frac{2}{3} \cdot f_{cc}$$

Therefore,  $\tau \approx f_{cc}/3$ .

b) For the possible role of the surrounding reinforcement (spiral, steel area  $A_s$ , hoop diameter  $d_s$ , spacing  $a_s$ ) one may think about the favourable consequences of the lateral pressure " $p_s$ " on the compressive strength of concrete, when the hoop is stressed by the wedging action (diagonal compressive stress  $\sigma_c$ , Fig. 2/11):

$$p_s \cdot d_s a_s \approx (2A_s f_{ys}) \cdot \gamma$$

where " $\gamma$ " is a corrective factor depending on the geometry of the surrounding reinforcement (Fig. 2/10).

Hence,  $p_s = \gamma \cdot \frac{2A_s}{a_s d_s} f_{ys}$  and its contribution to the

(triaxial) strength of teeth-concrete:

$$f_{cc}^* \approx f_{cc} + 4 \cdot p_s$$

Consequently,

$$\sigma_c (\approx 2\tau) \approx \frac{2}{3} f_{cc}^*$$

$$\text{and } \tau_u \approx \frac{1}{3} f_{cc} + \frac{8}{3} \gamma \frac{A_s}{a_s d_s} f_{ys}$$

c) In case of an external pressure  $p_y$ , an appropriate friction coefficient should also be selected and in this case an average value of  $\mu = \frac{1}{3}$  seems to be reasonable (see 2.5.a). Consequently,

$$\tau_u = \frac{1}{3} f_{cc} + \frac{8}{3} \gamma \frac{A_s}{a_s d_s} f_{ys} + \frac{1}{3} p_y$$

(only for deformed bars)

## 2.5. Friction coefficients

After the ultimate stage described in §2.4. for deformed bars (or in § 2.3 for plain bars), the only mechanism left is f r i c t i o n, which nevertheless has also partly contributed to previous stages. In the following, a short reference is made to possible values of friction coefficients.

a) Concrete to embedded steel: The values found for plain bars by Stocker + Sozen, [1970], highly scattered though (between 0,15 and 0,50), are practically centered around the limits 0,20 to 0,40, for a rather large slip equal to 3 mm approximately.

For deformed bars, and for slips of the order of 0,05 to 0,15 mm, Doerr [1978] offers experimental data leading to  $\mu$ -values equal to 0,26, 0,30 and 0,55. Consequently, it seems reasonable for (the time being) to expect friction coefficients around  $\frac{1}{4}$  for plain and  $\frac{1}{3}$  for deformed bars.

b) Concrete to concrete: Tassios + Tsoukantas [1978] have summarized several test results leading to friction coefficients as high as 1,0 to 3,0, valid for normal stresses lower than 1 MPa. Nevertheless, for normal stresses higher than, say, 5 MPa acting on keyed-patched joints, it seems that values lower than 0,8 should be used. For the purposes of this Report a value  $\mu = 0,6$  will be adopted. It is, however, understood that this will be a source of very large uncertainty.

## 2.6. Residual bond strength

a) An abrupt decrease of bond response should be expected under strain-controlled conditions, for slips larger than those corresponding to the peak bond value  $\tau_u$ .

As for all falling branches of stress-strain curves, here again there is a big uncertainty about the level of the residual bond strength  $\tau_r$  and the relevant transition curve (see Fig. 2/7). Nevertheless, Fig. 2/12 is an attempt to describe the mechanism which secures this residual "bond" (shear resistance) for very large slips, provided that splitting does not lead to a complete desintegration of the surrounding concrete (and this is feasible by means of a minimum of surrounding reinforcement or thanks to the contiguity of less stressed parts of the bar): The quasi-triangular sub-teeth have the

tendency to move along together with the bar. The main resistance against this movement seems to be due to the concrete-to-concrete interlocking along the compression cracks AB. The frictional resistance equals  $\tau_b = \mu_r \sigma_b$ , where  $\mu_r \approx 0,6$  (for  $\sigma > 10$  MPa), (see preceding paragraph), and  $\sigma_b$  may be estimated (\*) from its value at the moment of compressive rupture of teeth (§ 2.4., Fig. 2/11),

$$\sigma_b \approx \frac{1}{2} \cdot f_{cc} \cdot (1 - \sin \varphi).$$

Under these hypothetical conditions,

$$\begin{aligned} \tau_r &= \frac{b}{a} \tau_b \cdot \cos \frac{\varphi}{2} = \frac{b}{a} \mu_r \sigma_b \cos \frac{\varphi}{2} \\ &\approx 0,30 \cos \frac{\varphi}{2} (1 - \sin \varphi) \left( \sin \frac{\varphi}{2} + \sqrt{1 + \sin^2 \frac{\varphi}{2}} \right) f_{cc} \end{aligned}$$

or, for  $\varphi \approx 45^\circ$ ,  $\tau_r \approx 0,12 f_{cc}$ .

b) In order to take into account the surrounding reinforcement (Fig. A2/13), only dowel action will be considered here, as expressed by Rasmussen [1982] and modified by Tassios + Tsoukantas [1978]:

$$\tau_{rd} \pi d \cdot b \cos \frac{\varphi}{2} \cdot \left( \frac{a_s}{a} \right) \approx 2 A_s f_{ct} \sqrt{f_{ys}} \text{ [MPa]}$$

Consequently, for  $\varphi \approx 45^\circ$ ,  $\mu_r = 0,6$  and  $a \approx 0,7\varnothing$ ,

$$\tau_r \approx 0,12 f_{cc} + 0,30 \frac{A_s}{\varnothing a s} f_{ct} \sqrt{f_{ct}} \text{ [MPa]} + 1,40 \cdot p_y$$

(for deformed bars)

As a matter of fact, for clear "splitting" failures, an abrupt falling branch is expected with almost zero residual bond-strength (see line CG in Fig. 2/7).

c) In the above formula, the last term takes into consideration the possible action of external radial pressure:

$$\begin{aligned} \tau_f &= p_y \left( \frac{\sin \varphi}{2} + \mu_r \cdot \cos^2 \frac{\varphi}{2} \right) \\ \tau_{rf} &= \frac{b \cos \frac{\varphi}{2}}{a} \tau_f \approx 1,40 p_y \end{aligned}$$

This, however, is a rather doubtfully high value and should not be used for  $p_y > \frac{1}{6} f_{cc}$ .

d) For plain bars, an estimation of the residual bond-strength could be made if the residual  $\sigma_y$ -values were known after the bond failure discussed in §2.3.d. Under the actual state of knowledge, however, only the following rough proposal could be made, provided that splitting does not lead to a complete desintegration of the surrounding concrete (compare §2.6.a):

After a considerable amount of slip, it could be admitted that irregularities are smoothed and friction has come to its minimum value valid for smooth steel on sawn concrete surfaces ( $\mu \approx 0,15$ , Tassios + Demiris 1970). Consequently, under the assumption of "frozen" normal stress developed

(\*) This is a practical application of the assumption of "frozen" normal stress after shear yield of surface.



under the ultimate load  $\tau_u$ , it could be written.

$$\tau_r > 0,15 \sigma_{yu} \approx 0,3 (0,5 \sigma_{yu}) = 0,3 \tau_u$$

Obviously, for clear splitting failures, an abrupt falling branch is expected, with almost zero residual bond-strength (see line BF in Fig. 2/7). Nevertheless, such failures may be avoided, as previously mentioned, in many practical cases.

## 2.7. Unloading from $\tau_1 < \tau_u$ and reloading

a) Practically speaking, no rebound is expected after such an unloading between the points A and C of the descriptive curve of Fig.2/14: All internal cracks, as described in § 2.3. and 2.4., will practically remain open. Nevertheless, a very small amount of "elasticity" could possibly be expected: There are always some microscopic cantilevers of sound cement paste material, submitted to a kind of bending which may be released elastically after unloading. As a first approximation for the slope of this unloading branch PR, one could retain the initial slope of the loading curve  $0\tau_0$  (Fig.2/7), i.e., very roughly, equal to 5 MPa: 10  $\mu$  =  $K'_0$  = 0,5 MPa/ $\mu$ .

As soon as an opposite slip is imposed to the bar (representative points left to R' in Fig.2/14), a negative bond-stress  $\tau_{01}$  will be build-up. In order to make a rough estimation of the magnitude of this bond reaction against opposite slip, one may adopt once again the assumption of "frozen" normal stress. In such a case,  $\sigma_{y0} = \sigma_y = \tau_1$  (for  $\beta \approx 45^\circ$ ) and  $\tau_{01} = \mu(\sigma_{y0} + p_y)$  where  $\mu = \frac{1}{4}$  as it has been chosen in §2.3.c.

Therefore,  $\tau_{01} \approx - \frac{1}{4} (\tau_1 + p_y)$

b) This negative bond response will remain constant as a consequence of the assumption of "frozen"  $\sigma_y$ , as it has been developed at the moment of positive loading  $\tau = \tau_1$ .

As the opposite slips are further increasing the following modifications are induced to the surrounding concrete:

Transversal (diagonal) cracks start to close gradually. It is reasonable to admit that these cracks will be completely closed as soon as the previously observed slip will be withdrawn, i.e., approximately, when the horizontal line R'H will touch the antisymmetric monotonic curve OA'B'C'. From now on, should further opposite slips be still imposed, additional negative bond will be developed as anticipated by the curve OA'B'C': In fact, the surrounding concrete is "intact" again, since its diagonal cracks are closed and stressed under compression only. (Diagonal cracks perpendicular to the previous ones will possibly open if the negative bond should continue to increase). Nevertheless, the internal splitting cracks previously open (at "point" P) have remained open since  $\sigma_y$  - stresses were supposed to remain unchanged. Consequently, the negative loading

could not be described exactly by the antimetric curve OA'B'C'; somehow lower response should be expected (say arbitrarily, by two thirds).

c) When a new unloading will occur, a similar behaviour is expected. Nevertheless, in order to take into account the somehow degraded bond available at P', it seems reasonable to admit here

$$\tau_Q = \frac{1}{4}(\tau_{P'} + p_Y) = \frac{1}{4}(\frac{2}{3}\tau_1 + p_Y).$$

And during the "reloading" (slip to the right), the positive reaction  $\tau_Q$  will be kept constant for the same reasons as previously put forth for the value  $\tau_{01}$ . This time, the horizontal line QX of the diagramme (always in Fig. 2/14) will not rise-up unless the same slip is reached as at the beginning of the cycle, i.e. at the point X. In fact, it is at that moment that (i) diagonal cracks will gain their initial opening and they will react against additional opening, (ii) bursting stresses induced by the ribs will start to increase again and contribute to further splitting and/or to the compressive exhaustion of the concrete-teeth considered in §§ 2.3. and 2.4.

d) Similar cycling should be followed if the imposed slips would be larger (see loop YY'ZW, Fig. 2/14).

e) Further refinements of the model will be introduced in § 4, mainly on the basis of experimental evidence.

## 2.8. Combined bond and dowel action

For reasonably low values of concrete cover and/or transverse reinforcement, it is obvious that simultaneous dowel action will contribute to an early s p l i t t i n g of the surrounding concrete, thus increasing slip and diminishing bond strength.

Within this report only some rough experimental results will be mentioned [Sharma, 1969], although they have been found for large embedments:

Let " $P_{u,0}$ " be the characteristic bond-load at 0,5 mm end-slip under zero dowel load  $V_d = 0$ . The loss  $\Delta P$  in characteristic bond-load (for the same slip) due to a simultaneous action of a dowel load  $V_d$ , has been found (in a limited number of tests) to be  $\Delta P = 3V_d$ . Therefore for a small embedment "a" the following qualitative approximation could very roughly be made:  $\tau = P : \pi \phi a$ ,  $\sigma_d = V_d : \phi a$  and therefore  $\tau_{ud} \approx \tau_{u0} - \sigma_d$

## 2.9. Rate of pulling-out

Since bond-strength depends i.a. on compressive strength of concrete, it is reasonable to expect that bond-strength will be related to the rate of loading in a somehow similar way,

$$\tau_u : \tau_{u0} \approx 0,1 \left( \log \frac{\dot{t}}{\dot{t}_0} + 10 \right),$$

as it has been proposed by Kvirikadze [1977] for compressive strength.

Forty five percent (45%) higher local maximum bond-stresses

have been observed by Perry + Jundi [1969] near the loaded end of their long specimen (230 mm), for a rate  $\dot{\epsilon} = 160$  MPa/sec. After a correction of 20% due to the difference of strengths of concretes used in their static and dynamic tests (15,5 and 18,9 MPa respectively), the remaining net difference of 25% is approximately predictable by the above formula ( $\dot{\epsilon}_0 \approx 1 \frac{\text{MPa}}{\text{sec}}$ ).

## 2.10. Final corrections and summary

a) Against the conditions of concrete casting, the following corrective factors are applied as a first approximation.

Vertical casting parallel to the axis of the bar:  $\zeta = 1$ .  
Horizontal casting perpendicular to the axis of the bar:

$$\zeta = \frac{2}{3}$$

Particularly unfavourable conditions of casting (horizontal casting of high specimens, top or very small diameter bars):  $\zeta \leq \frac{1}{2}$

b) It is largely recognized that the location of the point considered along the interface has a very important influence on the local bond-slip characteristics. In fact, at points situated near a free end of the concrete block containing the bar, internal cracks (of all natures considered) may easily outbreak and diminish the local bond resistance. A rough proposal in order to quantify this phenomenon (coefficient " $\lambda$ ") is presented in Fig. 2/15, (based on Nilson's [1971], Fig. 13).

c) Summing-up of the formulae proposed for deformed bars:

$$\bullet \tau_A = \lambda \cdot \zeta \cdot f_{ct}$$

$\lambda$  = location factor, Fig. 2/15.

$\zeta$  = coefficient depending on the triaxial stress field acting on the surrounding concrete, Fig. 2/6.

$f_{ct}$  = tensile strength of concrete, mean value.

$$\bullet \tau_B = \xi \cdot \lambda \cdot \left( \frac{2}{3} \frac{c}{\phi} + \frac{1}{3} \right) f_{ct} + 80 \cdot \gamma \frac{A_s}{\phi a_s} + \frac{1}{4} p_y$$

$c$  = concrete cover } however  $\frac{c}{\phi} \leq 6$ .  
 $\phi$  = bar diameter }

$\gamma$  = geometry factor of the surrounding reinforcement Fig. 2/10.

$A_s$  = steel area of one bar of the surrounding reinforcement (separately for each direction)

$a_s$  = spacing of surrounding bars.

$p_y$  = externally applied pressure normally to the interface.

$$\bullet \tau_u = \frac{1}{3} \xi \cdot \lambda \cdot f_{cc} + \frac{8}{3} \gamma \frac{A_s}{a_s d_s} f_{ys} + \frac{1}{3} p_y$$

$f_{cc}$  = compressive strength of concrete.

$d_s$  = equivalent diameter of surrounding hoops.

$f_{ys}$  = yield strength of steel hoops.

- $\tau_r = 0,12 \cdot \xi \cdot \lambda \cdot f_{cc} + 0,30 \frac{A_s}{\phi a_s} f_{ct} \sqrt{f_{ys}^{MPa}} + 1,40 p_y$ , for  $p_y$  not higher of  $\frac{1}{6} f_{cc}$ .
- d) Summing-up for plain bars:
  - $\tau_A = \lambda \cdot \zeta \cdot f_{ct}$  as per deformed bars.
  - $\tau_u < 0,4 \xi \cdot \lambda \left( \frac{2}{3} \frac{c}{\phi} + \frac{1}{3} \right) f_{ct} + 30 \gamma \frac{A_s}{\phi a_s} + 0,4 p_y$   
 where  $0,4 \xi \left( \frac{2}{3} \frac{c}{\phi} + \frac{1}{3} \right) \geq \zeta$  and  $\frac{c}{\phi} \leq 6$
  - $\tau_r = 0,3 \tau_u$

**N o t e:**

Additional corrections might be necessary:

- For dowel loading of the bar pulled-out, a reduction of  $\tau_u$  equal to  $V_d : \phi \cdot a$  should be applied. Here,  $V_d$  denotes the dowel load supposed to be acting uniformly along the small length "a" where the pull-out force is reported.
- For dynamic bond-straining, an possible corrective factor could be equal to  $0,1 (\log \dot{\epsilon} + 10)$   
 where " $\dot{\epsilon}$ " denotes the rate of bond-stress in MPa/sec.

## 2.11. Characteristic slip values

Only characteristic bond-stresses have been considered so far, along the description of the conceptual model. The number of parameters influencing these characteristic bond-stresses is already vast and a very large scatter is to be expected around the proposed values. The situation will be plausibly worse when deformation is considered. As a consequence, the computational attempt made in Fig. 2/16 in order to get some rough estimations of the characteristic bond-slips, is but an oversimplified model which allows, nevertheless, to draw some first qualitative conclusions:

- Characteristic slip values seem to increase with the diameter of the bar, the concrete cover and the transverse reinforcement (\*). A similar increase is anticipated for larger rib spacings i.e. for larger  $a/v$  ratios (in Fig. 2/16  $a/v$  has been taken constantly equal to 16). Fig. 2/17 after Rehm [1961] is interesting to be reminded in this respect.
- For a typical case of  $\phi = 20$  mm and  $c = 40$  mm, one could find:  $S_A \approx 5 \mu$ ,  $S_B \approx 45 \mu$  and  $S_u \approx 170 \mu$ .

In connection with  $S_u$ , Rehm [1961] has stated that "the displacements occurring when shear resistance is overcome

(\*) This reinforcement was not taken into account in the numerical estimations of Fig.2/16, but its favourable influence towards higher  $\tau$ -values contributes directly to higher  $s$ -values.

are about 10% of the rib spacing".

c) Possible primary cracking, non-apparent though, may occur across an embedded long bar. In such cases, if these cracks are not separately considered, an apparent increase of local slips may be observed or adopted (in experiments or in calculations, respectively).

d) For the same rib's geometry, lower slips are expected for lower bond-strengths (e.g. next to primary cracks where  $\lambda \ll 1$ ).

### 3. EXPERIMENTAL EVIDENCE

#### 3.1. Monotonic loading

(local bond - local slip curves)

a) In Table I experimental and computed values of characteristic bond-stresses are shown and compared. Their ratios are brought to Fig. 3/2. A very poor agreement is found, yet on the basis of limited experimental data. Additional test results are bound to further worsen the validity of the proposed formulae, although a part of the scattering could be systematically explained if the differences in length of the "small" embedment were taken into account. In conclusion, the model set-forth in §2 is not able to serve but as qualitative tool, in order to locate or recognize the parameters of the problem, and to estimate their relative importance each time.

b) As it has been anticipated, characteristic slip-values are even less predictable than bond-stresses. The experimental arrangement, particularly the secondary stress-field induced by the supports, is one of the reasons for a much higher sensitivity of slip values. Table II shows some characteristic local slip values as found experimentally. No attempt is made here to find the corresponding computed values (§2.11, Fig. 2/16). The remark made in § 2.11.c, about possibly unnoticed internal primary cracks, should also be reminded here.

#### 3.2. Cyclic loading

Table III summarises some experimental results concerning local bond-slip under cyclic loading, (for "small" length of embedment, around 40mm). The scarcity of data does not allow for clear conclusion, although the temporary use of the values proposed is not excluded either. Experimental evidence concerning cyclic local bond-slip will be used again in § 4 for further refinements of the model.

#### 4. A SIMPLIFIED CONSTITUTIVE RULE FOR LOCAL BOND - SLIP UNDER CYCLIC LOADING

4.1. The monotonic curve of Fig. 2/7 (with characteristic  $\tau$ - $s$  values indicated in §2.10.c and Fig. 2/16) will serve as a guide-curve (not always an envelope).

#### 4.2. Degradation during slip-controlled cycles

In Fig. 4/1, unloading after the bond level  $\tau_{m1}$  leads to the bond level  $-\tau_{01} = \frac{1}{4} \tau_{m1}$  (as described in §2.7).

Further opposite slipping will take place on the constant level  $-\tau_{01}$  up to the point of intersection with the anti-metric curve ( $m'$ ) of monotonic loading reduced by  $\frac{2}{3}$ . The negative slip  $-s_1$  will, therefore, correspond to  $\frac{2}{3}$

the bond level  $-\frac{2}{3} \tau_{m1}$ . For the slip-controlled loading considered here, a positive slip will start to be imposed again; a positive bond level  $\tau_{01} = \frac{1}{4} (\frac{2}{3} \tau_{m1})$  will be reached soon, untill the initial slip  $+s_1$  is regained. If an opposite slip has to be imposed again, the absolute value of the residual bond  $-\tau_{r1,1}$  will be lower

than  $-\tau_{01}$ . In fact, it is reasonable to admit that after the successive opening, closing and re-opening of micro-cracks considered in §2.7.c, a certain loosening of the surrounding concrete will take place, so that for the  $n_1^{th}$  cycle:  $\tau_{r1,n1} < \tau_{01}$ . For assessing this "residual bond ratio" (more generally  $\rho_{ni} = \tau_{ri,ni} : \tau_{0i}$ ) experimental findings of Morita + Kaku [1973] and Plainis + Tassios [1978] have been used (see upper left part of Fig. 4/1).

It has also been admitted that this ratio equals the ratio between the corresponding peak-residual bond stresses  $\tau_{ri,n}$  and the initial stress  $\tau_{mi}$  (see lower right part of Fig. 4/1).

Thus when the full slip  $+s_i$  is imposed for  $n$  cycles, the corresponding extreme bonds are only equal to

$$+\rho_n \tau_{mi}, -\frac{2}{3} \rho_n \tau_{mi}$$

4.3. Next cycle, after a possible increase of  $s_i$  to  $s_{i+1}$ , will:

a) start from point  $[\tau'_{ri,ni}, s_i]$

b) go up (slope  $K'$ ) to the monotonic curve

c) continue on this curve, up to the point  $[\tau_{m,i+1}, s_{i+1}]$

Any unloading from this high point shall follow the previous rules.

- 4.4. An alternative possibility appears to be suggested by some experimental evidence (not yet reconfirmed though): Going up towards the monotonic curve (step 4.3.b) should stop at a level lower than that indicated by this curve; the next step (§ 4.3.c) should take place on a curve parallel to the corresponding part  $\tau_{mi}$ ,  $\tau_{m(i+1)}$  of the monotonic curve.

#### Note

A more precise (and somehow more complicated) rule has been proposed by Morita + Kaku [1973] based on their well known original work. The model proposed here has been inspired by:

- The somehow more severe degradation observed in our own tests (Plainis + Tassios, 1978).
- The sake for further simplicity, fitting to the simple conceptual model set-forth in this Report.

However, one cannot expect considerable differences between the results of computational applications of different models which are based on the same general lines.

#### 4.5. Repeated (not reversed) loading

For the sake of completeness, Fig. 4/2 shows an excellent example of experimental work on repeated local bond-slip. This example offers refinements useful for practical applications (stochastic approach included), as well as for the completion of the constitutive rule for bond-stress controlled loading. A somehow similar behaviour (gradual slip increase) is expected under sustained bond stress.

### 5. BOND AND CYCLIC LOADING OF R. C. ELEMENTS

#### 5.1. Tension stiffening degradation under cyclic loading

Higher peak bond-stresses reached in preceeding cycles produce a drastic bond reduction during unloading and reloading, as well as during subsequent cycles with lower peak stresses (Fig. 4/1). Consequently, higher steel stresses are expected between consecutive primary cracks, during unloading. This fact has been repeatedly confirmed experimentally, as e.g. by Ismail + Jirsa [1972], Fig. 5/1. An elementary analytical solution for the case shown in Fig. 5/1 is presented in Fig. 5/2 and Fig. 5/3. This solution is based in only one average local bond-slip curve, instead of a series of characteristic curves as suggested by Fig. 2/15. Besides, only three representative points have been considered along the half-length of the bar, in order to facilitate a direct

following up of this application (\*). Nevertheless, the phenomenon is clearly emerging from Fig. 5/3, although numerical values do not always coincide with those experimentally found.

## 5.2. Cyclic application of pull-out and/or push-in from one end

This problem is of fundamental importance, since it is encountered in all exterior beam-column joints. The main findings of some experimental investigations on the subject are summarized here-below very briefly, together with some analytical models.

5.2.1. A first category of tests comprises cantilever beams cast monolithically with heavily reinforced end blocks, to simulate exterior beam-column joints. The steel slips  $s_{FE}$  at the ("fixed-end") interface are measured, in order to find the corresponding rotation  $\theta$  which contributes (to an unexpectedly high percentage) towards the deflection of the beam's free end. Here are the main conclusions from these systematic test series (Brown + Jirsa, [1971], Ismail + Jirsa, [1972], Gosain + Jirsa [1978]):

- a) End-slips do not increase significantly after a small number of repetitions of the same peak load.
- b) For load-controlled loading below the level which produces steel yield, end-slips under a certain low load are markedly increased if higher peak loads were previously applied.
- c) For deflection-controlled loadings of large amplitude of almost fully reversed cycles, yield penetration along the reinforcing bar increases rapidly with the number of cycles, the bar diameter and the amplitude of imposed deflections (Fig. 5/4) after yielding.
- d) The "fixed-end" rotations due to slip may contribute considerably ( $\approx 50\%$ ) to the deflection of the cantilever.
- e) Under the conditions of these tests the order of magnitude of fixed-end slips after the 3<sup>d</sup> half cycle is shown in Fig. 5/5. A relatively small sensitivity against specific conditions is observed.

5.2.2. In a second category of tests, (Hassan + Hawkins, [1975, a]) a direct pull-out (or, subsequently push-in) was applied to one end of a bar embedded in a R.C. block (Fig. 5/6). Here are the main conclusions of this very important work:

- a) Progressive bond deterioration under reversed cycling, is highly dependable on the loading history (Fig. 5/7). If  $\delta_r$  = "end slip between the previous zero load and the maximum load, divided by the end-slip necessary for first yielding of the bar", decreasing  $\delta_r$  -values

---

(\*) A computerized application of this nature for fully reversed loading may be seen in Tassios + Yannopoulos [1979].



(Fig. 5/7a) lead to a stable condition, while constant  $\delta_r$  -values (Fig. 5/7b) rapidly lead to failure. Favourable is also the case of "compressive"  $\delta_r$  -values of half the amplitude of "tensile"  $\delta_r$  - values (Fig. 5/7c). The constitutive rule for local bond-slip shown in Fig. 4/1 may offer (qualitatively though) some physical justification of the above findings.

b) The performance of bars with lug-spacings much larger than the normal spacing (approx.  $\frac{3}{4} \emptyset$ ,  $\emptyset$  being the nominal bar diameter), is significantly inferior.

c) The overall structural integrity of the block (location, direction and width of diagonal primary cracks) is of great importance for the bond-slip characteristics of anchorage under cyclic loading.

5.2.3. Of particular interest is the analytical method proposed by Hassan + Hawkins [1975,b] for predicting anchorage characteristics under reversed cyclic loading. The model takes also in to account the yielding of reinforcement, its Bauschinger effect, together with the non-linearity of bond stresses. Fig. 5/8 gives a summary of the main points of this analytical model.

In spite of its physical inadequacies (empirical expression for fully "cracked" length, equilibrium - dependent  $\tau_{\max}$ -value, instead of being slip-dependent), the model has several practical possibilities for computational predictions of highly complicated cyclic bond loadings, for which simple models are not available.

5.2.4. Nevertheless, a more fundamental approach is still desirable. Local bond-slip relationships appear to be very promising for this kind of loading too: The constitutive rule presented e.g. in Fig. 4/1 may be used to the purpose, together with the modifications foreseen in Fig. 2/15 along the end-zones of the anchorage considered. Such a technique has been applied by Popov + Bertero + Cowell + Viathanepa [1978]: The bar is supposed to be connected to the surrounding concrete by means of springs in discrete spacings along the bar. The bond stress-displacement characteristics of each spring are dictated by several idealized relationship; details of this model were missing at the moment of writing this Report but the principle appears very sound. On the other hand, Morita + Kaku [1973] have successfully applied their local bond-slip law in a case of cyclic pull-out and push-in (from one end), although only a unique curve has been used for every point along the embedded length. In order to show the potentialities of this principle, an equally simple method (\*) is shown in Fig. 5/9, Fig. 5/10 and Fig. 5/11 (using rather arbitrary basic data) for the case studied by Hassan + Hawkins (op. cit.). Nevertheless, the use of just one bond-slip law for every

---

(\*) This numerical application has been prepared by S. Samaras, Dipl. Eng.

point along the bar is a basic handicap, limiting the versatility of the technique. In addition, only one " $\tau$ -s" curve does not allow the use of falling branch; supplementary assumptions are necessary instead, near the ends of the bar.

The complete technique (with varying curves near the ends) is actually studied in the Nat. Techn. University of Athens, by means of appropriate computer programmes.

### 5.3. Alternate application of pull-out from one end, and simultaneous push-in from the other

Alike the case of the previous paragraph, beam-column joints (interior joints this time) are particularly concerned with this type of bond cyclic loading (compare § 6.2). A fundamental research work on the subject, repeatedly reviewed here, has been performed by Bertero + Popov + Vivathanatepa [1978]. Data and some typical results are reproduced in Fig. 5/12 and Fig. 5/13. Some of the findings of this work are summarized here below:

- a) Before reaching yield of steel, a cone of unconfined concrete pulls away from the confined core; the corresponding length is no more available for transmitting bond stresses.

- b) Roughly speaking, almost symmetric or antisymmetric patterns of stresses and displacements are generated.

- c) Significant bond deterioration occurs, particularly when the applied displacements exceed those producing yield of steel.

The analytical models mentioned in §5.2.4 are expected to offer further insight and allow for low cost mathematical tests, instead of the physical ones.

## 6. SOME PRACTICAL IMPLICATIONS

Although the structural consequences of bond deterioration are included in the main topics of other Sessions of this Symposium, a minimum of similar remarks has been deemed necessary to be made here, as a closure, in order to underline the fundamental significance of the local bond-slip phenomena we have dealt within this Report.

### 6.1. Flexural stiffness, damping and crack width under cyclic loading.

This is a very well known topic supported by an extensive amount of experimental data.

This paragraph intends only to remind the practical potentiality of the local bond-slip approach, in this connection too. If we take back the computed end displacements (half crack-widths) of Fig. 5/3, we may consider a rectangular beam section as shown in Fig 6/1

and think of the two extreme axially stressed members,  $A_s$  and  $A_c$  (\*), under repeated bending. Table IV makes use of the results of Fig. 5/3, translating them into moment-curvature relationships (see Fig. 6/1). This approximate technique may be used for a n y cyclic loading or cyclic displacement characteristics, provided that good models for cyclic behaviour of steel and concrete are available (see also Tassios + Yannopoulos, [1979]). Therefore, stiffness degradation, hysteretic damping and crack width under cyclic loading, may be computed on the basis of an appropriate local bond-slip model.

## 6.2. Joints under seismic loading

Fig.6/2 illustrates very roughly the transmission of forces through the core of internal joints, before and after hinging of the beams. Initially, the compressive forces of beam and column, acting on their uncracked compressive zones, are d i r e c t l y transmitted from corner to corner through the core of the joint. Relatively little diagonal compression is initiated by means of bond along the bars (see also Fig. 6/3,a).

On the contrary, after the formation of large cracks on the vertical interfaces of joint (due to previous cyclic overloading), horizontal compressive forces from the beam have to be transmitted by means of the compressive reinforcement, so that  $C \approx T_s$ . The corresponding bond demand is higher and it is s further increased because of the coming yield penetration (Fig. 6/2,b). Direct diagonal transmission of compressive forces from corner to corner is no more possible, although the combination of column compression with the bond forces induced by horizontal bars, results in diagonal compressions directed to points B and B' in Fig.6/2,b. Parallely, intensive diagonal compressions are induced by the "concentrated" high bond stresses ( $\tau_u$ ). These compressions are directed to points A and A' in Fig. 6/2.b, where e q u i l i b r i u m is impossible, unless horizontal h o o p s are provided. This is the mechanism suggested by Paulay + Park + Priestley, [1978].

The patterns for distribution of bond stresses used in Fig. 6/2 and Fig. 6/3 have been encountered in previous paragraphs of this Report (mainly in § 6) both out of experimental or computational works. (Somehow similar distributions after overloading, may be taken from Fig.6a of the previously mentioned reference, Paulay et al. [1978] as shown in our Fig. 6/4).

It is believed that further study of bond-slip relationships within longitudinally and transversally reinforced concrete under cyclic loading, will directly contribute towards a r a t i o n a l model for the structural behaviour of joints under seismic action.

(\*) For this substitute flexural model see i.a. Ferry Borges, [1973]

### 6.3. Anchorage capacity under cyclic loading

After what it has been said in the previous paragraphs 5.2, 5.3 and 6.2, it becomes clear that it is still difficult to set forth general rules for the development lengths needed under cyclic loading: The s p e c i f i c geometrical, detailing and loading conditions should be taken into account to this purpose. Besides, the performance expectations should be more explicitly stated in each case of loading (Seckin + Uzumeri, [1978]). Nevertheless, the following simple rules may be temporarily considered:

- a) Development lengths should be counted only from the i n s i d e of the column bar (towards the confined core). In this respect, the very low  $\tau$ -values offered near the end-face of non-reinforced concrete (after primary cracking), and the risk of pulling-out of core (§5.3.a) should be avoided.
- b) Confinement of the anchorage zone must compulsorily be provided, in order to secure its overall integrity (mainly against external shear) and for local bond betterment. The oversimplified formulae, summarized in §2.10.c, offer an order of magnitude of the contribution of transversal reinforcement to the characteristic values of bond strength.
- c) Nevertheless, for large bar diameters (larger than, say, 35÷50 mm), splitting is very difficult to be avoided (compare also Morita + Kaku, [1977]). Consequently the characteristic value  $\tau_B$  should be considered as peak-value, and brittle failures are to be expected.
- d) For hooked bars (shortened "lead-in" lengths), fully reversed cycles can not be safely undertaken, unless hook movements for compression loading are effectively constrained: Shortened "lead-in" lengths (because of the provision of hooks) allow yield penetration to reach the hook and produce a brittle loss of concrete cover behind it, unless an appropriately strong constraint is provided (Hassan + Hawkins, [1977a]). Besides, 90° deg. hooks seem to be preferable to 180° deg. hooks (ACI-ASCE Committee 352, § 4.2.5.2, [1976]): Broader distribution of lateral stresses on the concrete, and easier constraint are possible, due to the vertical extension of the hook.
- e) Different expected histories of loading may have dramatically different effects on a given anchorage length:
  - When overloads of the same sign are expected, the additional permanent slip should be taken into consideration in serviceability design (see Fig.4/2).
  - When reversed loading ( $\pm \sigma_{s,max}$  or  $\pm \epsilon_{s,max}$ ) is expected, the following working hypothesis could be set forth as a temporary basis for discussion and as a research - incentive: Design the development lengths on the basis of a fraction of the statically "allowable" average bond-stress, roughly estimated as follows:

Loading conditions		Equivalent number of full reversed cycles "n"			Performance expectations
		$n \leq 3$	$4 \leq n \leq 10$	$10 < n$	
$\pm \sigma_{s,max} < f_{sy}$		$\beta \cdot \frac{\sigma_{s,serv}}{\sigma_{s,max}} \geq \frac{1}{3}$	$\frac{2}{3} \beta \cdot \frac{\sigma_{s,serv}}{\sigma_{s,max}} \geq \frac{1}{3}$	Special local measures for ensuring anchorage	Practical end-fixity (serviceability limit state)
$\pm \epsilon_{s,max} > \epsilon_{sy}$	$\frac{a}{a_y} \leq 2$	$\beta$	$\frac{2}{3} \beta$		No-collapse (ultimate limit state)
	$3 < \frac{a}{a_y} < 5$	$\frac{1}{2} \beta$	$\frac{1}{3} \beta$		
	$5 < \frac{a}{a_y}$	Special local measures for ensuring anchorage			

$\frac{a}{a_y}$  = ductility demand

$\beta$  = an appropriate reduction coefficient depending on transversal compression and degree of confinement.

In assessing these rough proposals, the data illustrated in Fig 4/1, Fig.5/3, Fig 5/4, Fig. 5/6 have been taken into account i.a.

#### 6.4. Splices under cyclic loading

This paragraph is intended to be a short one. No reference will be made to the stress field and the corresponding micro - and macro-cracking in the area of a splice, under monotonic loading (see i.a., Stoeckl, [1972], Tepfers, [1973], Orangun + Jirsa + Breen, [1977]).

The basic bond-slip model presented along this Report, may possibly serve as a basis for the extension of the knowledge from monotonic to the cyclic loading. However, a special reference will be made here of the completeness of the formula proposed by Orangun et al. (op. cit.), for the average (static) bond strength at the splice length  $l_s$ :

$$\bar{\tau}_u = 0,10 + 0,25 \frac{c}{\phi} + 4,15 \frac{\phi}{l_s} + \frac{A_{s,tr} f_{y,tr}}{42 a_s \phi} \sqrt{f_{cc}}$$

(For notation see Fig.2/10 and Fig.2/11, units: mm,MPa)

It is also important to remind here the specific study made by Tepfers (op.cit.) on the fatigue of lapped splices under pulsating bond load (from around 10% ÷ 30% up to 50% ÷ 90% of the average ultimate static bond strength, all one sign loads). The results seem encouraging, since a very large number of load repetitions were needed to produce bond fatigue failures, which, according to Tepfers, are governed by concrete tensile-strength fatigue characteristics, as foreseen by a typical Smith diagramme. Reversed

loading were not applied.

Finally, the consequences of "impact"-type of bond loading of splices (studied by Rezansoff et.al., 1975) do not appear very important. Many unidirectional or reversed impact loadings may be applied without failure, provided that the static capacity is not exceeded. For higher impact loading exceeding the static capacity by 50%, splice failure resulted after very few cycles. In this connection reversed loading did not appear to be clearly worse than unidirectional impact loading of the splice.

Systematic investigation on fully instrumented spliced bars under clear reversed bond-loading and/or related theoretical studies were not known to the writer of this Report at the moment of its writing.

## 7. SUGGESTED FIELDS OF ADDITIONAL RESEARCH

In the Preamble of this Report, it has been said:

"It is hoped that, precisely, the weak points of  
"this Report will engender the additional research  
"works urgently needed, so that after an extremely  
"short time this Report will be obsolete"

I sincerely wished it is already obsolete, thanks to the existing research works unknown to this Reporter. However, under the light of the material included in this Report, the following topics seem to need further intensive investigation:

### 7.1. On the physical model of local bond-slip relationship under monotonic and cyclic loading

- a) Radial compressive stresses on the lateral surface of the bar and longitudinal (incompatibility) stresses due to shrinkage, corresponding " $\tau$ -s" consequences.
- b) Internal microcracking tracing after bond loading (both transversal and splitting cracks are of interest, together with the hypothetical compression - shear cracks at the ultimate stage).
- c) Bond and radial normal stress interaction during loading.
- d) Effects of the rate of bond loading.
- e) Topological approach: Local bond-slip relationship near the end faces.
- f) The influence of clear cover on the  $\tau$ -s curve.
- g) Residual bond strengths.
- h) Creep and relaxation of slips and bond stresses.
- i) In-situ corrosion and its consequences on local  $\tau$ -s.

### 7.2. Technical parameters influencing the local $\tau$ -s relationship

- a) The influence of external (longitudinal and/or transversal) normal stresses on the  $\tau$ -s curve.
- b) Bond and dowel loading interaction.
- c) The influence of transversal and longitudinal reinforcement on local  $\tau$ -s curve.

- d) Loading history and detailed " $\tau$ -s" response
- e) The influence of spacing of parallel loaded bars.

### 7.3. Overall behaviour of anchorages and splices

- a) Structural behaviour of hooks under repeated compressive forces and the effectiveness of the necessary constraints.
- b) Mathematical models for predicting the structural behaviour of anchorages under cyclic loading from both ends.
- c) Structural behaviour of anchorages in repaired R.C. elements.
- d) Studies of splices under fully reversed loading (with the parameters mentioned in §§7.1. and 7.2.).
- e) Performance criteria for anchorages and splices under cyclic loading for serviceability and ultimate limit states conditions. Corresponding practical recommendations.

### A c k n o w l e d g e m e n t s

The writer of this Report gratefully acknowledges the information kindly sent to him by Prof. Bertero, Prof. Gergely, Prof. Hawkins, Prof. Jirsa, Prof. Morita, Prof. Nilson and Dr. Yannopoulos.

### R E F E R E N C E S

- ACI-ASCE Comm. 352: "Recommendations for design of beam-column joints in monolithic R.C. structures", Journal ACI, July, 1976.
- Berge + Losberg: "Partially prestressed 3L-concrete", Publ.78, 4, Div. Conc. Structures, Chalmers Univ. of Technology, Goeteborg, 1978.
- Bertero + Popov + Vivathanatepa: "Bond of reinforcing steel: Experiments and a mechanical model", Proc. IASS Symp. Nonlinear Behaviour of R.C. Spatial Structures, Darmstadt, 1978.
- Bresler + Bertero: "Behaviour of R.C. under repeated load", Journal ASCE, Str. Div., June 1968.
- Bresler B.: "R.C. Engineering", Vol. I, J. Wiley, N.York, 1974.
- Brown + Jirsa: "R.C. beams under load reversals", Journal ACI, May, 1971.
- Doerr K.: "Bond-behaviour of ribbed reinforcements under transversal pressure", Proc. IASS Symp. Nonlinear Behaviour of R. C. Spatial Structures, Darmstadt, 1978.
- Edwards + Yannopoulos: "Local bond-stress-slip relationships under repeated loading", Magazine of Concrete Research, Vol. 30, No 103, June 1978.
- Ferguson P.M.: "Bond stress - The State of the Art", ACI Journal, Nov. 1966.

Ferry Borges J.: "Structural behaviour under repeated loading", Working group on the resistance of structures, CEB, 1973.

Gosain + Jirsa: "Bond deterioration in R.C members under cyclic loads", Proc. 6th World Conf. on Earthquake Eng., New Delhi, 1977.

Goto + Ueda + Maki: "Investigation on tension cracks in R.C. members", Japan Society of Civil Eng., 2nd Symp. on Deformed Bars, Japan, Dec. 1965.

Goto Y.: "Cracks formed in concrete around deformed tension bars", ACI Journal, Apr. 1971.

Hassan + Hawkins: "Anchorage of reinforcing bars for seismic forces", ACI Special Publication 53, 1977(a).

Hassan + Hawkins: "Prediction of the seismic loading anchorage characteristics of reinforcing bars", ACI Special Publication 53, 1977 (b).

Ismail + Jirsa: "Bond deterioration in R.C. subject to low cycle loads", Journal ACI, June 1972.

Koufopoulos + Theocaris: "Shrinkage stresses in two-phase materials", Journal of Composite Materials, Apr. 1969.

Kvirikadze G.: "Determination of the ultimate strength and modulus of deformation of concrete at different rates of loading", RILEM, Symp. In-situ testing of concr. structures, Budapest, 1977.

Lutz + Gergely: "Mechanics of bond and slip of deformed bars in concrete", ACI Journal, Nov. 1967.

Martin H.: "Die Haftung der Bewehrung im Stahlbeton", Radex - Rundschau Apr. 1967, (as cited in Stocker + Sozen, 1970).

Morita + Kaku: "Local bond stress-slip relationship under repeated loading", Symposium: Resistance and ultimate deformability of structures acted on by well defined repeated loads, Lisboa 1973.

Morita + Kaku: "Cracking and deformation of R.C. prisms subjected to tension", Proc. Coll. Inter-Association (Behaviour in service of concrete structures): Liege, June, 1975.

Morita + Kaku: "Splitting bond failures of large deformed reinforcing bars", ACI Annual Convention, San Diego, 1977.

Nilson A.: "Bond stress-slip relations in R.C.", Report No 345, D/t of Struct. Eng., Cornell University, 1971.

Orangun + Jirsa + Breen: "A reevaluation of test data on development length and splices", Journal ACI, March 1977.

Paulay + Park + Priestley: "R.C. beam-column joints under seismic actions", Journal ACI, Nov. 1978.



Perry + Jund: "Pullout bond stress distribution under static and dynamic repeated loadings", Journal ACI, May, 1969.

Petrangeli + Menesto: "The effects of low cycle loads on the bond in R.C." Proc. 6th Eur. Conf. Earthquake Eng., Dubrovnik, 1978.

Plainis + Tassios: "Local bond-slip test results under cycling, creep and relaxation", (unpublished data), Nat. Techn. University, Athens, 1978.

Popov E.: "Mechanical characteristics and bond of reinforcing steel under seismic loading", Workshop on ERCBC, University of California, July, 1977.

Popov + Bertero + Cowell + Viwathanepa: "Reinforcing steel bond under monotonic and cyclic loadings", SEAOC Conf., Lake Tahoe, Sept. 1978.

Rasmussen B.H.: "Betoninstøbe tvaebelastede boltes og domes bæreevne", Laboratoriet for Bygningstatik, Danmark Tekn. Højskole, Meddelelse, Vol. 34, No 2, 1962.

Rehm G.: "Ueber die Grundlagen des Verbundes zwischen Stahl und Beton", D.A.f.S., Heft 138, 1961.

Rezansoff + Bufkin + Jirsa + Breen: "The performance of lapped splices under rapid loading", R.R. 152-2, Center for Highway Research, The University of Texas at Austin, 1975.

Schwing H.: "Zur wirklichkeitsnahen Berechnung von Wandscheiben aus Fertigteilen", Techn. Hochschule, (Dissertation), Darmstadt, 1975.

Seckin + Uzumeri: "Examination of design criteria for beam-column joints", 6th Eur. Conf. Earth. Eng., Dubrovnik, 1978.

Sharma N.K.: "Splitting Failures in R.C. members", Thesis, Cornell University, 1969.

Stocker + Sozen: "Investigation of prestressed R.C. for highway bridges, Part V: Bond characteristics of prestressing strand", Eng. Exp. Station, Bulletin 503, Univ. of Illinois, 1970.

Stoeckl S.: "Uebergreifungsstoesse von zugbeanspruchten Bewehrungsstäben", Beton und Stahlbetonbau, 10/ 1972.

Tassios + Demiris: "A new non-destructive method for concrete's strength determination", Scient. Publ. No 21, Nat. Techn. University, Athens, 1970.

Tassios T.: "Reinforced Concrete, a textbook", (ch. XX, p. 940), (in greek), Athens, 1976.

Tassios + Tsoukantas: "Serviceability and ultimate limit-states of large panels' connections under static and dynamic loading", Proc. RILEM-CEB-CIB Symp. Mech. Behaviour of Joints of Precast R.C. Elements, Athens, (Nat. Techn. University), 1978.

Tassios + Yannopoulos: "Fundamental computer studies on axially loaded and flexural members under cyclic loading", AICAP-CEB Symp. Structural Concrete under seismic actions, Roma 1979.

Taylor + Brooms: "Shear bond strength between coarse aggregate and cement paste or mortar", ACI Journal, Aug. 1964.

Tepfers R.: "A theory of bond, applied to overlapped tensile reinforcement splices for deformed bars", Publ. 73,2, Div. of Concrete Structures, Chalmers University, Göteborg, 1973.

Yannopoulos P.: "Fatigue, bond and cracking characteristics of R.C. tension members", Ph.D. thesis, Imp. College, London, Jan. 1976.

TABLE 1: Experimental evidence related to monotonic loading  
(characteristic bond - stresses).

No	Authors	Data										Results			
		$f_{cc}$	$f_{ct}$	$c$	$\phi$	$\rho_o$	cast	$A_s$	$d_s$	$f_{sy}$	$\rho$	$\tau_A : \tau_A^{comp}$	$\tau_B : \tau_B^{comp}$	$\tau_G : \tau_G^{comp}$	
1.	Bertero + Popov + Vivathanatepa, [1978] (see Fig. 3/1)	30	(2.6)	114	254	$\gg$	vert	380 113	200 100	1100 400	469 (equ)	$\frac{4.5}{3.9} = 1.2$	$\frac{11.0}{12.0} = 0.9$	$\frac{14.5}{12.9} = 1.1$	
		$\xi = 1, \eta = 1, (\text{pronounced confinement}) \tau_A = 1\frac{1}{2} \cdot 2.6 = 3.9$										$\tau_r^{exp} : \tau_r^{comp} = 8.0 : 5.6 = 1.4$			
		$\tau_B = \left( \frac{2}{3} \cdot \frac{114}{254} + \frac{1}{3} \right) \cdot 2.6 + 8.0 \cdot \frac{1}{254} \cdot \left( \frac{1}{4} \cdot \frac{380}{200} + \frac{1}{2} \cdot \frac{113}{100} \right) = 12.0$													
		$\tau_u = \frac{1}{3} \cdot 3.0 + \frac{8}{3} \cdot \frac{1}{2} \cdot 4.69 \left( \frac{380}{200 \cdot 1100} + \frac{113}{100 \cdot 400} \right) = 12.9$													
		$\tau_r = 0.12 \cdot 3.0 + 0.30 \cdot \frac{2.6}{254} \left( \frac{380}{200} + \frac{113}{100} \right) \sqrt{4.69} = 5.6$													
2.	Berge + Losberg [1978]	36.0	(2.9)	(90)	12	$\gg$	vert	$\tau_A = 4 \tau_B = 12.6$	$\tau_u = 13$						
		23.5	(2.2)	plus	$P_y = \frac{P}{2}$	50 MPa	3.3	9.5	8.5						
		13.5	(1.5)	$\therefore P_y = \frac{P}{4}$						$\frac{3.5}{3.3} = 1.1$ $\frac{2.0}{2.3} = 0.9$	$\frac{14.5}{10.0} = 1.5$ $\frac{7.0}{7.0} = 1.0$	$\frac{16.5}{11.5} = 1.4$ $\frac{7.9}{7.9} = 1.0$			
		$\frac{2}{3} \cdot 6 + \frac{1}{3} = 4.33, \tau_A = 1.5 \tau_{ct}$ (almost compressive loading) $\left( \frac{c}{\phi} = 7.5 \rightarrow 6 \right)$													
3.	Doerr [1978]	36	(3.2)	67	16 <sup>D</sup>	110	(horiz)	—					$\frac{2.3}{2.1} = 1.1$	$\frac{4.0}{4.3} = 0.9$	$\frac{6.0(?)}{5.2} = 1.1$
		$\frac{\rho_o}{c} = 1.64 \rightarrow \eta = 0.65, \tau_A = 0.65 \cdot 3.2 = 2.1, \xi = \frac{2}{3}$													
		$\frac{2}{3} \cdot 4.18 + \frac{1}{3} = 3.12, \tau_B = \frac{2}{3} \cdot 0.65 \cdot 3.12 \cdot 3.2 = 4.3, \tau_u = \frac{2}{3} \cdot 0.65 \cdot \frac{36}{3} = 5.2$													





TABLE II: Characteristic slip values

CHARACTERISTIC SLIP - VALUES	Fig.3/1, roughly based on Bertero et al. [1978]							
	a	b	c	d	e	f	g	h
		Berge + Losberg [1978]	Doerr [1978]	Yannopoulos [1976]	Morita + Kaku [1975]	Morita + Kaku [1973]	Nilson [1971] (for $l_0 > >$ )	Rehm [1961], $\frac{v}{a} = 1 : 15$ (one rib)
$s_A$	60	-	7	5	35	25	6	-
$s_B$	180	150	30	60	100	50	20	100
$s_u$	320	500	150?	160	350	400	35	1000
$(s_r)$	(750)	(>2000)	-	-	-	-	-	

TABLE III: Experimental evidence related to cyclic loading

No	Author	Miscellaneous comparisons
1	Doerr [1978]	<p><u>Data</u>: Unloading from <math>\tau_1 = 3,25</math> under <math>p_y = 0</math>  " = 6,00 " = 15</p> <p><u>Results</u>: <math>\tau_{01}^{\text{exp}} : \tau_{01}^{\text{comp}} = 0,75 : \frac{1}{4} 3,25 = 0,9</math>  " = 4,5 : <math>\frac{1}{4} (6+15) = 0,9</math></p>
2	Edwards + Yannopoulos [1978]	Unloading slope ranging from $K' = 0,5 \text{ MPa}/\mu$ , to $K' = 0,2 \text{ MPa}/\mu$ , for lower and higher bond-stresses respectively.
3	Plainis + Tassios [1978]	$\frac{\tau_{01}}{\tau_1} \approx 0,15 \div 0,25$
4	Morita + Kaku [1973]	<p>Unloading slope <math>K'_{\text{exp}} = 0,4 \frac{\text{MPa}}{\mu}</math> (vs. 0,5 proposed)</p> <hr/> <p><math>\frac{\tau_{01}}{\tau_1} = 0,25</math> for low <math>\tau_1</math>-values  " = 0,15 for high " (vs. 0,20 proposed)</p>

**TABLE IV:** Calculation of  $M - \frac{1}{r}$  relationship (Fig. 6/1)

$$(M = N \cdot z, \frac{1}{r} = \left[ \epsilon_c + \left( \frac{\Delta l}{l} \right)_t \right] : z, \quad \epsilon_c \approx \sigma_c : E_c)$$

No	$\sigma_s$ MPa	$N_t$ KN	$\left( \frac{\Delta l}{l} \right)_t \cdot 10^3$	$\sigma_c$ MPa	$\epsilon_c \cdot 10^3$	$\frac{1}{r} \cdot 10^3$	$M$ KN m
a	140	49	0,51	2,18	0,07	1,05	26,9
b	0	0	0,05	0	0	0,09	0
c	280	98	1,20	4,35	0,15	2,45	53,9
d	0	0	0,06	0	0	0,11	0
e	140	49	0,64	2,18	0,07	1,29	26,9



Stress distributions, (Lutz+Gergely, [1967]).

Constant or triangular shear "r" along a strip of finite length "l" on the boundary of elastic half-space (plane).

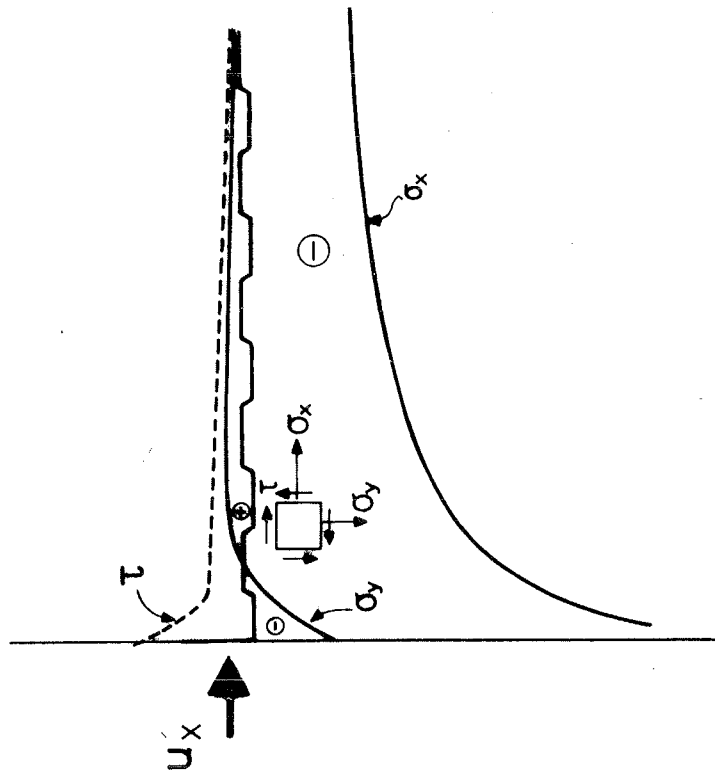
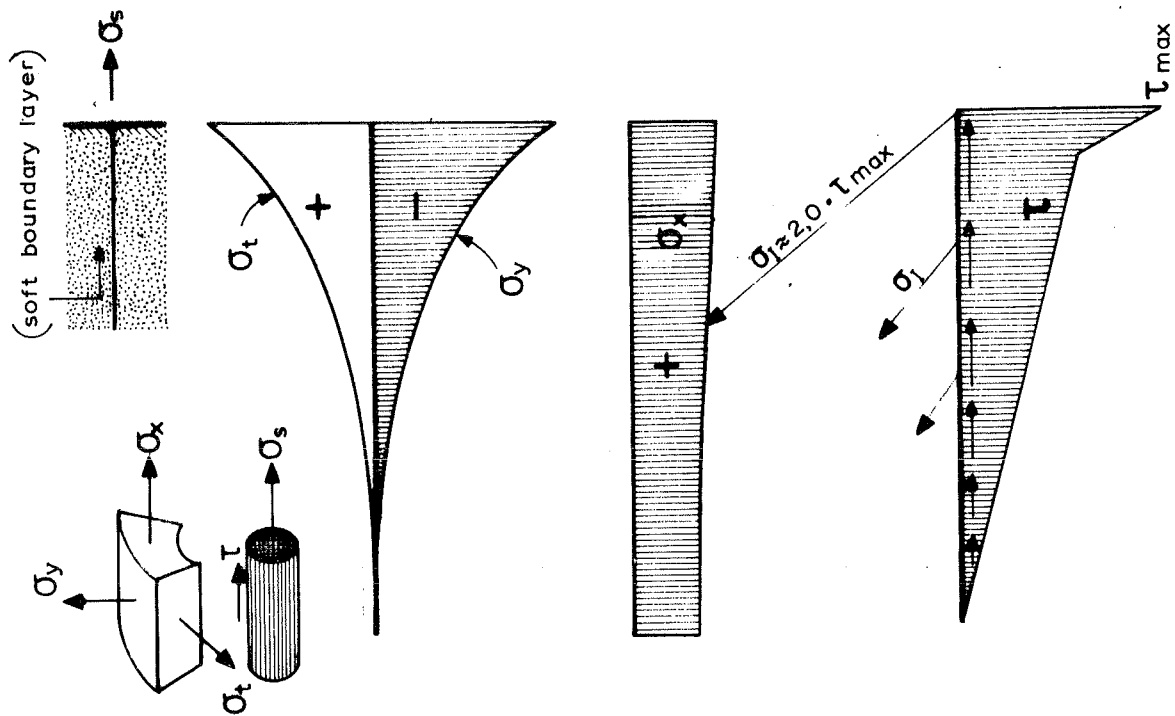


Fig 2/4:

Stress distributions along a joint between precast large panels under imposed displacements  $u_x$ . ( J. Laing, in Schwing, [1975] )

Fig. 2/3:

Stress distributions ( Bresler+Bertero, [1968] )

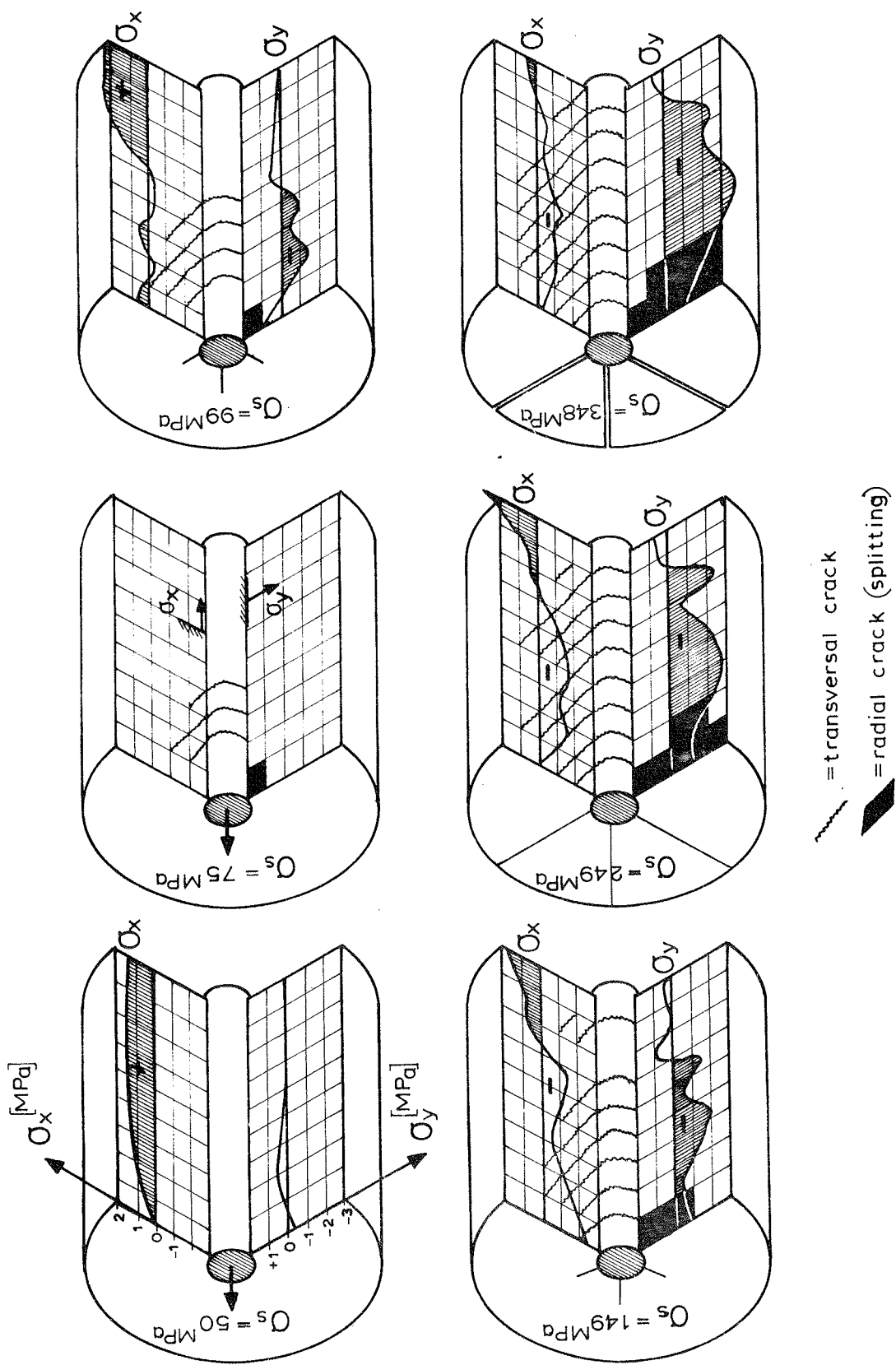


Fig. 2/5:  
Internal crack formation and propagation in a small length (90 mm) specimen. (Finite elements analysis, Yannopoulos, [1976]). Stresses are supposed acting on steel-concrete interface.

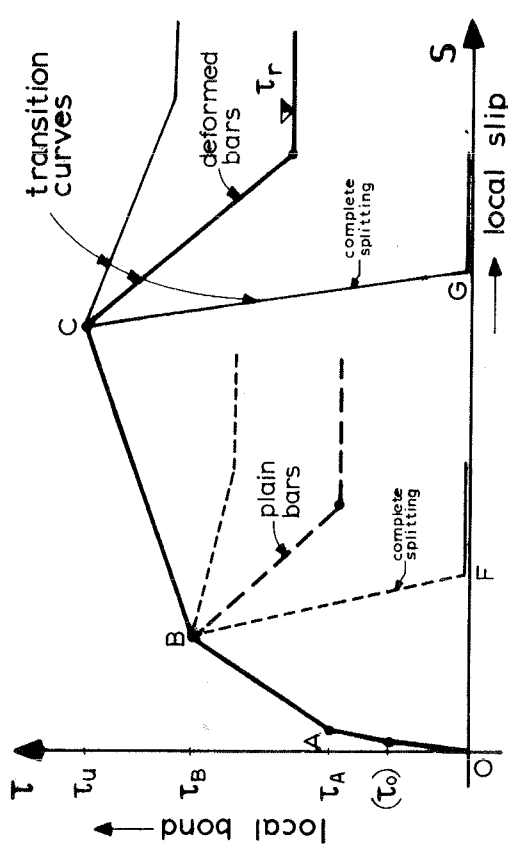


Fig. 2/7:

Local bond-local slip between a reinforcing bar and the surrounding concrete, (an oversimplified description).

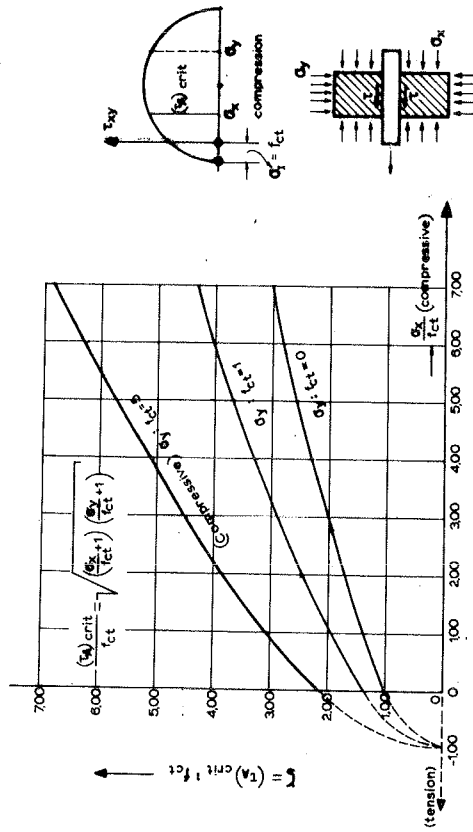


Fig. 2/6:

Critical shear-bond stress  $\tau_l \text{ crit}$  (for transverse cracking) depends on longitudinal ( $\sigma_x$ ) and radial ( $\sigma_y$ ) stresses.



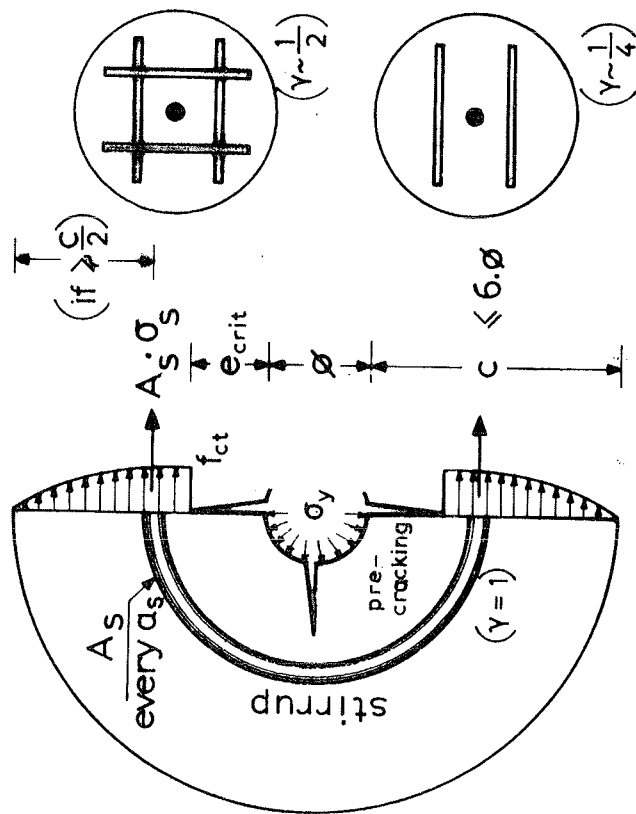


Fig. 2/10:

Estimated stress conditions at the moment of splitting outburst.

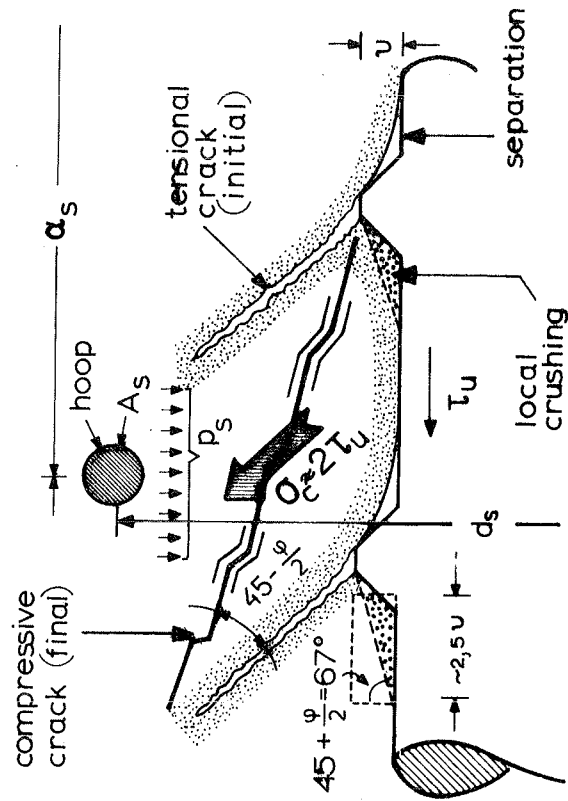


Fig 2/11:

Possible stage at bond-failure: Rupture of concrete teeth and favourable pressure of surrounding reinforcement.

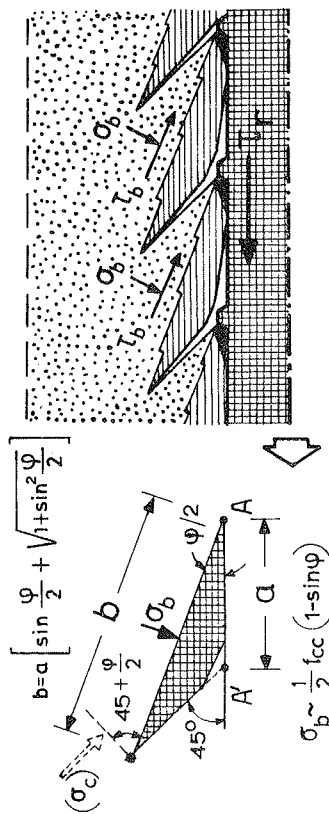


Fig. 2/12:  
Mechanics of residual bond strength  $\tau_r$ ,  
(hypothesis).

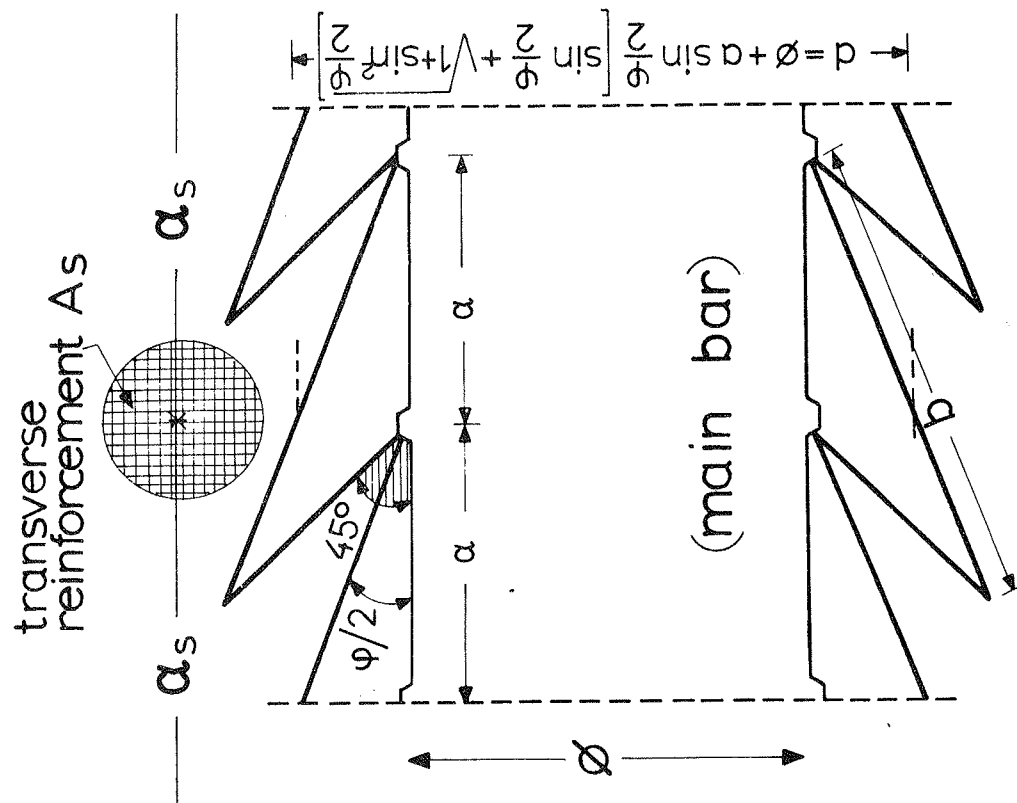


Fig. 2/13:  
Sketch for consideration of dowel action  
of surrounding reinforcement.

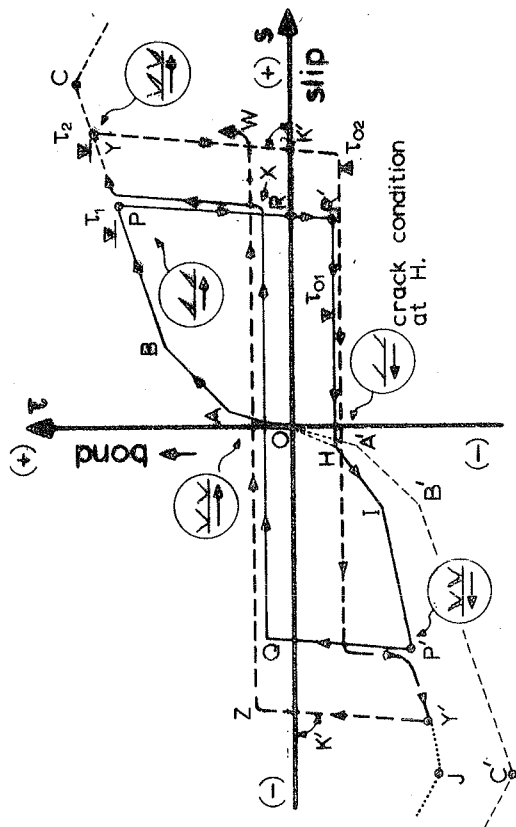


Fig. 2/14:  
Cyclic bond-slip relationships as foreseen  
by conceptual model set-forth.

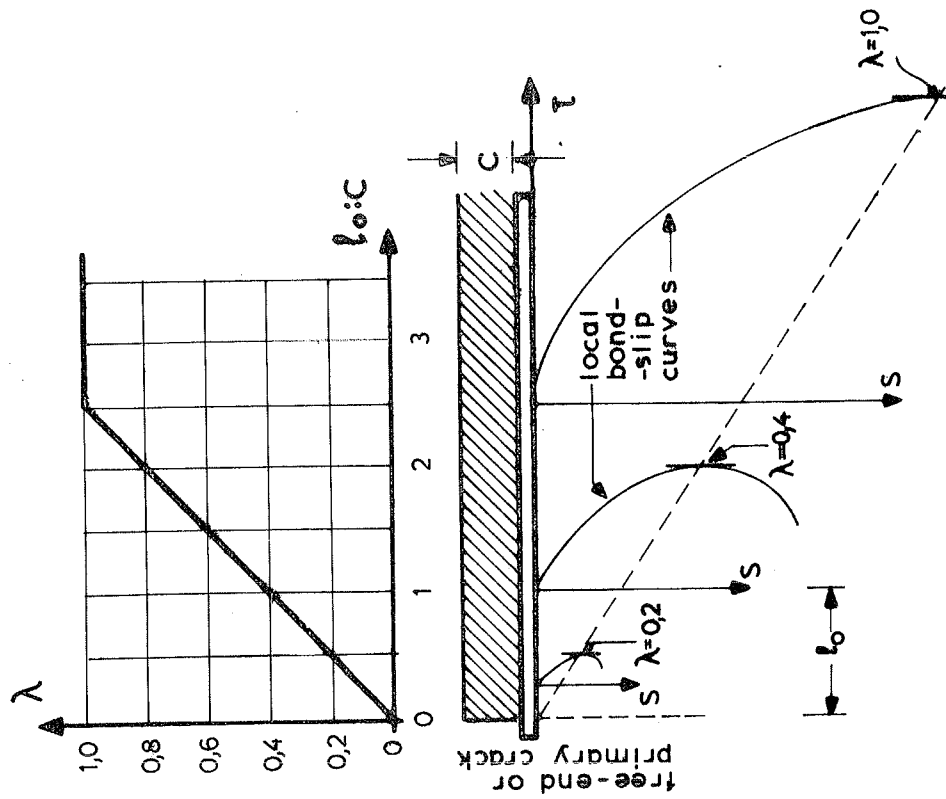


Fig. 2/15: Empirical "location" factor  $\lambda$ .



$$S_A^{[\mu]} = \Delta x_1 + \Delta \alpha_1 \approx 0,3 \varnothing \text{ [mm]}$$

The diagram illustrates the cross-section of a reinforced concrete beam under load. Key features include:

- Dimensions:** Total height \$C\$, effective depth \$d\$, and width \$B\$.
- Stress Distribution:** A linear stress profile across the section, with maximum compressive stress \$\sigma\_c \approx 2\tau\_B\$ at the top fiber and zero stress at the neutral axis.
- Strain:** Compressive strain indicated by arrows pointing towards the neutral axis.
- Reinforcement:** Longitudinal bars at the bottom and stirrups are shown.
- Parameters:**
  - \$\Delta C\_{\text{B}}^{[\mu]} = C \cdot \frac{2\tau\_B}{E\_c} = 0,5 \cdot 10^{-3} \cdot C \approx 0,5 C [\text{mm}]\$
  - \$\Delta x\_2^{[\mu]} = x \Delta \epsilon\_c \approx \emptyset [\text{mm}]\$
  - \$S\_B^{[\mu]} = 1,3 \emptyset^{[\text{mm}]} + 0,5 \cdot c^{[\text{mm}]}\$
  - \$\tau\_B \approx 2f\_{ct} \approx \frac{f\_{cc}}{5}\$
  - \$\sigma\_y = \tau\_B\$
  - \$\sigma\_h)\_B \approx \frac{1}{2} \cdot \tau\_B \cdot \frac{\alpha}{U} \approx 8 \cdot \tau\_B \approx f\_{cc}^\*\$
  - \$f\_{cc}^\* \approx f\_{cc} + 4\sigma\_y \approx \frac{9}{5} f\_{cc}\$
  - \$E\_{cu}^\* = E\_{co} + 30 \left( \frac{\sigma\_y}{f\_{cc}} \right) \approx 8 \%\$

[Tassios 1976]

$$\tau_u = f_{cc}/3, \quad \sigma_y/f_{cc} = 1/3, \quad \varepsilon_u^* = 11 + 57 \cdot (0,33 - 0,30) = 12,7\text{‰}, \quad \Delta \varepsilon_{cc}^* = 4,7\text{‰}$$

$$S_u = 0,3 \varnothing + 1,0 \varnothing \cdot \left(1 + \frac{4,7}{8,0}\right) + c (3,5 \text{‰})$$

$$S_u^{[\mu]} \approx 1,9 \phi^{[mm]} + 3,5 \cdot C^{[mm]}$$

Fig. 2/16: Estimated characteristic slips corresponding to  $\tau_A$ ,  $\tau_B$  and  $\tau_u$ .

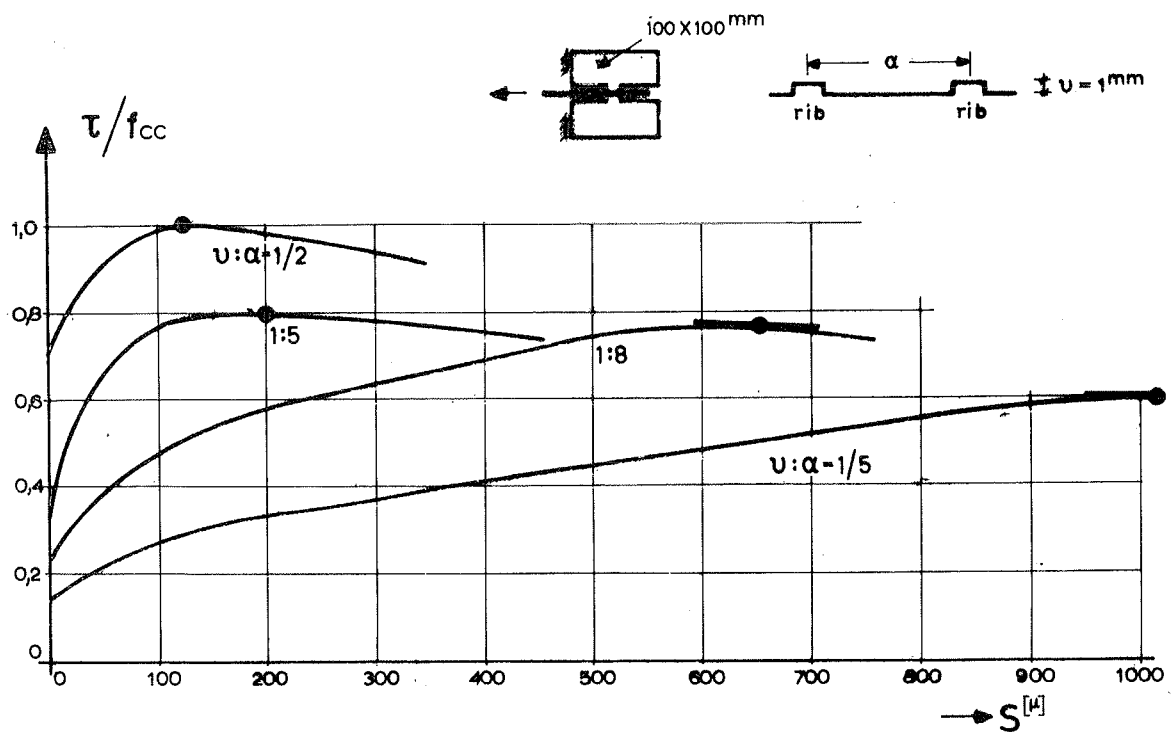


Fig. 2/17:

Local bond-slip curves after Rehm [1961], for various rib spacings.

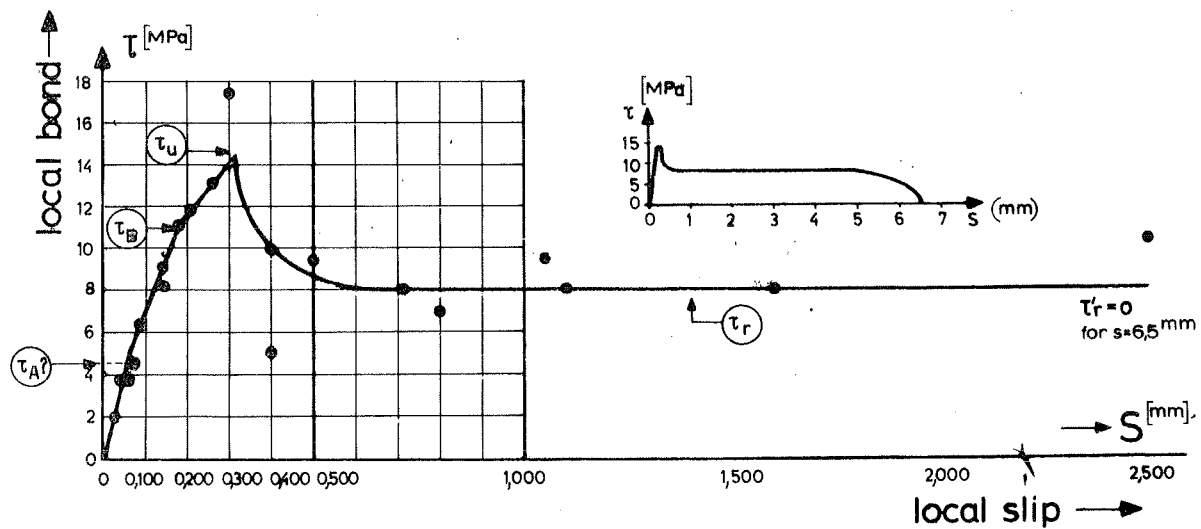


Fig. 3/1:

A probable local bond-slip relationship, roughly based on Bertero+Popov+Vivianathepa ([1978], Fig. 5)

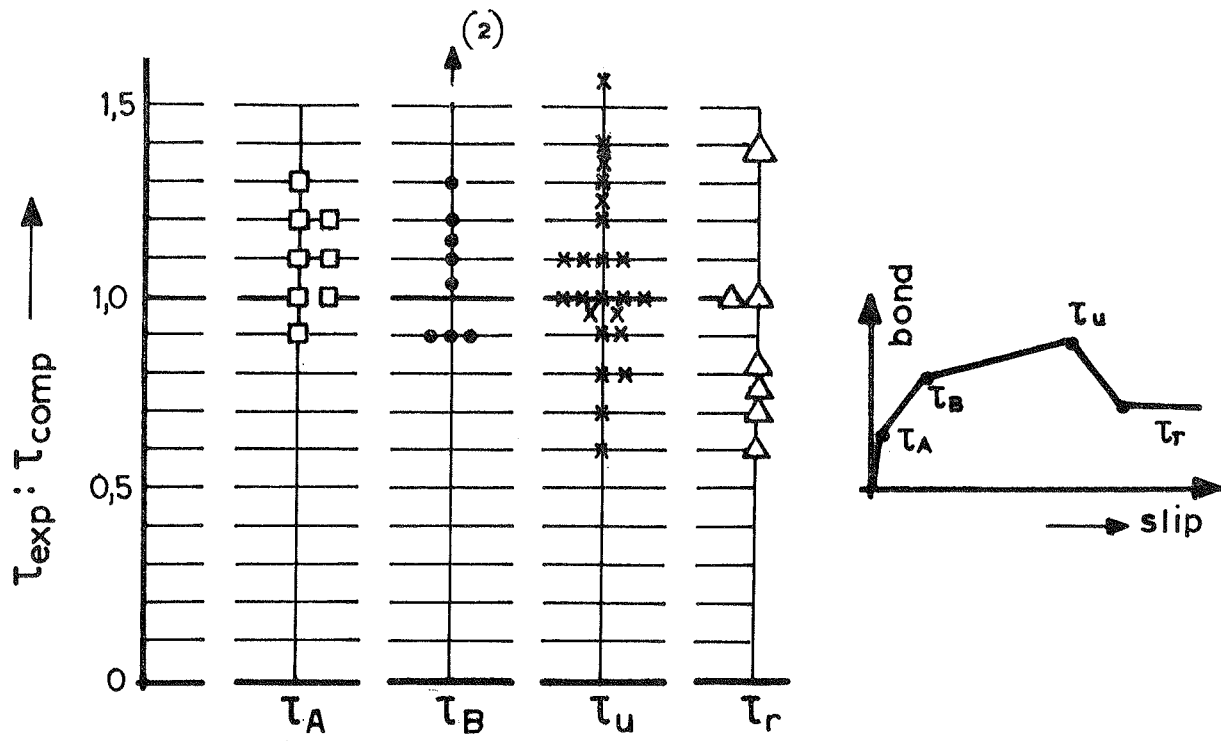


Fig. 3/2: Characteristic local-bond-stress values ratio  
(experimental over computed, see Table I).



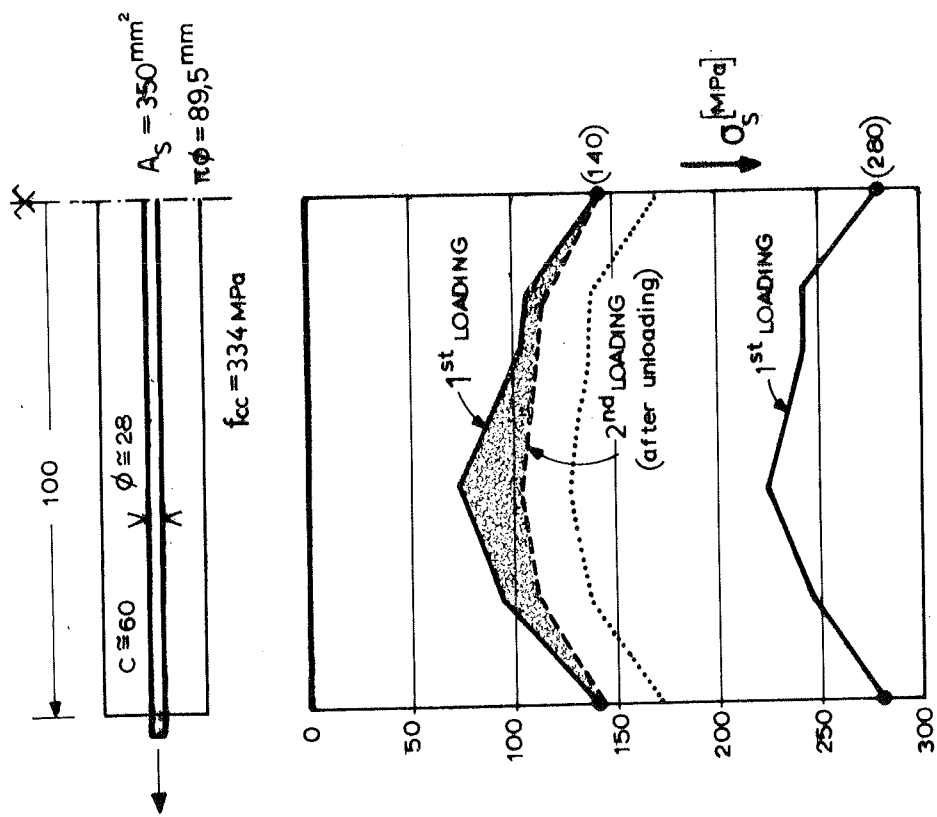


Fig. 5/1:

Steel stress distribution during repeated loading, (based on Ismail+Jirsa, [1972]).

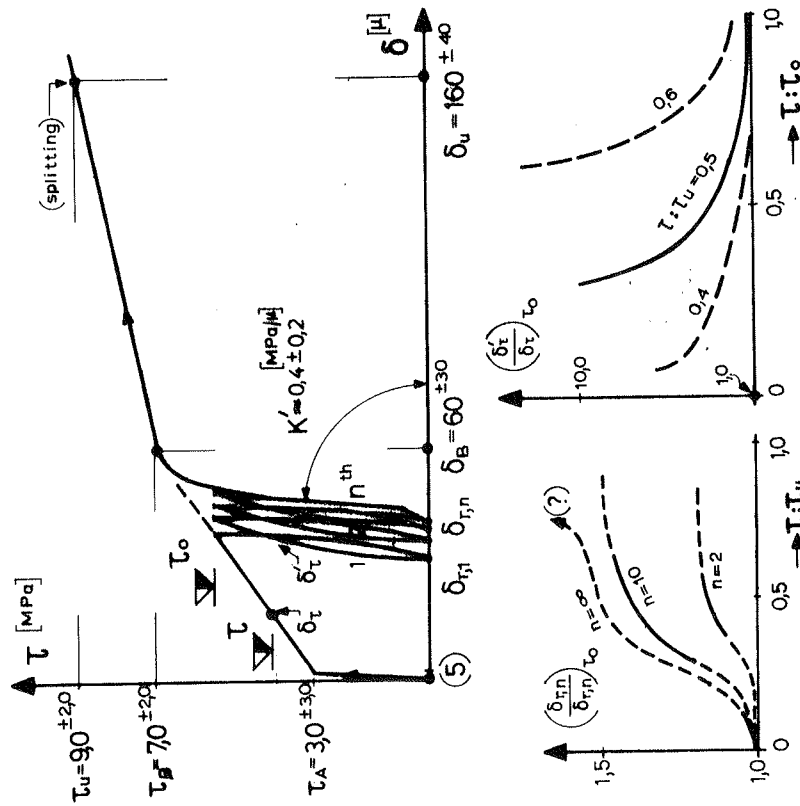


Fig. 4/2:

Repeated local bond-slip. An experimental example together with scatter limits ( $l = 38$  mm,  $C = 25 \div 35$  mm,  $\phi = 16$  def.,  $f_{cc} = 43$  MPa). (Based on Edwards+Yannopoulos [1978]).

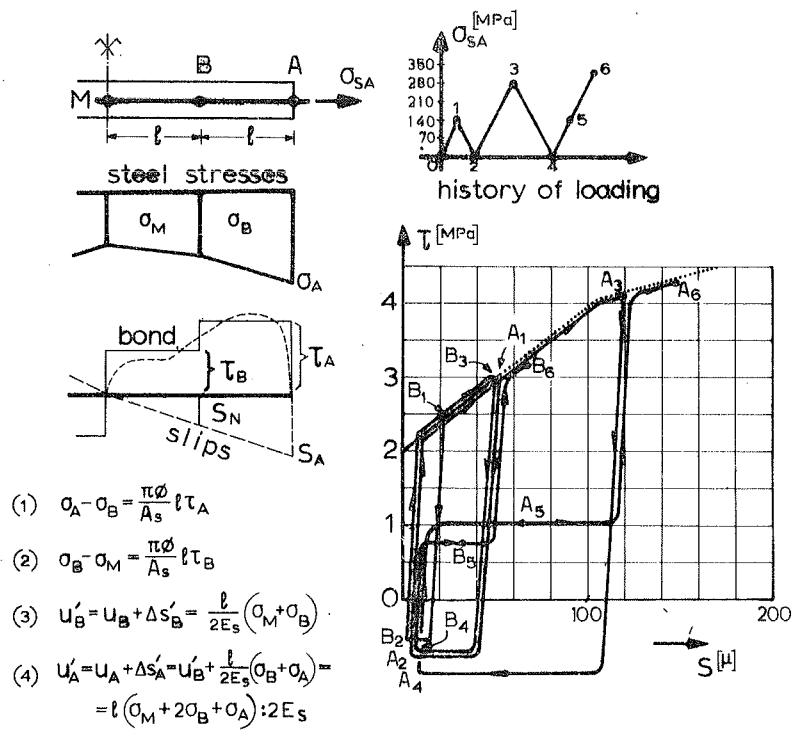


Fig. 5/2: Elementary analytical solution of the case shown in Fig. 5/1 (for bond and steel stress distributions see Fig. 5/3).

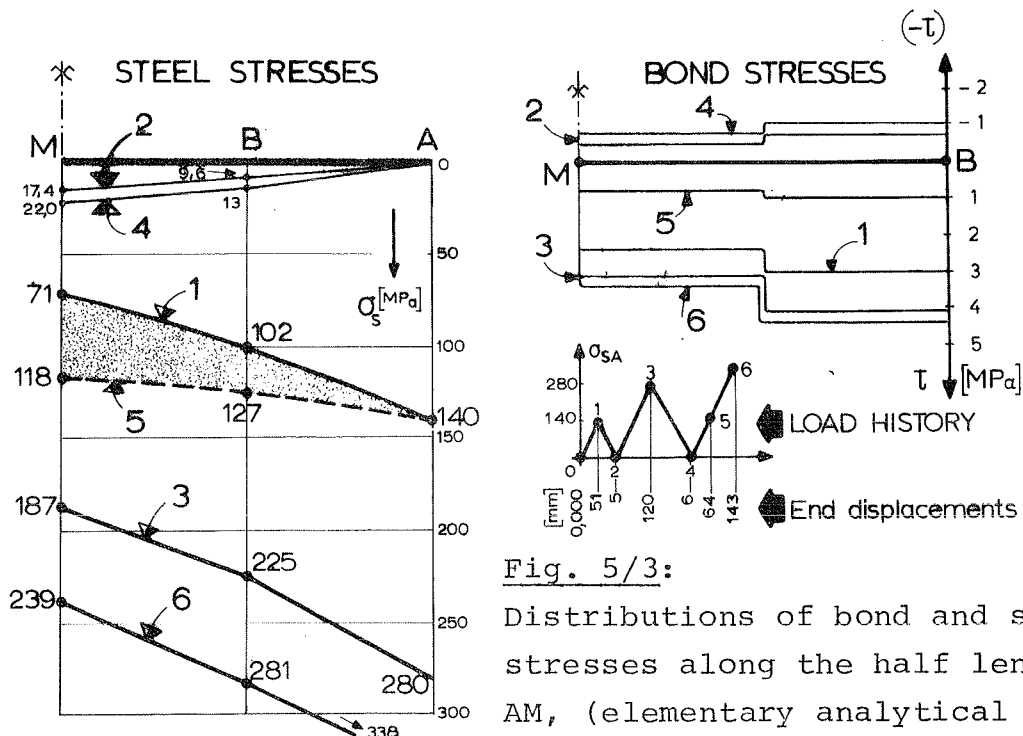


Fig. 5/3: Distributions of bond and steel stresses along the half length AM, (elementary analytical solution, Fig. 5/2).



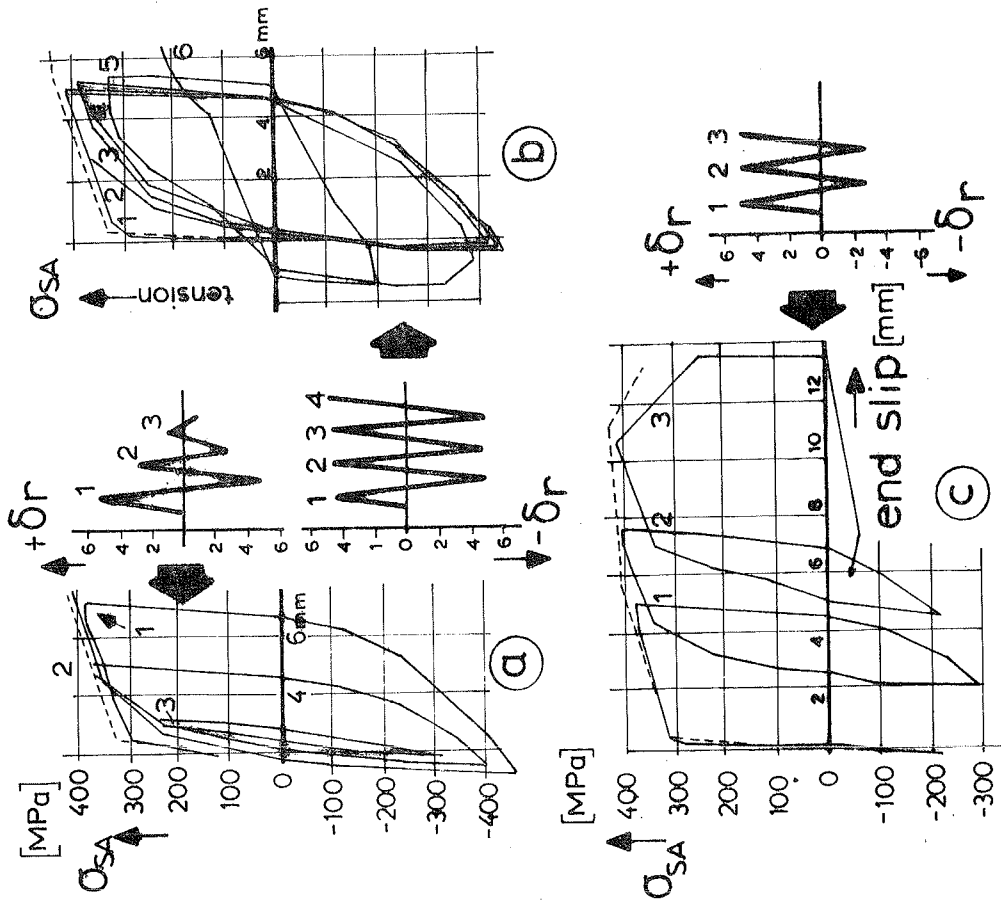


Fig. 5/7: Load history dependent stress-slip relations of the anchorage shown in Fig. 5/6.

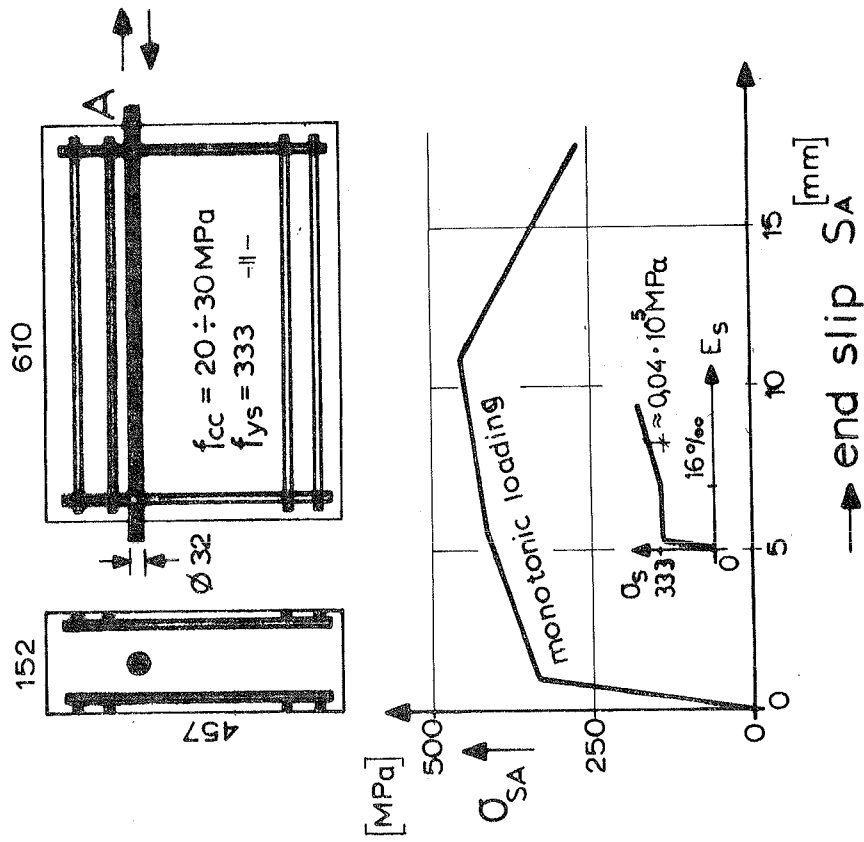
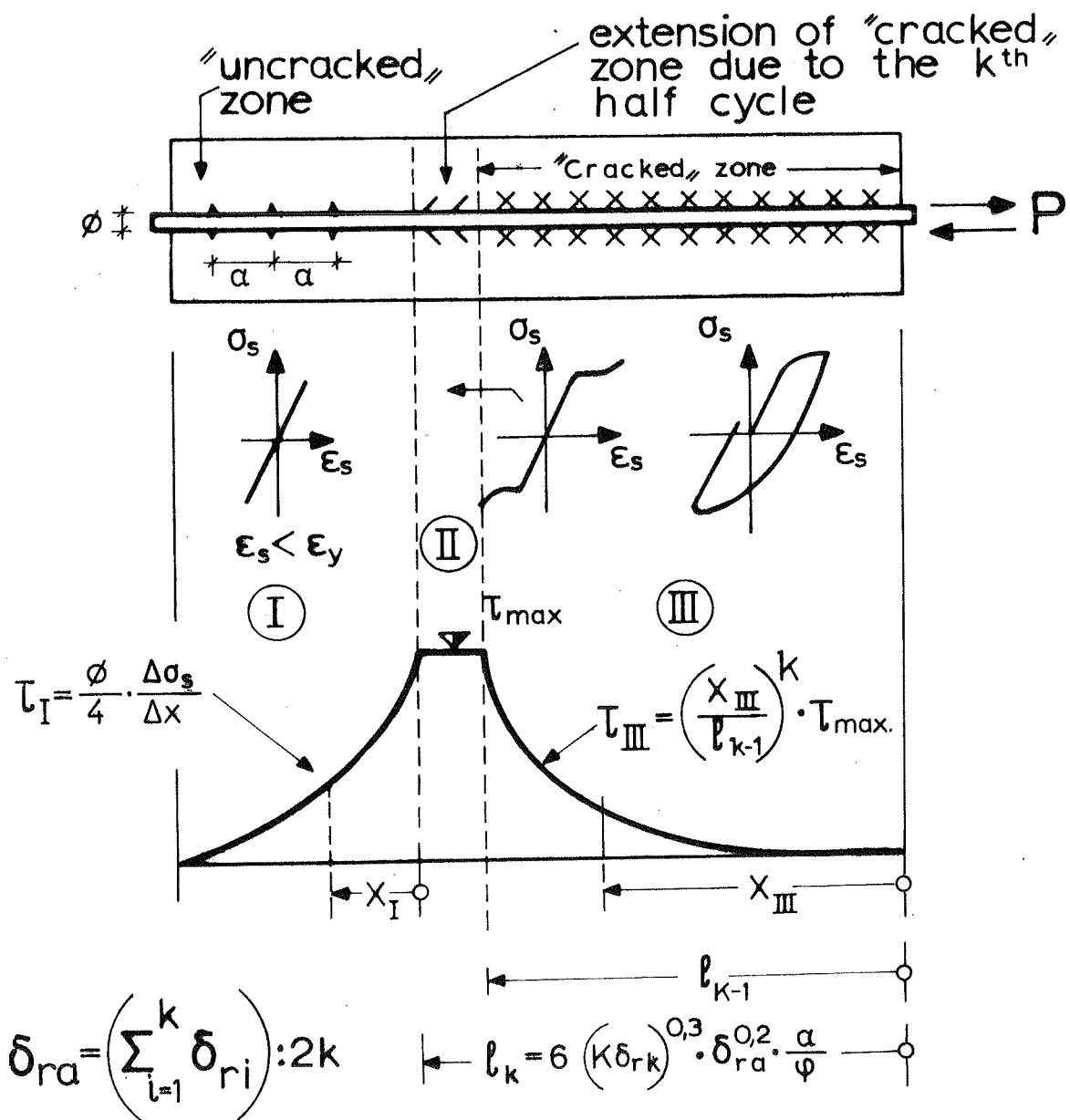


Fig. 5/6: Anchorage under monotonic and reversed loading according to Hassan + Hawkins, [1974].





$i, k = \text{half cycles order (1,0/1,5/2,0/2,5 etc.)}$

Fig. 5/8:

The main characteristics of the semi-empirical analytic model of Hassan+Hawkins, [1975], for reversed cyclic loading of anchorage.

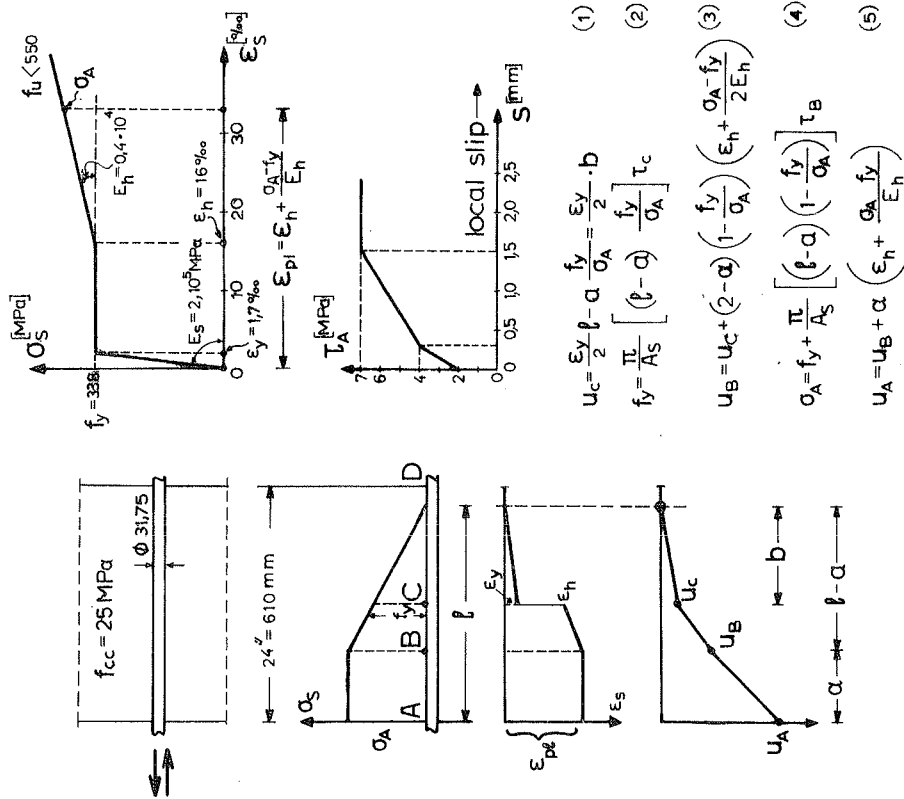


Fig. 5/9:

Basic assumptions for the analytical solution of cyclic pull-out and push-in studied experimentally by Hassan+Hawkins [1977]

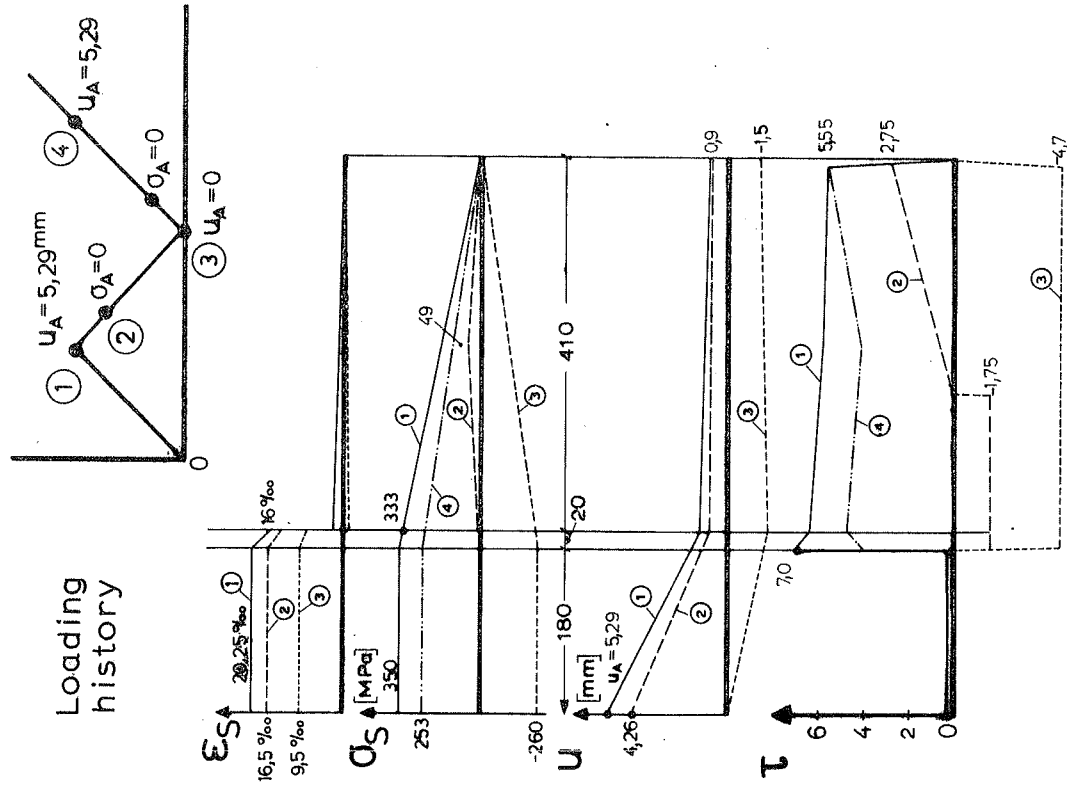


Fig. 5/10: Stresses, strain and displacement distributions of the case of Fig. 5/9. (elementary analytical solution).

# STEEL-MODEL

# BOND-SLIP MODEL

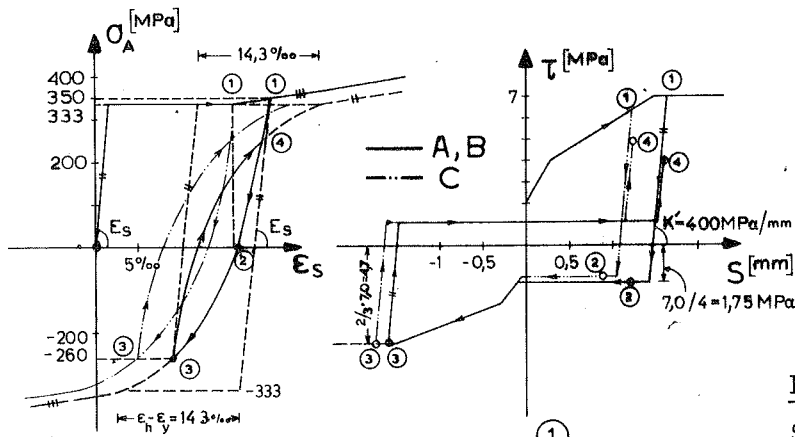


Fig. 5/11:

Stress-displacements diagramme for the case shown in Fig. 5/9 and 5/10, as found by means of a simple analytical model.

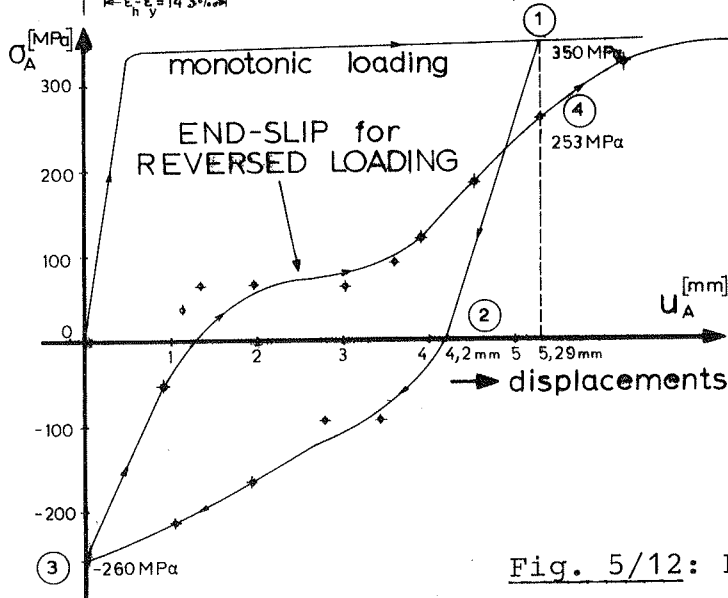
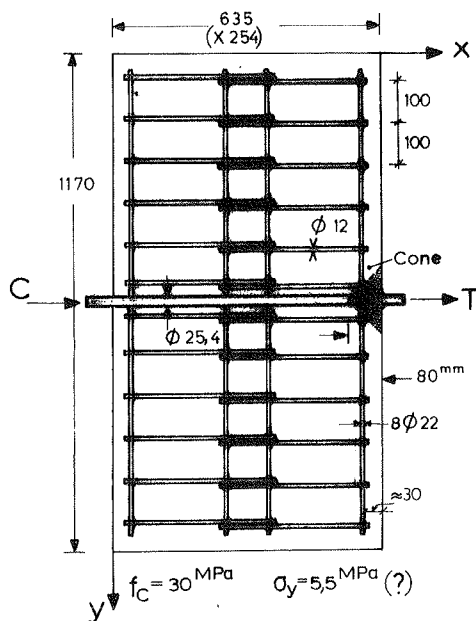


Fig. 5/12: Experimental details of cyclic pull-out (T) and simultaneous push-in (C) experiments of Popov + Bertero + Vivathanatepa, [1978].



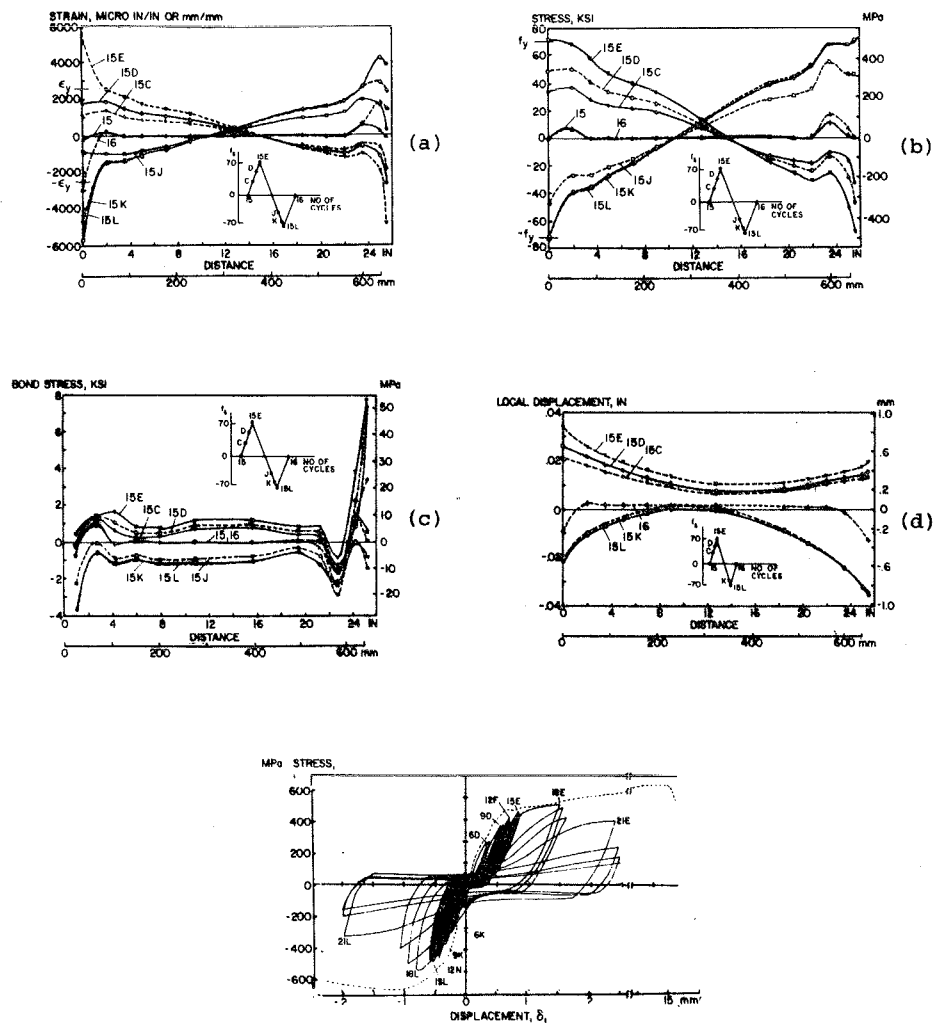


Fig. 5/13: Typical results of two-ends simultaneous bond cyclic loading (Popov+Bertero+Vivathanatepa, [1978]).

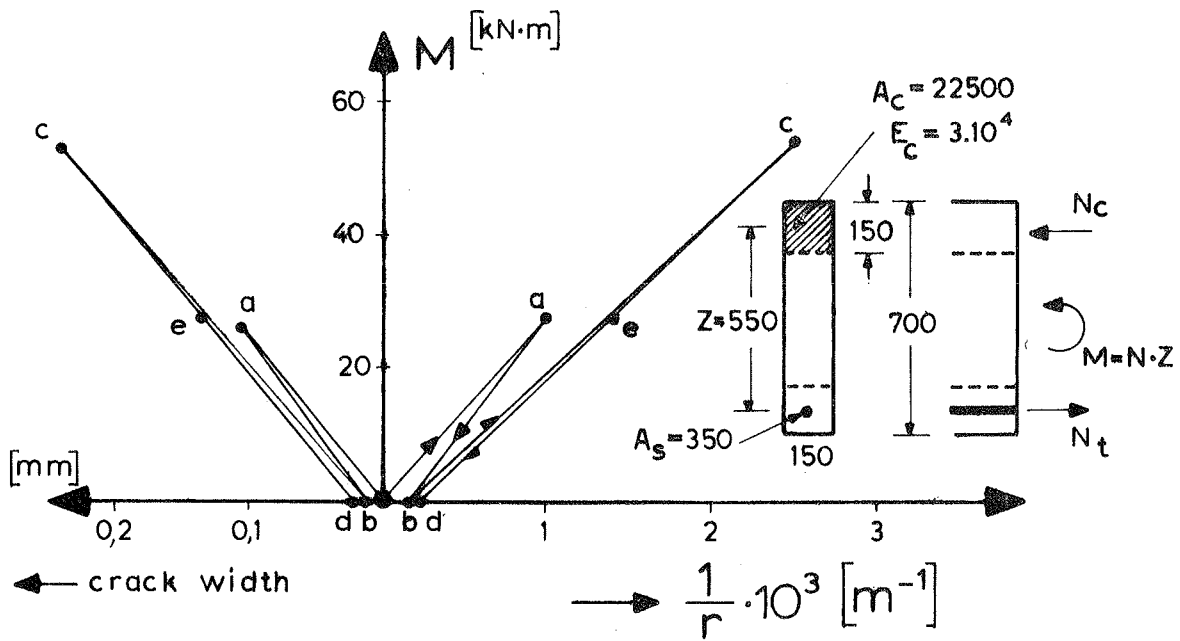


Fig. 6/1: Computed moment-curvature and moment-crack width diagrammes under repeated loading (Table III)

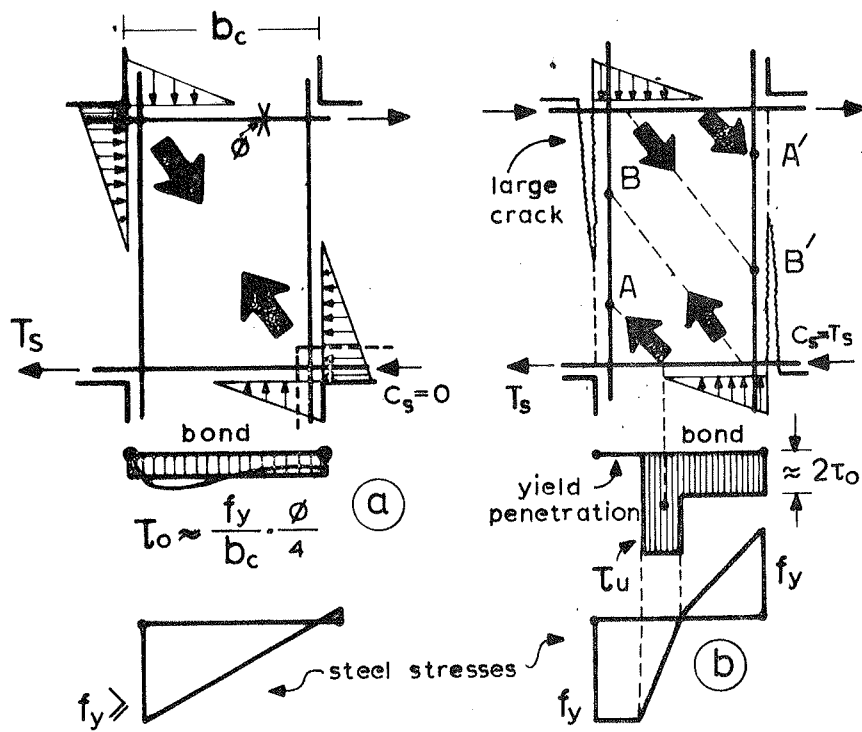
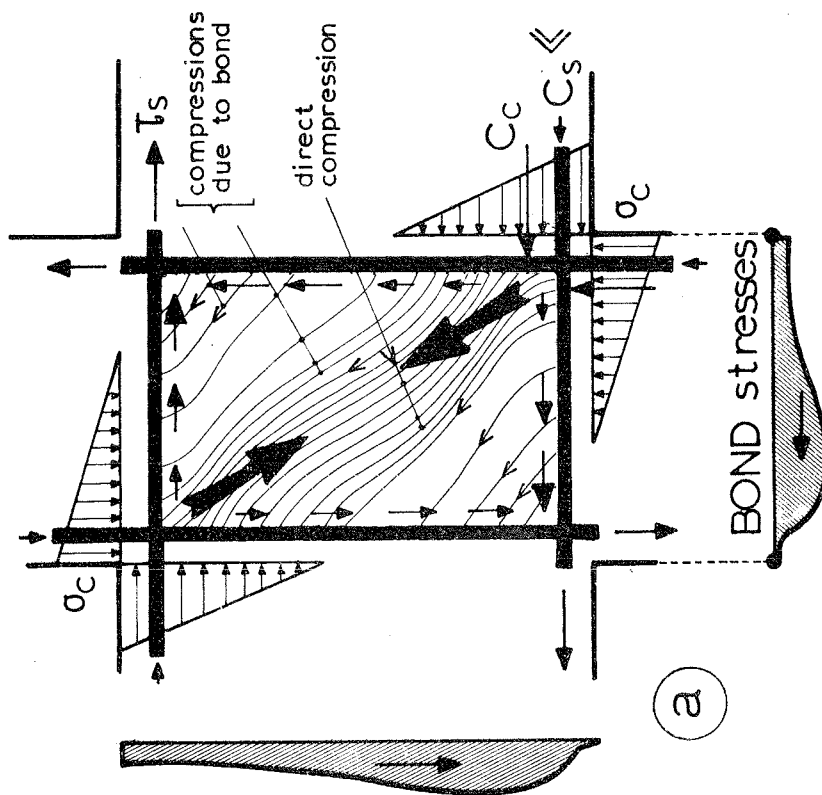


Fig. 6/2: Transmission of forces trough the core of an intact joint (a) and a joint after yield penetration (b).

# INTACT JOINT Monotonic loading



# HEAVILY CRACKED JOINT Reversed loading

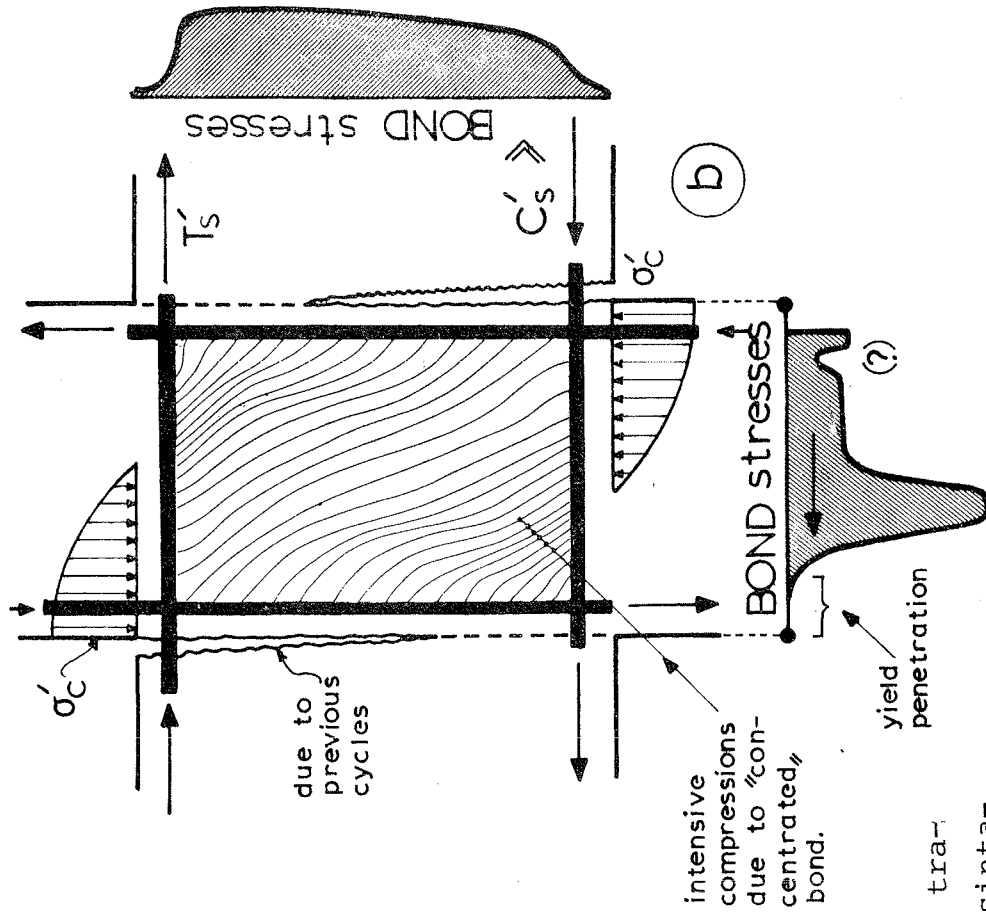


Fig. 6/3:

A qualitative image of compressive stress trajectories in an intact and a cyclicly desintegrated joint.

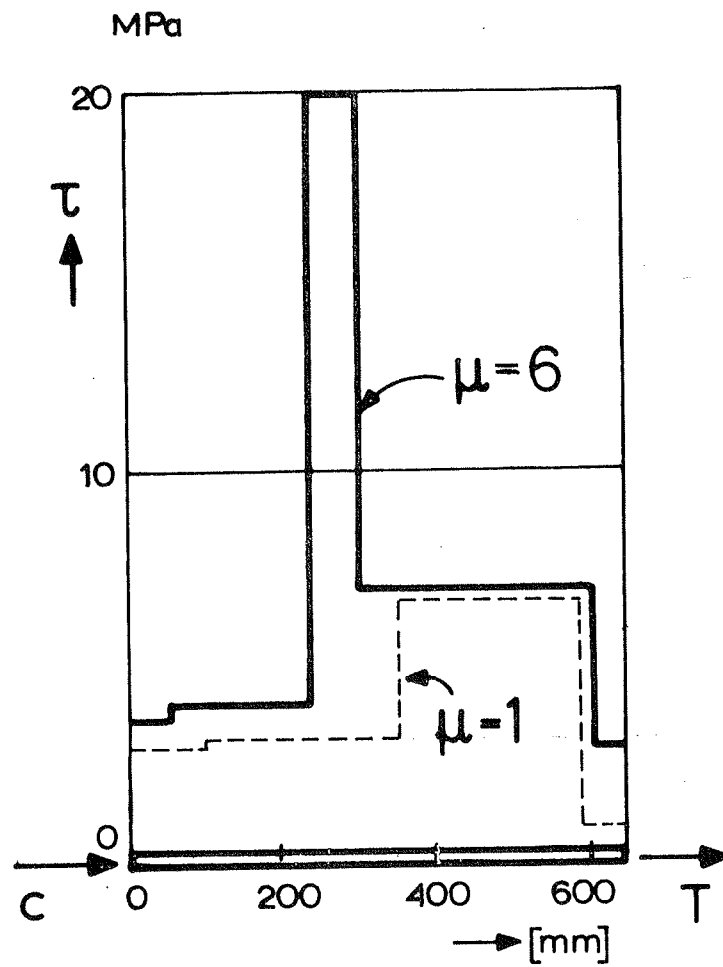


Fig. 6/4: Bond stress distribution along a joint, for various ductilities (based on Paulay et.al., [1978]).

## C O N T E N T S

- 1.- Preamble.
- 2.- For a conceptual physical model of bond.
  - 2.0.- Before loading.
  - 2.1.- Loading of bar within uncracked concrete.
  - 2.2.- First internal cracking.
  - 2.3.- Loading of the bar after the first cracking.
  - 2.4.- Loading of deformed bars up to the bond failure.
  - 2.5.- Friction coefficients.
  - 2.6.- Residual bond strength.
  - 2.7.- Unloading from  $\tau_1 < \tau_u$ .
  - 2.8.- Combined bond and dowel action.
  - 2.9.- Rate of pulling-out.
  - 2.10.- Final corrections and summary.
  - 2.11.- Characteristic slip values.
- 3.- Experimental evidence.
  - 3.1.- Monotonic loading.
  - 3.2.- Cyclic loading.
- 4.- A simplified constitutive rule for local bond-slip under cyclic loading.
  - 4.1.- The monotonic curve.
  - 4.2.- Degradation during slip-controlled cycles.
  - 4.3.- Next cycles.
  - 4.4.- An alternative possibility.
  - 4.5.- Repeated loading.
- 5.- Bond and cyclic loading of R.C. elements.
  - 5.1.- Tension stiffening degradation under cyclic loading.
  - 5.2.- Cyclic application of pull-out and/or push-in from one end.
  - 5.3.- Alternate application of pull-out from one end, and simultaneous push-in from the other.
- 6.- Some practical implications.
  - 6.1.- Flexural stiffness, damping and crack-width under cyclic loading.
  - 6.2.- Joints under seismic loading.
  - 6.3.- Anchorage capacity under cyclic loading.
  - 6.4.- Splices under cyclic loading.
- 7.- Suggested fields of additional research.
- 8.- References.
- 9.- Tables.
- 10.- Figures.